REGULATION OF CELL DEATH PROCESSES BY METABOLIC STRESS

A Dissertation

Presented to the Faculty of the Weill Cornell Graduate School

of Medical Sciences

in Partial Fulfillment of the Requirements for the Degree of

Doctor of Philosophy

by

Sung Eun Kim

May 2016

REGULATION OF CELL DEATH PROCESSES BY METABOLIC STRESS

Sung Eun Kim, Ph.D.

Cornell University 2016

In the recent few years, there have been numerous studies describing newly discovered cell death programs and the metabolic regulation of these cell death processes is poorly understood. Here we investigate two different cell death forms, ferroptosis and entosis, to examine how these death mechanisms are affected by conditions of metabolic stress. We have found that amino acid starvation can lead to ferroptosis of cells that have been treated with ultrasmall particles through depletion of cellular glutathione levels. This suggests that these ultrasmall silica nanoparticles, under nutrient-deprived conditions, can be utilized as inducers of ferroptosis. We have found that *in vivo* xenograft growth, which is accompanied by nutrient deprivation, was also inhibited with intravenous injections of these nanoparticles, suggesting the potential utilization of these particles as therapeutic agents to induce ferroptosis. We have also found that the death of live engulfed cells can be regulated by amino acids and mTOR activity. We find that amino acid withdrawal or mTOR inhibition induces apoptosis of engulfed cells and also disrupts entotic cell death that is associated with the lipidation of LC3 to entotic vacuoles. Cells ingested by two other live cell engulfment programs, homotypic cell cannibalism (HoCC) and anti-CD47 antibody-mediated phagocytosis, also known as phagoptosis, also undergo a similar vacuole maturation sequence involving LC3 lipidation and lysosome fusion, but only HoCC involves mTOR-dependent regulation of vacuole maturation and cell death, similar to entosis. We further find that the regulation of apoptosis by mTOR involves the 4E-BP1 protein

that is a known regulator of mRNA translation. The knockout of 4E-BP1 in engulfed cells rescues these cells from undergoing apoptosis caused by mTOR inhibition. These data identify amino acid signaling and the mTOR-4EBP-1 pathway as a survival pathway for live engulfed cells formed by entosis and HoCC. Together, my studies have uncovered novel roles of amino acid signaling in controlling cell death, and have identified, for ferroptosis, a potential new therapeutic strategy.

BIOGRAPHICAL SKETCH

Sung Eun Kim was born in Seoul, Republic of Korea, to Tae-won Kim and Myung-soon Han. She lived in both Korea and the United States during her childhood with her parents and brother, Sang Yoon. During her high school years, she discovered her passion for biology and went on to study Biotechnology and Genetic Engineering at Korea University, Seoul, Korea, where she obtained her B.S. degree in 2006. During her senior year, she became fascinated in cell biology and decided to further obtain her M.S degree in the laboratory of Dr. Jong-hoon Kim, studying the differentiation processes of human embryonic stem cells. In 2009, she moved to New York to attend Weill Cornell Graduate School of Medical Sciences to pursue doctoral studies, where she joined the lab of Michael Overholtzer at Memorial Sloan Kettering Cancer Center. During her stay at the Overholtzer lab, she worked on investigating the regulation of the cell death processes, ferroptosis and entosis.

To my parents for all of their love and support

To my husband, Donghyuk, for being my biggest supporter and best friend

ACKNOWLEDGEMENTS

I would first like to thank my mentor, Dr. Michael Overholtzer, for being a wonderful advisor. His dedication to science and supportive guidance has been an extremely inspiring experience to me and I have learned so much from him. I would also like to thank my thesis committee members, Dr. Alan Hall, Dr. Xuejun Jiang, and Dr. Cole Haynes, who have been very supportive and insightful throughout my graduate studies and it has been a great environment of sharing ideas and resources with their labs. Although Dr. Alan Hall is no longer with us, he was always very supportive and provided many great ideas during our weekly joint lab meetings. I am also grateful to Dr. Philipp Niethammer for scientific discussions and for chairing my thesis defense.

I would like to thank all the current and former members of the Overholtzer lab for making my Ph. D. experience a wonderful and exciting process: Oliver Florey, Qiang Sun, Matej Krajcovic, Shefali Krishna, Jens Hamann, Yongchan Lee, Urmi Bandyopadhyay, Chan Lee, Ruoyao Chen, and Michelle Riegman. They have made our lab such an enjoyable place to work and I will truly miss working with these talented colleagues.

Next, I would like to express my appreciation to my collaborators for their professional advice and discussions. In particular, Dr. Michelle Bradbury for initiating our collaboration and carrying out *in vivo* experiments of the ferroptosis project. I'd also like to thank Dr. Ulrich Wiesner at Cornell University for providing the ultrasmall silica nanoparticles and Dr. Thomas Quinn at University of Missouri for providing peptides that have been the main resource for my studies of ferroptosis.

I would also like to thank my friends that I met during grad school, Bongnam Jung, Minhee Kim, Minjung Kang, Myungjoo Kim, Ty El Rayes, Stephanie Agbu,

and Xin Tan, for making the entire Ph. D. experience so much fun. I would not have had such an enjoyable time in school and New York without all my friends. Lastly, I am most grateful to my family for all of their support and love throughout my graduate studies: my father for watching over me, my mother for always believing in me, and my husband, Donghyuk, for being with me throughout this journey.

TABLE OF CONTENTS

BIOGRAPHICAL SKETCH iii
ACKNOWLEDGEMENTS v
TABLE OF CONTENTS vii
LIST OF FIGURES xi
CHAPTER 1: Introduction 1
1.1 HISTORICAL PERSPECTIVE 1
1.2 CELL DEATH FORMS 2
1.2.1 Apoptosis 2
1.2.2 Autophagic cell death 3
1.2.3 Necrosis 4
1.2.4 Engulfment-dependent cell death 6
1.3 REGULATION OF CELL DEATH BY AMINO ACID METABOLISM 8
1.3.1 mTOR pathway 9
1.3.2 GCN2pathway 10
1.3.3 Glutamine 11
1.3.4 Asparagine 12
1.3.5 Arginine 13
1.3.6 Serine & Glycine 13
1.3.7 Cystine & Cysteine 14
1.4 THESIS AIMS 16
1.5 REFERENCES 16
CHAPTER 2: Ultrasmall nanoparticle treatment induces ferroptosis of amino acid-deprived cells 26

2.1 INTRODUCTION 26
2.2 MATERIALS AND METHODS 27
2.2.1 Cell culture and constructs 27
2.2.2 Reagents 28
2.2.3 Peptide synthesis 29
2.2.4 Synthesis and characterization of αMSH-PEG-C' dots 29
2.2.5 Western blotting 30
2.2.6 Time-lapse microscopy 30
2.2.7 Analysis of reactive oxygen species 30
2.2.8 Animal models and tumor inoculation 31
2.2.9 In vivo dosing strategy and examination 31
2.2.10 In vivo fluorescence imaging 32
2.2.11 Histological analysis 32
2.2.12 Statistics 33
2.3 RESULTS 33
2.3.1 αMSH-PEG-C' dot particles localize to the lysosome network 33
2.3.2 αMSH-PEG-C' dot particles induce cell death in amino acid-deprived conditions 34
2.3.3 αMSH-PEG-C' dot particle-induced cell death is not apoptosis, necroptosis or autosis 38
2.3.4 Ferroptosis is the underlying mechanism of αMSH particle-induced cell death 41
2.3.5 αMSH-PEG-C' dots induce partial tumor regression and growth inhibition in HT1080 xenograft models 43
2.4 DISCUSSION 47
2.5 REFERENCES 54

CHAPTER 3: Amino acids and mTOR regulate the fate of live engulfed cells 58
3.1 INTRODUCTION 58
3.2 MATERIALS AND METHODS 60
3.2.1 Cell culture and constructs 60
3.2.2 Reagents 61
3.2.3 Immunofluorescence 61
3.2.4 Western blotting 62
3.2.5 siRNA and shRNA mediated protein knockdown 62
3.2.6 CRISPR/Cas9 gene knockout system 62
3.2.7 Time-lapse microscopy 63
3.2.8 BrdU incorporation assay 63
3.2.9 Phagoptosis assay 63
3.3 RESULTS 64
3.3.1 Amino acid starvation or mTOR inhibition induces apoptosis of live engulfed entotic cells 64
3.3.2 Amino acid starvation or mTOR inhibition induces apoptosis of live engulfed cells during HoCC 66
3.3.3 mTOR activity is required within engulfed cells for survival 66
3.3.4 4E-BP1 is required for apoptosis occurring in response to mTOR inhibition 68
3.3.5 Non-apoptotic death of engulfed cells in entosis is also regulated by amino acids and mTOR 71
3.3.6 mTOR does not act through autophagy to regulate non-apoptotic death during entosis 73
3.3.7 The fates of live engulfed cells within HoCC cell-in-cell structures, but not CD47-blockade-induced phagocytosis, are regulated by amino acids and mTOR 73

3.4 DISCUSSION 78
3.5 REFERENCES 81
CHAPTER 4: Conclusions and perspectives 84
4.1 SUMMARY 84
4.2 FUTURE DIRECTIONS 85
4.2.1 Molecular mechanism of ferroptosis 85
4.2.2 Synchronous cell-to-cell spreading of ferroptosis 87
4.2.3 Nutrient uptake of live engulfed cells 88
4.2.4 mTOR-dependent upstream trigger of entotic death 89
4.3 CONCLUSION 90
4.4 REFERENCES 91

LIST OF FIGURES

Figure 2.1 αMSH-PEG-C' dot particles and their localization to lysosomal networks 35
Figure 2.2 αMSH-PEG-C' dot particles induce cell death in amino acid-deprived conditions 37
Figure 2.3 αMSH-PEG-C' dot particle-induced cell death is not apoptosis, necroptosis or autosis 39
Figure 2.4 Control assays for apoptosis and necroptosis-inhibited cells 40
Figure 2.5 Ferroptosis is the underlying mechanism of αMSH particle-induced cell death 42
Figure 2.6 αMSH-PEG-C' dots induce cell death in different types of cancer cells 44
Figure 2.7 αMSH-PEG-C' dots induce partial tumor regression and growth inhibition in HT1080 xenograft models 46
Figure 2.8 Differential sensitivity of HT1080 cancer cells to αMSH-PEG-C' dot-induced ferroptosis 50
Figure 2.9 ROS, glutathione, and cell death measurements in MCF10A cells treated with and without αMSH-PEG-C' dots or PEG-C' dots 52
Figure 2.10 Cell death measurements in HT1080 cells treated with different sized PEG-C' dots 53
Figure 3.1. Amino acid starvation or mTOR inhibition induces apoptosis of live engulfed cells in entosis 65
Figure 3.2. The live engulfed cells of HoCC cell-in-cell structures can also undergo apoptosis and are regulated by amino acid starvation and mTOR 67
Figure 3.3. The activity of mTOR in required in the engulfed cell for survival 69
Figure 3.4. Knockout of 4E-BP1 specifically in engulfed cells rescues cells from apoptosis 70

Figure 3.5. Amino acid starvation or mTOR inhibition inhibits non-apoptotic death in entosis and HoCC 72
Figure 3.6. Autophagy-inhibited cells still have decreased rates of non-apoptotic death with mTOR inhibition 74
Figure 3.7. The live engulfed cells of HoCC cell-in-cell structures can undergo non-apoptotic death and are regulated by amino acid starvation and mTOR..... 76
Figure 3.8 Live engulfed cells of phagoptosis undergo non-apoptotic death but are not affected by amino acid starvation and mTOR 77

CHAPTER 1: Introduction

1.1 HISTORICAL PERSPECTIVE

The concept of cell death as a physiological process was first recognized in1842 by Carl Vogt when he made the observation that cell death was involved in removal of the notochord during amphibian development (Vogt, 1842). Then in 1964, more than a century later, Richard Lockshin and Carroll Williams observed that cell death is a regulated process by studying insect metamorphosis (Lockshin and Williams, 1965). Further progress in the field was made by using the model organism *Caenorhabditis elegans* which revealed that apoptosis, the most studied cell death form, has a genetically defined program and its biochemical mechanisms are conserved in various animal systems (Ellis and Horvitz, 1986). For many following years, apoptosis was considered to be the only major form of programmed cell death and was the focus of numerous studies that lead to many significant findings. Recently, however, an expanding number of new studies have revealed that there are many other diverse forms of non-apoptotic cell death programs that occur in various contexts. Most of these cell death forms occur in an active manner, as a consequence of distinct signaling events to specific stimuli. Dysregulation of cell death signaling is involved in various pathological conditions such as cancer, autoimmune, and neurodegenerative diseases. In particular, cancer cells have been shown to evade cell death and this is recognized as one of the hallmarks of cancer development (Hanahan and Weinberg, 2011). Another hallmark of cancer that is emerging as a focus of numerous studies is the reprogramming of metabolic pathways. Although some results suggest that metabolism and cell death are linked, they are mostly focused on the regulation of apoptosis. It will be important to learn how metabolic changes can induce or regulate

other non-apoptotic cell death forms in various contexts. In the following sections, I will introduce the characteristics of regulated cell death programs with a focus on non-apoptotic cell death forms, and discuss how cell death processes can be regulated by metabolic stress.

1.2 CELL DEATH FORMS

It is now well accepted that programmed cell death is required for normal tissue development and homeostasis of organisms. Cell death supports the development of various tissues as well as the turnover of aged cells or unwanted immune cells (Lee et al., 2002; Lindsten et al., 2000; Rathmell et al., 2002). Cell death is also relevant in the context of pathological processes such as degenerative diseases and cancer, and has been recognized as an important barrier to tumor development. Classically, mammalian cell death programs are categorized into three major types of morphologically distinct cell death forms: apoptosis (type 1), autophagic cell death (type II), and necrosis (type III) (Schweichel, 1973).

1.2.1 Apoptosis

Apoptosis has been the main focus of the cell death field for several decades and its molecular mechanism and clinical applications have been well studied (Fulda, 2015; Korsmeyer, 1992; Wong, 2011). Morphologically, apoptosis is characterized by cell shrinkage, membrane blebbing, condensation of chromatin, and cell and nuclear fragmentation that leads to the formation of apoptotic bodies (Xiong et al., 2014). Apoptosis can be triggered when cell-surface death receptors such as Fas are bound by their ligands (extrinsic pathway) or when the pro-apoptotic Bcl-2 (B-cell lymphoma 2) family proteins cause permeabilization of the mitochondrial outer membrane (intrinsic

pathway). Both pathways converge on the activation of caspase proteases, which are ultimately responsible for the dismantling of the cell. Deficiencies for key caspases of the apoptotic pathway cause pre- or neonatal lethality due to impaired organ development demonstrating the importance of apoptosis during embryonic development (Hakem et al., 1998; Kuida et al., 1996). Apoptosis can influence tumor progression in multiple ways as oncogenic alterations that disrupt apoptosis (e.g. Bcl-2 translocation, mutation of phosphatidylinositol-3-kinase (PI3K) catalytic subunit p110α) can lead to cancer development, but conversely other oncogenic changes (e.g. c-Myc amplification) can promote apoptosis (Korsmeyer, 1992; McDonnell et al., 1989). Further research of signaling pathways and molecular mechanisms leading to apoptosis in specific contexts will provide new avenues for cancer therapy.

1.2.2 Autophagic cell death

Autophagy is a catabolic process in which parts of the cytosol and specific organelles are engulfed by a double membrane structure, known as the autophagosome, and eventually degraded inside lysosomes to be recycled. The autophagy pathway is induced when cells are deprived of nutrients or when cells are under conditions of stress. Although autophagy mostly acts as a survival mechanism, there are a few examples of autophagy functioning as a death mechanism, (hence the term "autophagic cell death"), where components of the autophagic signaling pathway actively promote cell death. During *Drosophila* metamorphosis, involution of the midgut and salivary glands involves massive autophagy-induced cell death triggered by the steroid hormone ecdysone (Berry and Baehrecke, 2007; Denton et al., 2009). In this scenario, a deficiency in autophagy-related (ATG) genes, which are required for the autophagy protein microtubule-associated protein 1A light chain 3 (LC3) lipidation and elongation of autophagosomal membranes, inhibits cell death. Also,

forced expression of ATG1, which is a component of the upstream initiation complex needed for the induction of the autophagy pathway, is sufficient to promote cell death in this context (Scott et al., 2007). Despite this clear genetic evidence for a pro-death function of autophagy in development, a mechanistic link between the formation of autophagosomes and the execution of cell death, to explain how autophagy can kill cells, has remained lacking. A recent study has suggested that autophagic cell death also occurs in mammalian cells and involves activity of the plasma membrane Na^+/K^+-ATPase (Liu et al., 2013), but it remains controversial whether autophagic cell death contributes to development and disease in humans.

1.2.3 Necrosis

Although necrosis was thought for a long time to be an accidental process that occurred in response to physiochemical insults, it has become evident in the past few years that necrosis can be initiated and executed in a regulated and genetically controlled manner (Degterev et al., 2008; Degterev et al., 2005). This relatively recent finding has spawned a new generation of research into many non-apoptotic cell death mechanisms. Necrosis is morphologically characterized by cell swelling and rapid plasma membrane rupture, and a loss of organelle structure without chromatin condensation. The best-characterized form of programmed necrosis is RIP-dependent necrosis, referred to as necroptosis, which requires the kinase activity of RIP1 and RIP3. Necroptosis can be initiated from tumor necrosis factor receptor 1 (TNFR1) ligation, which is followed by the recruitment and activation of RIP3 by RIP1. Phosphorylation of RIP3 triggers oligomerization of the pseudokinase mixed lineage kinase-like (MLKL) and translocation to the plasma membrane, which leads to a disruption in ionic homeostasis and cell rupture (Sun et al., 2012). Although RIP3 or MLKL deficiency does not lead to defects in development or adulthood (Newton et

al., 2004; Wu et al., 2013), RIP3-deficient mice die after challenge with vaccinia virus, highlighting the physiological relevance of necroptosis as a viral defense mechanism (Cho et al., 2009; Wu et al., 2013).

Aside from necroptosis, there has been an expansion of other regulated necrotic death forms that are consistent with the morphological definition of necrosis, but are independent of RIP1 or RIP3 activity. Ferroptosis, one of these additional necrotic cell death forms, was discovered several years ago and has been the topic of numerous recent studies. It was shown by initial studies that RAS-transformed cells treated with a lethal small molecule called erastin undergo regulated necrosis, resulting from inhibition of the system X_C-Cys/Glu antiporter that is required for generation of the key antioxidant glutathione (GSH) (Dixon et al., 2012). This type of cell death was named ferroptosis because it also crucially depends on intracellular iron, perhaps to support, through Fenton chemistry, the accumulation of lethal reactive oxygen species (ROS). GSH peroxidase 4 (GPX4) has been shown to be an important enzyme that defends cells against ferroptosis by scavenging lipid peroxides, and its activity relies on cellular GSH levels (Yang et al., 2014). Therefore, GSH depletion typically leads to loss of GPX4 function, resulting in ROS-mediated lipid peroxidation. This is most likely similar to the cell death process named oxytosis in which neuronal cells die through the inhibition of the X_C-Cys/Glu antiporter by excess glutamate-induced excitotoxicity (Tan et al., 2001).

In addition to necroptosis and ferroptosis, still additional forms of regulated necrosis have also emerged, including cyclophilin D (CypD)-dependent necrosis, pyroptosis, NETosis, and parthanatos. Ischemia/reperfusion injury (I/R) leads to cell death caused by mitochondrial permeability transition (mPT) in which CypD plays an active role (Baines et al., 2005). Pyroptosis is a caspase 1-dependent death of macrophages in response to pathogens that leads to inflammation (Fink and Cookson,

2006). NETosis is a NADPH oxidase (NOX)-induced cell death of neutrophils that acts as an antibacterial immune defense mechanism (Remijsen et al., 2011), and Parthanatos is caused by overactivation of PARP1, an ADP-ribosyl transferase enzyme, that leads to NAD^+ depletion and, consequently, cell death (Andrabi et al., 2008).

1.2.4 Engulfment-dependent cell death

While three morphological categories of cell death have proven to be useful descriptors historically, it has now become evident that a much broader spectrum is needed to define the myriad metazoan cell death mechanisms that have recently been discovered (Galluzzi et al., 2015). Among numerous cell death forms that do not fit neatly into the historical categories, several cell death processes have been identified that share a common characteristic: they require the involvement of engulfing cells for cell death execution. This unique feature suggests that some metazoan cell deaths are not executed as cell suicides, but rather as cell murders, as they are triggered in a non-cell-autonomous manner by engulfing cells. One of these mechanisms, called entosis, involves the engulfment and death of mammary epithelial cells and can be observed in breast tumors (Overholtzer et al., 2007). Engulfment by entosis is controlled by cadherin cell adhesion proteins and Rho-mediated cytoskeletal tension, where cells with high mechanical tension are engulfed by neighbors with lower tension. Ingested cells are then killed by a mechanism involving lipidation of the autophagy protein LC3 onto entotic vacuoles, leading to lysosome fusion and engulfed cell death and degradation (Florey et al., 2011).

Intriguingly, engulfed entotic cells can actually survive inside of their hosts for extended periods before being killed (from hours to more than a day), and they can also escape from their hosts altogether, suggesting that the decision to initiate cell

death is made not before, but after, engulfment. Engulfed cells residing inside their hosts appear to be deprived of growth factors and nutrients from media, and subsequently activate autophagy that supports cell survival, as a block of autophagy induces apoptosis (Florey et al., 2011). Thus, autophagy machinery functions during entosis both to promote cell survival, by acting within engulfed cells, and also to promote cell death by modifying entotic vacuoles within engulfing cells.

The engulfment mechanism that initiates entosis can be induced in breast cancer cells by expression of E- or P-cadherin, which suppresses transformed growth in soft agar, suggesting that entosis may have a tumor-suppressive role (Sun et al., 2014). On the contrary, entosis can also induce aneuploidy within host cells, which is known to promote tumor progression (Krajcovic et al., 2011). In addition, host cells can recover nutrients from degraded engulfed cells and support proliferation and survival in starved conditions (Krajcovic et al., 2013), suggesting that on balance, while entosis acts as a mechanism of cell death that can suppress transformed growth, it may in fact promote tumor progression in the long-term.

Other examples of live engulfment programs include emperitosis, suicidal emperipolesis, phagoptosis, and homotypic cell cannbalism (HoCC). Emperitosis refers to the apoptotic death of engulfed natural killer cells in tumor cells caused by the secretion of granzyme B (Wang et al., 2013). Suicidal emperipolesis involves the clearance of autoreactive T cells by invasion into the liver *in vivo* (Benseler et al., 2011). Phagoptosis involves the engulfment and death of cells that have downregulated “don’t-eat-me” signals, such as CD47, by macrophages and is being considered for potential therapeutic applications (Brown and Neher, 2012; Vonderheide, 2015). HoCC is a form of cell engulfment observed in pancreatic tumors and found to inversely correlate with metastasis (Cano et al., 2012).

1.3 REGULATION OF CELL DEATH BY AMINO ACID METABOLISM

It has become clear in recent years that the regulation of cell death and metabolism are closely connected with multiple layers of interplay (Green et al., 2014). One classic example of crosstalk between metabolism and cell death is mitochondria, which mediate energy production in cells and also act as key inducers of apoptosis. Similarly, numerous metabolic intermediates (e.g. adenosine triphosphate (ATP), reactive oxygen species (ROS), acetyl-coenzyme (CoA), etc.) have been shown to influence the regulation of cell death. Understanding how metabolism affects specific cell death mechanisms, particularly in disease states, such as cancer, may reveal novel controls over disease progression, and could also lead to the identification of new therapeutic opportunities. Cancer cells are known to experience chronic metabolic stress, unlike normal cells, and undergo metabolic reprogramming to support their increased biosynthetic and energy demands for continued proliferation. Metabolic stress in cancers arises not only due to the effects of mutations to tumor suppressors and oncogenes that disrupt normal metabolism (e.g. p53 and Kras mutations), but also many solid tumors (e.g. pancreatic and breast carcinoma) experience chronically limited blood supplies due to insufficient vascularization. This leads to low availability of key nutrients (glucose, amino acids, and oxygen) for cells that are driven to be metabolically active by loss of normal cellular homeostatic controls. These specific nutrient deficiencies can have severe effects on cells that can trigger cell death, and may represent an Achilles' heel that could be exploited for cancer therapy. In particular, recent studies have revealed that amino acids are essential to support the high metabolic demands of tumors and can also function as nutrient signals that regulate signaling pathways leading to cell survival or death. Thus, amino

acid availability can influence cell death regulation in a complex manner either through signaling or by more direct requirements to support cell metabolism.

1.3.1 mTOR pathway

Amino acid levels are sensed by cells through two major adaptive pathways, the mammalian target of rapamycin complex 1 (mTORC1) pathway, and the general control nonderepressible 2 (GCN2) pathway. The mTOR complex 1 (mTORC1) is a serine/threonine kinase complex that senses amino acid availability to control mRNA translation and autophagy. mTORC1 is scaffolded to the surface of lysosomal membranes, where it senses the presence of particular amino acids such as leucine, glutamine, and arginine, as well as energy availability (through AMPK regulation) and growth factor signaling, and integrates these nutrient signals to suppress autophagy and promote translation when nutrients are plentiful. mTORC1 signaling has been shown to influence multiple cell death pathways in a complex manner. Apoptosis is inhibited by the mTORC1-dependent the translation of mRNAs that encode key anti-apoptotic proteins, such as myeloid cell leukemia 1 (MCL-1), and cellular FLICE-like inhibitory protein (cFLIP) (Meynet et al., 2013; Munoz-Pinedo et al., 2003). MCL-1 functions to bind and inhibit the pro-apoptotic proteins Bcl-2-associated X (Bax) and Bcl-2 homologous antagonist/killer (Bak), and cFLIP functions to block caspase-8 or prevent death-inducing signaling complex (DISC) formation. As the ratio of anti-apoptotic to pro-apoptotic Bcl-2 family proteins can regulate apoptosis sensitivity, the loss of MCL-1 or cFLIP expression in amino acid-starved cells with decreased mTORC1 activity can induce apoptosis. In addition to modulating apoptosis senstitivity, mTORC1 is also implicated in regulating necroptosis, in this case by promoting the necroptotic cell death of neuronal cells in response to TNF-α signaling. The inhibition of mTOR or Akt, an upstream regulator of mTOR, blocked necroptosis

without affecting the RIP1-RIP3 complex assembly, suggesting a role for Akt and mTOR downstream of RIP1 activation in regulating necroptosis (Liu et al., 2014).

1.3.2 GCN2 pathway

Another pathway that functions as an adaptive mechanism to fluctuating amino acid levels is the GCN2 pathway that regulates mRNA translation initiation and lipid metabolism, by detecting uncharged tRNAs that accumulate in the absence of amino acids. When activated, GCN2, a serine/threonine kinase, can phosphorylate eukaryotic translation initiation factor 2α (eIF2α), resulting in reduced rates of translation initiation and a decline in protein synthesis. While phosphorylated eIF2α generally suppresses protein synthesis, it can also promote translation of specific mRNAs that contain unique 5' untranslated regions (UTR), such as the activating transcription factor 4 (ATF4) (Harding et al., 2000). ATF4 can then induce expression of many genes involved in amino acid metabolism, such as amino acid synthetases, transporters, and amino acyl tRNA synthetases (Baird and Wek, 2012; Ye et al., 2010). ATF4 is overexpressed in several human tumor tissues and is upregulated in response to hypoxic stress. As ATF4 is a critical regulator of genes involved in amino acid metabolism, cells that have been depleted of ATF4 cannot survive or proliferate in the absence of non-essential amino acids (NEAAs). Likewise, the GCN2-ATF4 pathway has been shown to be important for the survival of c-Myc-overexpressing neuroblastoma cells under conditions of glutamine deprivation (Qing et al., 2013). Sestrin2, a stress response protein that is upregulated through GCN2 signaling, was shown to be essential for keeping cells from undergoing apoptosis in response to glutamine starvation (Ye et al., 2015).

1.3.3 Glutamine

Among the twenty-two standard amino acids, nine are considered to be "essential" because they must be obtained through nutritional intake. However, some cells, such as cancer cells, may conditionally depend on different amino acids based on microenvironmental context or genetic mutations. Several amino acids have been shown to be required for the survival of cancer cells due to particular metabolic requirements. For example, deprivation of glutamine has been shown to be synthetically lethal toward cancer cells with loss-of-function of p53 (Reid et al., 2013). Glutamine is a critical nutrient for cancer cells as a carbon and nitrogen source for macromolecule synthesis, an ATP source through conversion to α-ketoglutarate, and glutamate source for GSH synthesis. The concentration gradient of glutamine can also drive specific antiporters expressed at the plasma membrane to uptake other amino acids. Cancer cells consume glutamine to a degree that exceeds their need for the molecules in anabolic macromolecular synthesis and glutamine metabolism is highly regulated by several factors such as c-Myc, Ras, p53 and HIF. p53 can increase expression of the mitochondrial isoform of glutaminase (GLS2), which converts glutamine to glutamate, leading to enhanced mitochondrial respiration and ATP generation along with reduction in ROS due to increased glutathione levels (Hu et al., 2010). Likewise, expression of c-Myc in mouse embryonic fibroblasts leads to induction of GLS1 along with lactate dehydrogenase and glutamine transporters, suggesting that c-Myc is sufficient to drive cellular dependence on glutamine (Chen and Cui, 2015). Therefore, not surprisingly, inhibitors of GLS, such as BPTES and 968, have been shown to induce the cell death of cancer cells (Li et al., 2015; Simpson et al., 2012). Glutamine deprivation has also been reported to sensitize cells to Fas ligand, TNF-α, and heat shock-mediated apoptosis (Ko et al., 2001), and to induce apoptosis through reduction of GSH, the main antioxidant in cells. Glutamate, an

essential component of GSH, is mostly derived from glutamine uptake by cells and is necessary for cystine uptake through the X_C-Cys/Glu antiporter. Glutamine deprivation-induced apoptosis can be reversed by inhibition of ROS production highlighting the importance of ROS production during apoptosis (Reid et al., 2013).

1.3.4 Asparagine

As mentioned above, glutamine deprivation can lead to cell death and this was initially thought to be caused by the role of glutamine to replenish tricarboxylic acid (TCA) cycle intermediates and support synthesis of nucleotides and non-essential amino acids. However, a recent study has shown that cell death induced by glutamine deprivation was prevented by suppression of citrate synthase, the first tricarbosylic acid cycle enzyme (Zhang et al., 2014). In the absence of glutamine, citrate synthase depletion lead to the synthesis of aspartate and asparagine and it was further shown that addition of asparagine was sufficient to prevent glutamine-deprivation-induced death. In support of this model, knockdown of asparagine synthetase (ASNS), the enzyme that generates asparagine, induced apoptosis even in the presence of glutamine, highlighting the importance of asparagine. The anti-apoptotic function of asparagine was dependent on its ability to suppress C/EBP-homologous protein (CHOP), a pro-apoptotic regulator of the unfolded protein response, without affecting induction of ASNS by the GCN2-ATF4 pathway. Some cancers that lack ASNS depend on extracellular asparagine for survival (Galluzzi et al., 2013) and use of asparaginase, which hydrolyzes extracellular asparagine, in patients with acute lymphoblastic leukemia has shown successful results (Avramis and Panosyan, 2012). Recently, upregulated ASNS was associated with aggressiveness in ovarian, prostate, and pancreatic cancers, suggesting that asparaginase may also hold therapeutic potential in these contexts (Panosyan et al., 2014).

1.3.5 Arginine

The amino acid arginine is an important precursor for the synthesis of protein, urea, creatine, and nitric oxide. The enzyme that generates arginine, arginino-succinate synthase 1 (ASS1), is lacking in some cancers, rendering them to be dependent on exogenous supplies of arginine for survival (Galluzzi et al., 2013). For example, osteosarcoma and bladder cancer cell lines expressing low levels of ASS1 fail to grow in an arginine-free medium, suggesting that ASS1 may be a good target for therpeutic agents (Allen et al., 2014; Kobayashi et al., 2010). It has been shown that arginine depletion induces Bax conformation changes and mitochondrial inner membrane depolarization in ASS1-negative cells, which leads to apoptosis in mesothelioma cells (Szlosarek et al., 2006). Ongoing research of arginine deprivation therapy has led to the development of arginine depleters, such as pegylated arginine deiminase that may represent a potential treatment method for various cancers. The treatment of ASS1-deficient prostate cell lines with these pegylated arginine deiminase resulted in cell death resembling an autophagic mechanism, suggesting that although some cancers have a common requirement for arginine metabolism, they may undergo different types of cell death in response to arginine depletion (Changou et al., 2014).

1.3.6 Serine & Glycine

The amino acids serine and glycine are interconvertible and interconnected via the glycine cleavage system, a major metabolic pathway in one-carbon metabolism that provides cofactors for nucleotide synthesis for proliferating cancer cells. The overexpression of several enzymes that function in serine and glycine metabolism can promote oncogenic transformation of breast and lung cancer, respectively, suggesting that serine and glycine metabolism can promote the growth of some cancers (Possemato et al., 2011; Zhang et al., 2012). Similarly, the removal of these amino

acids by dietary restriction was shown to limit tumor growth without impacting animal health (Maddocks et al., 2013). When cells are deprived of serine or glycine, the enzymes of the serine-glycine metabolism pathway accumulate and stabilize p53, resulting in the activation of multiple genes, including cyclin-dependent kinase inhibitor 1A (CDKN1A), coding for the cell cycle inhibitor $p21^{Cip1}$ (Maddocks et al., 2013). In the case of some cancers where p53 functions are compromised, cells succumb to serine-glycine deprivation, similarly to glutamine deprivation, suggesting that p53 has a role of suppressing cell death in this scenario (Maddocks et al., 2013; Reid et al., 2013).

Some cancer cells have an increased capacity for *de novo* serine synthesis via the phosphoglycerate dehydrogenase (PHGDH) pathway. PHGDH converts the glycolytic intermediate 3-phosphogycerate to yield serine following a three-step enzymatic reaction. Suppression of PHGDH in cell lines with elevated PHGDH expression causes a decrease in reduction of serine synthesis and cell proliferation (Locasale et al., 2011). In addition, serine hydroxymethyl transferase (SHMT), the enzyme that converts serine to glycine, has also been implicated in tumorigenesis. The two isoforms of SHMT have been described as targets of c-Myc and have been shown to rescue the growth defects of cells depleted for c-Myc (Nikiforov et al., 2002). These metabolic enzymes are the focus of several clinical studies to test the efficacy of targeting the serine-glycine metabolic pathway for anti-tumor therapies.

1.3.7 Cystine & Cysteine

Redox control of cell death has attracted increasing interest in recent years and the metabolism of glutathione (GSH), the most abundant cellular antioxidant, has emerged as a possible target for development of anti-cancer treatments. Cysteine, typically present in its oxidized form cystine in the extracellular space, is regarded as the rate-

limiting substrate for GSH synthesis. Cystine, the predominant form in plasma, extracellular body fluids and cell culture medium, is transported into cells by the amino acid system X_C-Cys/Glu antiporter. Recently, the X_C-Cys/Glu antiporter has been shown to play an important role in promoting cell survival by blocking the induction of ferroptosis, as inhibition of the antiporter by excessive glutamate or erastin treatment can induce ferroptosis of cells (Albrecht et al., 2010; Dixon et al., 2012). Similar results have been observed for cancer cells and several clinically approved drugs, such as sulfasalazine, sorafenib, and artesunate, which have been shown to induce ferroptosis in various types of cancer cells (Dixon et al., 2014; Eling et al., 2015; Louandre et al., 2015).

Amino acids in general can provide reducing equivalents to increase the cellular capacity for redox homeostasis, and deprivation of amino acids has been shown to lead to an accumulation of ROS, most likely through mitochondrial dysregulation (Chen et al., 2009). ROS have been implicated in controlling not only in the execution of cell death but also to the signal transduction pathways leading to the initiation of cell death (Trachootham et al., 2008). ROS can be generated from both intracellular and extracellular sources, and there are multiple cellular defense mechanisms, including GSH, superoxide dismutases (SODs), GPXs, and catalases. The mitochondria are a major source of ROS, especially superoxide anion ($O_2\bullet^-$) and hydrogen peroxide (H_2O_2), which are normally cleared by SODs. In the cytoplasm, ROS may be generated from the arachidonic acid pathway or cytochrome P-450 isozymes, which can be scavenged by GSH. In addition to these intracellular sources, many other extracellular agents may contribute to the formation of ROS in cells. Several cytotoxic agents induce ROS, such as H_2O_2 and $O_2\bullet^-$, which are involved in the induction of apoptosis (Gorman et al., 1997). H_2O_2 can promote cytochrome *c* release from mitochondria upon activation of the intrinsic pathway of apoptosis, and

can also activate transcription factors that upregulate death proteins or inhibitors of survival proteins (Meyer et al., 1993). H_2O_2 can also upregulate Fas-FasL, leading to caspase activation. Also, nitric oxide (NO•) has been shown to inactivate antioxidant enzymes such as superoxide dismutases, GPXs, and catalase, as well as induce apoptosis by activating caspase-3 and the Fas system (Bosca and Hortelano, 1999; Dobashi et al., 1997).

1.4 THESIS AIMS

While apoptosis has been the most studied form of cell death for the past several decades, in the recent few years, there have been numerous studies describing non-apoptotic cell death programs, including ferroptosis and entosis. These new mechanisms may also contribute to organismal homeostasis and pathophysiology, yet their roles *in vivo* remain unclear. Similarly the molecular mechanisms that regulate these forms of cell death remain poorly understood. My thesis aims were to investigate two different cell death forms, ferroptosis and entosis, to examine how these death mechanisms are affected by conditions of metabolic stress. My studies have uncovered novel roles of amino acid signaling in controlling cell death, and have identified, for ferroptosis, a potential new therapeutic strategy.

1.5 REFERENCES

Albrecht, P., J. Lewerenz, S. Dittmer, R. Noack, P. Maher, and A. Methner. 2010. Mechanisms of oxidative glutamate toxicity: the glutamate/cystine antiporter system xc as a neuroprotective drug target. *CNS & Neurological Disorders-Drug Targets (Formerly Current Drug Targets-CNS & Neurological Disorders)*. 9:373-382.

Allen, M.D., P. Luong, C. Hudson, J. Leyton, B. Delage, E. Ghazaly, R. Cutts, M. Yuan, N. Syed, C. Lo Nigro, L. Lattanzio, M. Chmielewska-Kassassir, I. Tomlinson, R. Roylance, H.C. Whitaker, A.Y. Warren, D. Neal, C. Frezza, L. Beltran, L.J. Jones, C. Chelala, B.-W. Wu, J.S. Bomalaski, R.C. Jackson, Y.-J. Lu, T. Crook, N.R.

Lemoine, S. Mather, J. Foster, J. Sosabowski, N. Avril, C.-F. Li, and P.W. Szlosarek. 2014. Prognostic and Therapeutic Impact of Argininosuccinate Synthetase 1 Control in Bladder Cancer as Monitored Longitudinally by PET Imaging. *Cancer Research*. 74:896-907.

Andrabi, S.A., T.M. Dawson, and V.L. Dawson. 2008. Mitochondrial and Nuclear Cross Talk in Cell Death: Parthanatos. *Annals of the New York Academy of Sciences*. 1147:233-241.

Avramis, V.I., and E.H. Panosyan. 2012. Pharmacokinetic/Pharmacodynamic Relationships of Asparaginase Formulations. *Clinical Pharmacokinetics*. 44:367-393.

Baines, C.P., R.A. Kaiser, N.H. Purcell, N.S. Blair, H. Osinska, M.A. Hambleton, E.W. Brunskill, M.R. Sayen, R.A. Gottlieb, G.W. Dorn, J. Robbins, and J.D. Molkentin. 2005. Loss of cyclophilin D reveals a critical role for mitochondrial permeability transition in cell death. *Nature*. 434:658-662.

Baird, T.D., and R.C. Wek. 2012. Eukaryotic Initiation Factor 2 Phosphorylation and Translational Control in Metabolism. *Advances in Nutrition: An International Review Journal*. 3:307-321.

Benseler, V., A. Warren, M. Vo, L.E. Holz, S.S. Tay, D.G. Le Couteur, E. Breen, A.C. Allison, N. van Rooijen, C. McGuffog, H.J. Schlitt, D.G. Bowen, G.W. McCaughan, and P. Bertolino. 2011. Hepatocyte entry leads to degradation of autoreactive CD8 T cells. *Proceedings of the National Academy of Sciences*. 108:16735-16740.

Berry, D.L., and E.H. Baehrecke. 2007. Growth arrest and autophagy are required for salivary gland cell degradation in Drosophila. *Cell*. 131:1137-1148.

Bosca, L., and S. Hortelano. 1999. Mechanisms of Nitric Oxide-Dependent Apoptosis: Involvement of Mitochondrial Mediators. *Cellular Signalling*. 11:239-244.

Brown, G.C., and J.J. Neher. 2012. Eaten alive! Cell death by primary phagocytosis: 'phagoptosis'. *Trends in Biochemical Sciences*. 37:325-332.

Brunelle, J.K., E.H. Shroff, H. Perlman, A. Strasser, C.T. Moraes, R.A. Flavell, N.N. Danial, B. Keith, C.B. Thompson, and N.S. Chandel. 2007. Loss of Mcl-1 Protein and Inhibition of Electron Transport Chain Together Induce Anoxic Cell Death. *Molecular and Cellular Biology*. 27:1222-1235.

Cano, C.E., M.a.J. Sand√¯≠, T. Hamidi, E.L. Calvo, O. Turrini, L. Bartholin, C.l. Loncle, V.r. Secq, S.p. Garcia, G. Lomberk, G. Kroemer, R. Urrutia, and J.L. Iovanna. 2012. Homotypic cell cannibalism, a cell-death process regulated by the nuclear protein 1, opposes to metastasis in pancreatic cancer: Cell cannibalism and metastasis. *EMBO Molecular Medicine*. 4:964-979.

Changou, C.A., Y.-R. Chen, L. Xing, Y. Yen, F.Y.S. Chuang, R.H. Cheng, R.J. Bold, D.K. Ann, and H.-J. Kung. 2014. Arginine starvation-associated atypical cellular death involves mitochondrial dysfunction, nuclear DNA leakage, and chromatin autophagy. *Proceedings of the National Academy of Sciences of the United States of America*. 111:14147-14152.

Chen, L., and H. Cui. 2015. Targeting Glutamine Induces Apoptosis: A Cancer Therapy Approach. *International Journal of Molecular Sciences*. 16:22830-22855.

Chen, Y., M.B. Azad, and S.B. Gibson. 2009. Superoxide is the major reactive oxygen species regulating autophagy. *Cell Death Differ*. 16:1040-1052.

Cho, Y.S., D. Challa S Fau - Moquin, R. Moquin D Fau - Genga, T.D. Genga R Fau - Ray, M. Ray Td Fau - Guildford, F.K.-M. Guildford M Fau - Chan, and F.K. Chan. 2009. Phosphorylation-driven assembly of the RIP1-RIP3 complex regulates programmed necrosis and virus-induced inflammation. *Cell*. 137:1112-1123.

Degterev, A., J. Hitomi, M. Germscheid, I.L. Ch'en, O. Korkina, X. Teng, D. Abbott, G.D. Cuny, C. Yuan, G. Wagner, S.M. Hedrick, S.A. Gerber, A. Lugovskoy, and J. Yuan. 2008. Identification of RIP1 kinase as a specific cellular target of necrostatins. *Nature Chemical Biology*. 4:313-321.

Degterev, A., Z. Huang, M. Boyce, Y. Li, P. Jagtap, N. Mizushima, G.D. Cuny, T.J. Mitchison, M.A. Moskowitz, and J. Yuan. 2005. Chemical inhibitor of nonapoptotic cell death with therapeutic potential for ischemic brain injury. *Nature Chemical Biology*. 1:112-119.

Denton, D., B. Shravage, R. Simin, K. Mills, D.L. Berry, E.H. Baehrecke, and S. Kumar. 2009. Autophagy, not apoptosis, is essential for midgut cell death in Drosophila. *Current biology : CB*. 19:1741-1746.

Dixon, S.J., K.M. Lemberg, M.R. Lamprecht, R. Skouta, E.M. Zaitsev, C.E. Gleason, D.N. Patel, A.J. Bauer, A.M. Cantley, W.S. Yang, B. Morrison, and B.R. Stockwell. 2012. Ferroptosis: An Iron-Dependent Form of Nonapoptotic Cell Death. *Cell*. 149:1060-1072.

Dixon, S.J., D.N. Patel, M. Welsch, R. Skouta, E.D. Lee, M. Hayano, A.G. Thomas, C.E. Gleason, N.P. Tatonetti, B.S. Slusher, and others. 2014. Pharmacological inhibition of cystine-glutamate exchange induces endoplasmic reticulum stress and ferroptosis. *Elife*. 3:e02523.

Dobashi, K., K. Pahan, A. Chahal, and I. Singh. 1997. Modulation of Endogenous Antioxidant Enzymes by Nitric Oxide in Rat C6 Glial Cells. *Journal of Neurochemistry*. 68:1896-1903.

Eling, N., L. Reuter, J. Hazin, A. Hamacher-Brady, and N.R. Brady. 2015. Identification of artesunate as a specific activator of ferroptosis in pancreatic cancer cells. *Oncoscience*. 2:517-532.

Ellis, H.M., and H.R. Horvitz. 1986. Genetic control of programmed cell death in the nematode C. elegans. *Cell*. 44:817-829.

Fink, S.L., and B.T. Cookson. 2006. Caspase-1-dependent pore formation during pyroptosis leads to osmotic lysis of infected host macrophages. *Cellular Microbiology*. 8:1812-1825.

Florey, O., S.E. Kim, C.P. Sandoval, C.M. Haynes, and M. Overholtzer. 2011. Autophagy machinery mediates macroendocytic processing and entotic cell death by targeting single membranes. *Nature Cell Biology*. 13:1335-1343.

Fulda, S. 2015. Targeting extrinsic apoptosis in cancer: Challenges and opportunities. *Seminars in Cell & Developmental Biology*. 39:20-25.

Galluzzi, L., J.M. Bravo-San Pedro, I. Vitale, S.A. Aaronson, J.M. Abrams, D. Adam, E.S. Alnemri, L. Altucci, D. Andrews, M. Annicchiarico-Petruzzelli, E.H. Baehrecke, N.G. Bazan, M.J. Bertrand, K. Bianchi, M.V. Blagosklonny, K. Blomgren, C. Borner, D.E. Bredesen, C. Brenner, M. Campanella, E. Candi, F. Cecconi, F.K. Chan, N.S. Chandel, E.H. Cheng, J.E. Chipuk, J.A. Cidlowski, A. Ciechanover, T.M. Dawson, V.L. Dawson, V. De Laurenzi, R. De Maria, K.M. Debatin, N. Di Daniele, V.M. Dixit, B.D. Dynlacht, W.S. El-Deiry, G.M. Fimia, R.A. Flavell, S. Fulda, C. Garrido, M.L. Gougeon, D.R. Green, H. Gronemeyer, G. Hajnoczky, J.M. Hardwick, M.O. Hengartner, H. Ichijo, B. Joseph, P.J. Jost, T. Kaufmann, O. Kepp, D.J. Klionsky, R.A. Knight, S. Kumar, J.J. Lemasters, B. Levine, A. Linkermann, S.A. Lipton, R.A. Lockshin, C. Lopez-Otin, E. Lugli, F. Madeo, W. Malorni, J.C. Marine, S.J. Martin, J.C. Martinou, J.P. Medema, P. Meier, S. Melino, N. Mizushima, U. Moll, C. Munoz-Pinedo, G. Nunez, A. Oberst, T. Panaretakis, J.M. Penninger, M.E. Peter, M. Piacentini, P. Pinton, J.H. Prehn, H. Puthalakath, G.A. Rabinovich, K.S. Ravichandran, R. Rizzuto, C.M. Rodrigues, D.C. Rubinsztein, T. Rudel, Y. Shi, H.U. Simon, B.R. Stockwell, G. Szabadkai, S.W. Tait, H.L. Tang, N. Tavernarakis, Y. Tsujimoto, T. Vanden Berghe, P. Vandenabeele, A. Villunger, E.F. Wagner, et al. 2015. Essential versus accessory aspects of cell death: recommendations of the NCCD 2015. *Cell Death Differ*. 22:58-73.

Galluzzi, L., O. Kepp, M.G.V. Heiden, and G. Kroemer. 2013. Metabolic targets for cancer therapy. *Nat Rev Drug Discov*. 12:829-846.

Gorman, A., A. McGowan, and T.G. Cotter. 1997. Role of peroxide and superoxide anion during tumour cell apoptosis. *FEBS Letters*. 404:27-33.

Graeber, T.G., C. Osmanian, T. Jacks, D.E. Housman, C.J. Koch, S.W. Lowe, and A.J. Giaccia. 1996. Hypoxia-mediated selection of cells with diminished apoptotic potential in solid tumours. *Nature*. 379:88-91.

Green, D.R., L. Galluzzi, and G. Kroemer. 2014. Metabolic control of cell death. *Science*. 345:1250256.

Hakem, R., A. Hakem, G.S. Duncan, J.T. Henderson, M. Woo, M.S. Soengas, A. Elia, J.L. de la Pompa, D. Kagi, W. Khoo, J. Potter, R. Yoshida, S.A. Kaufman, S.W. Lowe, J.M. Penninger, and T.W. Mak. 1998. Differential Requirement for Caspase 9 in Apoptotic Pathways In Vivo. *Cell*. 94:339-352.

Hanahan, D., and R.A. Weinberg. 2011. Hallmarks of Cancer: The Next Generation. *Cell*. 144:646-674.

Harding, H.P., I. Novoa, Y. Zhang, H. Zeng, R. Wek, M. Schapira, and D. Ron. 2000. Regulated Translation Initiation Controls Stress-Induced Gene Expression in Mammalian Cells. *Molecular Cell*. 6:1099-1108.

Hu, W., C. Zhang, R. Wu, Y. Sun, A. Levine, and Z. Feng. 2010. Glutaminase 2, a novel p53 target gene regulating energy metabolism and antioxidant function. *Proceedings of the National Academy of Sciences of the United States of America*. 107:7455-7460.

Ko, Y.-G., E.-K. Kim, T. Kim, H. Park, H.-S. Park, E.-J. Choi, and S. Kim. 2001. Glutamine-dependent Antiapoptotic Interaction of Human Glutaminyl-tRNA Synthetase with Apoptosis Signal-regulating Kinase 1. *Journal of Biological Chemistry*. 276:6030-6036.

Kobayashi, E., M. Masuda, R. Nakayama, H. Ichikawa, R. Satow, M. Shitashige, K. Honda, U. Yamaguchi, A. Shoji, N. Tochigi, H. Morioka, Y. Toyama, S. Hirohashi, A. Kawai, and T. Yamada. 2010. Reduced Argininosuccinate Synthetase Is a Predictive Biomarker for the Development of Pulmonary Metastasis in Patients with Osteosarcoma. *Mol Cancer Ther*. 9:535-544.

Korsmeyer, S.J. 1992. Bcl-2: an antidote to programmed cell death. *Cancer surveys*. 15:105-118.

Krajcovic, M., N.B. Johnson, Q. Sun, G. Normand, N. Hoover, E. Yao, A.L. Richardson, R.W. King, E.S. Cibas, S.J. Schnitt, J.S. Brugge, and M. Overholtzer. 2011. A non-genetic route to aneuploidy in human cancers. *Nature Cell Biology*. 13:324-330.

Krajcovic, M., S. Krishna, L. Akkari, J.A. Joyce, and M. Overholtzer. 2013. mTOR regulates phagosome and entotic vacuole fission. *Mol. Biol. Cell*. 24:3736-3745.

Kuida, K., T.S. Zheng, S. Na, C.-Y. Kuan, D. Yang, H. Karasuyama, P. Rakic, and R.A. Flavell. 1996. Decreased apoptosis in the brain and premature lethality in CPP32-deficient mice. *Nature*. 384:368-372.

Lee, C.-Y., B.A.K. Cooksey, and E.H. Baehrecke. 2002. Steroid Regulation of Midgut Cell Death during Drosophila Development. *Developmental Biology*. 250:101-111.

Li, J., A. Csibi, S. Yang, G.R. Hoffman, C. Li, E. Zhang, J.J. Yu, and J. Blenis. 2015. Synthetic lethality of combined glutaminase and Hsp90 inhibition in mTORC1-driven tumor cells. *Proceedings of the National Academy of Sciences of the United States of America*. 112:E21-E29.

Lindsten, T., A.J. Ross, A. King, W.-X. Zong, J.C. Rathmell, H.A. Shiels, E. Ulrich, K.G. Waymire, P. Mahar, K. Frauwirth, Y. Chen, M. Wei, V.M. Eng, D.M. Adelman, M.C. Simon, A. Ma, J.A. Golden, G. Evan, S.J. Korsmeyer, G.R. MacGregor, and C.B. Thompson. 2000. The Combined Functions of Proapoptotic Bcl-2 Family Members Bak and Bax Are Essential for Normal Development of Multiple Tissues. *Molecular Cell*. 6:1389-1399.

Liu, Q., J. Qiu, M. Liang, J. Golinski, K. van Leyen, J.E. Jung, Z. You, E.H. Lo, A. Degterev, and M.J. Whalen. 2014. Akt and mTOR mediate programmed necrosis in neurons. *Cell Death Dis*. 5:e1084.

Liu, Y., S. Shoji-Kawata, R.M. Sumpter, Y. Wei, V. Ginet, L. Zhang, B. Posner, K.A. Tran, D.R. Green, R.J. Xavier, S.Y. Shaw, P.G.H. Clarke, J. Puyal, and B. Levine. 2013. Autosis is a Na(+),K(+)-ATPase,Äìregulated form of cell death triggered by autophagy-inducing peptides, starvation, and hypoxia,Äìischemia. *Proceedings of the National Academy of Sciences of the United States of America*. 110:20364-20371.

Locasale, J.W., A.R. Grassian, T. Melman, C.A. Lyssiotis, K.R. Mattaini, A.J. Bass, G. Heffron, C.M. Metallo, T. Muranen, H. Sharfi, A.T. Sasaki, D. Anastasiou, E. Mullarky, N.I. Vokes, M. Sasaki, R. Beroukhim, G. Stephanopoulos, A.H. Ligon, M. Meyerson, A.L. Richardson, L. Chin, G. Wagner, J.M. Asara, J.S. Brugge, L.C. Cantley, and M.G. Vander Heiden. 2011. Phosphoglycerate dehydrogenase diverts glycolytic flux and contributes to oncogenesis. *Nature genetics*. 43:869-874.

Lockshin, R.A., and C.M. Williams. 1965. Programmed cell death,ÄîI. Cytology of degeneration in the intersegmental muscles of the Pernyi silkmoth. *Journal of Insect Physiology*. 11:123-133.

Louandre, C., I. Marcq, H. Bouhlal, E. Lachaier, C. Godin, Z. Saidak, C. Fran√ßois, D. Chatelain, V.r. Debuysscher, J.-C. Barbare, B. Chauffert, and A. Galmiche. 2015. The retinoblastoma (Rb) protein regulates ferroptosis induced by sorafenib in human hepatocellular carcinoma cells. *Cancer Letters*. 356:971-977.

Maddocks, O.D.K., C.R. Berkers, S.M. Mason, L. Zheng, K. Blyth, E. Gottlieb, and K.H. Vousden. 2013. Serine starvation induces stress and p53-dependent metabolic remodelling in cancer cells. *Nature*. 493:542-546.

McDonnell, T.J., N. Deane, F.M. Platt, G. Nunez, U. Jaeger, J.P. McKearn, and S.J. Korsmeyer. 1989. bcl-2-immunoglobulin transgenic mice demonstrate extended B cell survival and follicular lymphoproliferation. *Cell*. 57:79-88.

Meyer, M., R. Schreck, and P.A. Baeuerle. 1993. H2O2 and antioxidants have opposite effects on activation of NF-kappa B and AP-1 in intact cells: AP-1 as secondary antioxidant-responsive factor. *The EMBO Journal*. 12:2005-2015.

Meynet, O.l., B. Zunino, L. Happo, L.A. Pradelli, J. Chiche, M.A. Jacquin, L. Mondrag√≥n, J.-F.o. Tanti, B. Taillan, G. Garnier, J. Reverso-Meinietti, N. Mounier, J.-F.o. Michiels, E.M. Michalak, M. Carles, C.L. Scott, and J.-E. Ricci. 2013. Caloric restriction modulates Mcl-1 expression and sensitizes lymphomas to BH3 mimetic in mice. *Blood*. 122:2402-2411.

Munoz-Pinedo, C., C. Ruiz-Ruiz, C. Ruiz de Almodovar, C. Palacios, and A. Lopez-Rivas. 2003. Inhibition of Glucose Metabolism Sensitizes Tumor Cells to Death Receptor-triggered Apoptosis through Enhancement of Death-inducing Signaling Complex Formation and Apical Procaspase-8 Processing. *Journal of Biological Chemistry*. 278:12759-12768.

Newton, K., X. Sun, and V.M. Dixit. 2004. Kinase RIP3 Is Dispensable for Normal NF- κ Bs, Signaling by the B-Cell and T-Cell Receptors, Tumor Necrosis Factor Receptor 1, and Toll-Like Receptors 2 and 4. *Molecular and Cellular Biology*. 24:1464-1469.

Nikiforov, M.A., S. Chandriani, B. O'Connell, O. Petrenko, I. Kotenko, A. Beavis, J.M. Sedivy, and M.D. Cole. 2002. A Functional Screen for Myc-Responsive Genes Reveals Serine Hydroxymethyltransferase, a Major Source of the One-Carbon Unit for Cell Metabolism. *Molecular and Cellular Biology*. 22:5793-5800.

Overholtzer, M., A.A. Mailleux, G. Mouneimne, G. Normand, S.J. Schnitt, R.W. King, E.S. Cibas, and J.S. Brugge. 2007. A Nonapoptotic Cell Death Process, Entosis, that Occurs by Cell-in-Cell Invasion. *Cell*. 131:966-979.

Panosyan, E.H., Y. Wang, P. Xia, W.-N.P. Lee, Y. Pak, D.R. Laks, H.J. Lin, T.B. Moore, T.F. Cloughesy, H.I. Kornblum, and J.L. Lasky. 2014. Asparagine Depletion Potentiates the Cytotoxic Effect of Chemotherapy Against Brain Tumors. *Molecular cancer research : MCR*. 12:694-702.

Possemato, R., K.M. Marks, Y.D. Shaul, M.E. Pacold, D. Kim, K. Birsoy, S. Sethumadhavan, H.-K. Woo, H.G. Jang, A.K. Jha, W.W. Chen, F.G. Barrett, N. Stransky, Z.-Y. Tsun, G.S. Cowley, J. Barretina, N.Y. Kalaany, P.P. Hsu, K. Ottina,

A.M. Chan, B. Yuan, L.A. Garraway, D.E. Root, M. Mino-Kenudson, E.F. Brachtel, E.M. Driggers, and D.M. Sabatini. 2011. Functional genomics reveals serine synthesis is essential in PHGDH-amplified breast cancer. *Nature*. 476:346-350.

Qing, G., B. Li, A. Vu, N. Skuli, Z.E. Walton, X. Liu, P.A. Mayes, D.R. Wise, C.B. Thompson, J.M. Maris, M.D. Hogarty, and M.C. Simon. 2013. ATF4 Regulates MYC-Mediated Neuroblastoma Cell Death upon Glutamine Deprivation. *Cancer Cell*. 22:631-644.

Rathmell, J.C., T. Lindsten, W.-X. Zong, R.M. Cinalli, and C.B. Thompson. 2002. Deficiency in Bak and Bax perturbs thymic selection and lymphoid homeostasis. *Nat Immunol*. 3:932-939.

Reid, M.A., W.-I. Wang, K.R. Rosales, M.X. Welliver, M. Pan, and M. Kong. 2013. The B55a Subunit of PP2A Drives a p53-Dependent Metabolic Adaptation to Glutamine Deprivation. *Molecular Cell*. 50:200-211.

Remijsen, Q., T.W. Kuijpers, E. Wirawan, S. Lippens, P. Vandenabeele, and T. Vanden Berghe. 2011. Dying for a cause: NETosis, mechanisms behind an antimicrobial cell death modality. *Cell Death and Differentiation*. 18:581-588.

Saikumar, P., Y. Dong Z Fau - Patel, K. Patel Y Fau - Hall, U. Hall K Fau - Hopfer, J.M. Hopfer U Fau - Weinberg, M.A. Weinberg Jm Fau - Venkatachalam, and M.A. Venkatachalam. 1998. Role of hypoxia-induced Bax translocation and cytochrome c release in reoxygenation injury. *Oncogene*. 17:3401-3415.

Schweichel, J., Merker, HJ. 1973. The morphology of various types of cell death in prenatal tissues. *Tertology*. 7:253-266.

Scott, R.C., G. Juhasz, and T.P. Neufeld. 2007. Direct Induction of Autophagy by Atg1 Inhibits Cell Growth and Induces Apoptotic Cell Death. *Current Biology*. 17:1-11.

Simpson, N.E., V.P. Tryndyak, M. Pogribna, F.A. Beland, and I.P. Pogribny. 2012. Modifying metabolically sensitive histone marks by inhibiting glutamine metabolism affects gene expression and alters cancer cell phenotype. *Epigenetics*. 7:1413-1420.

Sun, L., H. Wang, Z. Wang, S. He, S. Chen, D. Liao, L. Wang, J. Yan, W. Liu, X. Lei, and X. Wang. 2012. Mixed Lineage Kinase Domain-like Protein Mediates Necrosis Signaling Downstream of RIP3 Kinase. *Cell*. 148:213-227.

Sun, Q., E.S. Cibas, H. Huang, L. Hodgson, and M. Overholtzer. 2014. Induction of entosis by epithelial cadherin expression. *Cell Res*. 24:1288-1298.

Szlosarek, P.W., A. Klabatsa, A. Pallaska, M. Sheaff, P. Smith, T. Crook, M.J. Grimshaw, J.P. Steele, R.M. Rudd, F.R. Balkwill, and D.A. Fennell. 2006. In vivo Loss of Expression of Argininosuccinate Synthetase in Malignant Pleural

Mesothelioma Is a Biomarker for Susceptibility to Arginine Depletion. *Clinical Cancer Research*. 12:7126-7131.

Tan, S., D. Schubert, and P. Maher. 2001. Oxytosis: a novel form of programmed cell death. *Current topics in medicinal chemistry*. 1:497-506.

Trachootham, D., W. Lu, M.A. Ogasawara, N.R.-D. Valle, and P. Huang. 2008. Redox Regulation of Cell Survival. *Antioxidants & Redox Signaling*. 10:1343-1374.

Vogt, C. 1842. Untersuchungen ü ber die Entwicklungsgeschichte der Geburtshelferkröte (Alytes obstetricans). (Solothurn: Jent und Gassmann,1842).

Vonderheide, R.H. 2015. CD47 blockade as another immune checkpoint therapy for cancer. *Nat Med*. 21:1122-1123.

Wang, S., M.f. He, Y.h. Chen, M.y. Wang, X.m. Yu, J. Bai, H.y. Zhu, Y.y. Wang, H. Zhao, Q. Mei, J. Nie, J. Ma, J.f. Wang, Q. Wen, L. Ma, Y. Wang, and X.n. Wang. 2013. Rapid reuptake of granzyme B leads to emperitosis: an apoptotic cell-in-cell death of immune killer cells inside tumor cells. *Cell Death Dis*. 4:e856.

Wong, R.S. 2011. Apoptosis in cancer: from pathogenesis to treatment. *Journal of Experimental & Clinical Cancer Research*. 30.

Wu, J., J. Huang Z Fau - Ren, Z. Ren J Fau - Zhang, P. Zhang Z Fau - He, Y. He P Fau - Li, J. Li Y Fau - Ma, W. Ma J Fau - Chen, Y. Chen W Fau - Zhang, X. Zhang Y Fau - Zhou, Z. Zhou X Fau - Yang, S.-Q. Yang Z Fau - Wu, L. Wu Sq Fau - Chen, J. Chen L Fau - Han, and J. Han. 2013. Mlkl knockout mice demonstrate the indispensable role of Mlkl in necroptosis. *Cell Res*. 23:994-1006.

Xiong, S., T. Mu, G. Wang, and X. Jiang. 2014. Mitochondria-mediated apoptosis in mammals. *Protein & Cell*. 5:737-749.

Yang, W.S., R. SriRamaratnam, M.E. Welsch, K. Shimada, R. Skouta, V.S. Viswanathan, J.H. Cheah, P.A. Clemons, A.F. Shamji, C.B. Clish, L.M. Brown, A.W. Girotti, V.W. Cornish, S.L. Schreiber, and B.R. Stockwell. 2014. Regulation of Ferroptotic Cancer Cell Death by GPX4. *Cell*. 156:317-331.

Ye, J., M. Kumanova, L.S. Hart, K. Sloane, H. Zhang, D.N. De Panis, E. Bobrovnikova,ÄêMarjon, J.A. Diehl, D. Ron, and C. Koumenis. 2010. The GCN2-ATF4 pathway is critical for tumour cell survival and proliferation in response to nutrient deprivation. *The EMBO Journal*. 29:2082-2096.

Ye, J., W. Palm, M. Peng, B. King, T. Lindsten, M.O. Li, C. Koumenis, and C.B. Thompson. 2015. GCN2 sustains mTORC1 suppression upon amino acid deprivation by inducing Sestrin2. *Genes & Development*. 29:2331-2336.

Zhang, J., J. Fan, S. Venneti, J.R. Cross, T. Takagi, B. Bhinder, H. Djaballah, M. Kanai, E.H. Cheng, A.R. Judkins, B. Pawel, J. Baggs, S. Cherry, J.D. Rabinowitz, and C.B. Thompson. 2014. Asparagine Plays a Critical Role in Regulating Cellular Adaptation to Glutamine Depletion. *Molecular Cell*. 56:205-218.

Zhang, W.C., N. Shyh-Chang, H. Yang, A. Rai, S. Umashankar, S. Ma, B.S. Soh, L.L. Sun, B.C. Tai, M.E. Nga, K.K. Bhakoo, S.R. Jayapal, M. Nichane, Q. Yu, D.A. Ahmed, C. Tan, W.P. Sing, J. Tam, A. Thirugananam, M.S. Noghabi, Y. Huei¬†Pang, H.S. Ang, W. Mitchell, P. Robson, P. Kaldis, R.A. Soo, S. Swarup, E.H. Lim, and B. Lim. 2012. Glycine Decarboxylase Activity Drives Non-Small Cell Lung Cancer Tumor-Initiating Cells and Tumorigenesis. *Cell*. 148:259-272.

CHAPTER 2: Ultrasmall nanoparticle treatment induces ferroptosis of amino acid-deprived cells

2.1. INTRODUCTION

As discussed in chapter one, ferroptosis is a recently identified non-apoptotic cell death mechanism that is induced by oxidative stress. Ferroptosis is triggered by inhibition of the system X_C-Cys/Glu antiporter, or following direct inhibition of glutathione (GSH) peroxidase 4 (GPX4), leading to a decreased capacity to resist oxidative stress. Ferroptosis has been implicated in several pathological processes, such as neurodegeneration, acute renal failure, ischemia/reperfusion injury, immunity, and cancer (Xie et al., 2016). In cancer, ferroptosis has been shown to contribute to p53-mediated tumor suppression activity (Jiang et al., 2015), due to p53-mediated repression of the expression of the system X_C-Cys/Glu antiporter gene SLC7A11. Ferroptosis may also be induced in cancers as a result of deprivation for amino acids due to poor vascularization, resulting in depletion of GSH. Deprivation of cystine, or amino acids in general, has been shown to induce ferroptosis in some contexts in cultured cells (Gao et al., 2015; Hayano et al., 2015). Whether potential ferroptosis-inducing agents could synergize with amino acid deprivation to induce cancer cell death *in vivo* is an important open question.

An approach that is receiving increasing attention for the therapeutic targeting of cancer is treatment with various nano-sized materials that can be targeted to tumor sites. Cancer-targeted nanoparticles can be used to deliver therapeutic compounds, and can be modified with fluorescent or radioactive tracers to be used as imaging agents to detect cancer lesions (Davis et al., 2008; Duncan and Gaspar, 2011; Duncan and

Richardson, 2012; Phillips et al., 2014). While nanoparticle-based targeting of cancer is receiving increasing attention, there remains relatively little understood about how particles of different chemistries, as well as sizes and shapes, might be best designed to achieve proper targeting and therapeutic efficacy (Chen et al., 2014; Li et al., 2009; Li et al., 2010; Ma et al., 2011; Stern et al., 2012). Here we investigated the effects of the delivery of ultrasmall (~6 nm diameter) poly(ethylene glycol) (PEG)-coated silica nanoparticles, functionalized with melanoma-targeting peptides, into cells and tumors *in vivo*. These particles, called Cornell dots or C' dots, are currently in clinical trials for use as imaging agents for the detection of cancer. We examined the effects of particle loading on cell viability under conditions of increasing dosage and nutrient deprivation. Remarkably, we discovered that C' dot nanoparticle treatment induces ferroptosis when cells are also starved for amino acids. Moreover, intravenous particle delivery to tumor-bearing mice leads to tumor regression in a ferroptosis-dependent manner. These data identify ultrasmall silica nanoparticles, utilized under nutrient-deprived conditions, as novel inducers of ferroptosis.

2.2 MATERIALS AND METHODS

2.2.1 Cell culture and constructs

MEF and HT1080 cells (American Type Culture Collection (ATCC)) were cultured in Dulbecco's modified Eagle's medium (DMEM) (MSKCC Media Preparation Facility) supplemented with 10% fetal bovine serum (FBS, Sigma, St. Louis, MO) with penicillin/streptomycin (Corning, Corning, NY). MCF10A cells (ATCC) were cultured in DMEM/F12 (Gibco, Grand Island, NY) supplemented with 5% horse serum (Atlanta Biologicals, Flowery Branch, GA), 20 ng/ml EGF (Peprotech, Rocky Hill, NJ), 10 μg/ml insulin (Sigma), 0.5 μg/ml hydrocortisone (Sigma), and 100 ng/ml

cholera toxin (Sigma) with penicillin/streptomycin. M21, BxPC3 (ATCC), and H1650 cells were cultured in RPMI-1640 (Gibco) supplemented with 10% FBS with penicillin/streptomycin. Cells were routinely verified as mycoplasma-free by DAPI imaging. Amino acid-free medium was prepared by dialyzing heat-inactivated FBS (for MEF, HT1080, M21, BxPC3, and H1650 cells) or horse serum (for MCF10A cells) for 4 h, followed by overnight incubation at 4°C in phosphate-buffered saline (PBS) in MWCO 3500 dialysis tubing (21-152-9; Fisherbrand, Pittsburgh, PA) and addition to base media prepared without amino acids. pRetro–Lamp1–GFP was introduced into M21 cells by retroviral transduction, and stable cell lines were selected with puromycin (2 μg/ml).

2.2.2 Reagents

The following reagents were used at the indicated concentrations: Concanamycin A (ConA) (Sigma) 100 nM; SYTOX Green Nucleic Acid Stain (S7020; Invitrogen, Carlsbad, CA) 5 nM; Ferrostatin-1 (Fer-1) (EMD Millipore, Billerica, MA) 1 μM; Deferoxamine (DFO) (Sigma) 100 μM; Butylated hydroxyanisole (BHA) (Sigma) 50 μM; Ascorbic acid (AA) (Sigma) 200 μM; Trolox (Sigma) 100 μM; N-acetylcysteine (NAC) (Sigma) 10 mM; Glutathione (GSH) (Sigma) 5 mM; TNFα (Sigma) 100 ng/ml; Cycloheximide (CHX) (Sigma) 1 μg/ml and 50 μg/ml to induce necroptosis and apoptosis, respectively; zVAD (Sigma) 20 μM; Necrostatin-1 (Sigma) 30 μM; Buthionine sulphoximine (BSO) (Sigma) 400 μM. Reagents were added to cultures at the start of biological assays with the exception of ConA which was added 1 hour prior to lysis for western blotting.

2.2.3 Peptide synthesis

A modified melanocortin-1 receptor targeting peptide Re(Arg11)CCMSH (Miao et al., 2007) with a double aminohexanoic acid (Ahx_2) aliphatic linker and N-Ac-Cys was synthesized using standard solid phase Fmoc peptide chemistry. The rhenium-cyclized αMSH peptide analog, Ac-Cys^1-$(Ahx)_2$-dLys2-Re[Cys-Cys-Glu-His-dPhe-Arg-Trp-Cys]-Arg-Pro-Val-NH_2, was analyzed and purified on a Beckman Coulter High Performance Liquid Chromatography (HPLC) system coupled with an LCQ FLEET Ion Trap Mass spectrometer (Thermo Fisher Scientific) and finally recovered by lyophilization.

2.2.4 Synthesis and characterization of αMSH-PEG-C' dots

Fluorescent silica nanoparticles (C' dots), encapsulating the organic dye, Cy5, were synthesized in water as previously described (Ma et al., 2015). αMSH peptides were conjugated to maleimido-terminated heterobifunctional polyethylene glycol silane (mal-PEG-silane) via its N-terminal acetylated cysteine thiol to form αMSH-PEG-silane. Conjugates were attached to the particle surface in the PEGylation step to generate αMSH functionalized C' dots, or αMSH-PEG-C' dots. Synthesized particle samples were dialyzed in water and purified by gel permeation chromatography (GPC, Bio-Rad Laboratories, Inc, Hercules, California) prior to further characterization. Absorption and emission spectral profiles for the encapsulated and native Cy5 dye were obtained using a Varian Cary 5000 spectrophotometer (Varian, Palo Alto, CA) and a fluorescence spectrofluorometer (Photon Technology International, Inc, Birmington, NJ). Hydrodynamic radius, brightness, and concentration of αMSH-PEG-C' dots, as against free Cy5 dye, were determined using a homebuilt fluorescence correlation spectroscopy (FCS) set up configured with a solid-state 633-nm excitation (Sadasivan et al., 1998).

2.2.5 Western blotting

Cells were scraped into ice-cold RIPA buffer (50 mM Tris at pH 7.4, 150 mM NaCl, 2 mM EDTA, 1% NP40, 0.1% SDS with protease inhibitor cocktail) and lysed for 10 min on ice. Lysates were then centrifuged at 15,870g for 20 min at 4 °C and protein was quantified by BCA assay (Pierce, Waltham, MA). Samples were separated on 15% polyacrylamide SDS–PAGE gels and transferred to a polyvinyldifluoride membrane which was blocked with TBST plus 5% BSA and incubated overnight at 4 °C with primary antibodies (anti-LC3A/B (4108; Cell Signaling, Danvers, MA) and anti-Actin (A1978; Sigma)), diluted in blocking buffer. Blots were incubated with horseradish peroxidase conjugated to secondary antibodies and protein was detected using enhanced chemiluminescence detection (Invitrogen). Densitometry analysis was carried out using ImageJ software (NIH).

2.2.6 Time-lapse microscopy

Cells were plated onto glass-bottom dishes (MatTek, Ashland, MA) overnight and fluorescence and differential interference contrast (DIC) images were acquired every 30 min for indicated times using a Nikon TI-E inverted microscope, a CoolSNAP HQ^2 CCD (charge-coupled device) camera (Photometrics, Tucson, AZ), a live-cell incubation chamber to maintain cells at 37 °C and 5% CO_2, and NIS Elements software (Nikon, Melville, NY). Cell fates, including cell survival, death, and proliferation, were manually quantified and processed using NIS Elements software and Image J.

2.2.7 Analysis of reactive oxygen species

Cells were treated with or without 15 μM α-MSH-PEG-C' dots for 24 hours, then harvested and resuspended in 500 μL Hanks Balanced Salt Solution (HBSS) (Gibco)

supplemented with either H_2DCFDA (25 μM) or C11-BODIPY(581/591) (2 μM) (both from Invitrogen) and incubated for 15 minutes at 37°C. Cells were then resuspended in 500 μL of fresh HBSS and analyzed using the FL1 channel of a flow cytometer (MoFlo, Beckman Coulter). Data were collected from a minimum of 10,000 cells per condition.

2.2.8 Animal models and tumor inoculation

All animal experiments were performed in accordance with protocols approved by the Institutional Animal Care and Use Committee of Memorial Sloan-Kettering Cancer Center and followed NIH guidelines for animal welfare. Human melanoma (M21) xenografts were generated on the shaved flanks of immunodeficient male SCID/Beige C.B-17/IcrHsd-*Prkdc*^{scid}*Lyst*$^{bg\text{-}J}$ mice (6-8 weeks old, Harlan Laboratories, South Easton, MA). Human sarcoma HT1080 flank xenografts (~2.0×10^6 cells/100 ml) were additionally generated in the same model. Average initial tumor volumes of 55 - 75 mm^3 were used for all studies.

2.2.9 In vivo dosing strategy and examination

Five million M21 cells, cultured in serum-supplemented media, were subcutaneously implanted into the right flank of mice using a 23-gauge trocar needle to establish melanoma xenografts 2 days after particle exposure (n=3) or without exposure (n=3). In a subsequent study, mice were assigned to one of two different treatment groups to evaluate the response of HT-1080 tumors to high-concentrations (60 μM) of i.v.-injected αMSH-PEG-C' dots (n=5 mice; 200 μl) administered three times over a 10-day period (i.e., days 0, 4, 7). Control mice (n=3) were administered 0.9% saline vehicle at the same time points. In a third treatment study, mice were again assigned to one of two groups to evaluate the response of HT-1080 tumors to three, high-

concentration doses (60 μM) of i.v.-injected αMSH-PEG-C' dots (n=3 mice; 200 μl) alone or with i.p.-administered liproxstatin-1 (n=3 mice, 10 mg/kg) over a 10-day period (as above). Tumor sizes were measured using calipers over the treatment interval. All mice were examined by palpation at the site of tumor cell inoculation, and were observed daily over until the termination of tumor growth studies for signs of morbidity or mortality. Two perpendicular diameters ($d_1 \leq d_2$) of the tumor used to calculate the tumor volume (V; $4/3 \cdot \pi \cdot d_1^2 \cdot d_2/8$) were measured with calipers daily following the injection of cells.

2.2.10 In vivo fluorescence imaging

Animals were anesthetized using isoflurane and whole body optical fluorescence imaging was acquired to identify nanoparticle fluorescence at the tumor site. Mice were scanned for 0.1 to 1 seconds using the IVIS Spectrum photon-counting device optical imaging system (Xenogen, Alameda, CA) with the blocks and filters for Cy5 fluorescence (excitation 650 nm, emission 680 nm), and for background fluorescence (excitation 465 nm, emission 600 nm), selected according to the manufacturer's recommendations. Fluorescence background was likewise subtracted according to the manufacturers' instructions. Fluorescence signal was reported as radiant efficiency ((photons/s/cm^2/sr) / mW/cm^2).

2.2.11 Histological analysis

Immediately after terminating the *in vivo* imaging study, mice were euthanized by CO_2 inhalation, and representative particle-exposed (n=2) and control (n=1) tumors were excised at necropsy. Excised tumors were fixed in 10% neutral buffered formalin for 24 hours, processed in alcohol and xylene, embedded in paraffin, sectioned at 5-micron thickness, and stained with hematoxylin and eosin (H&E). Additional sections

were stained by immunohistochemistry for Mac-2 (primary antibody Cedarlane CL8942B applied at concentration of 1:100 following heat-induced epitope retrieval [HIER] in a pH 6.0 buffer), myeloperoxidase (Dako A0398, 1:1000, HIER pH 6.0), cleaved caspase-3 (Cell Signaling Technology 9661, 1:250, HIER pH6.0), and Ki-67 (Abcam ab16667, 1:100, HIER pH 9.0). Mac-2 staining was performed manually with an avidin-biotin detection system (Vectastain ABC Elite Kit, Vector Laboratories, PK-6100). Other stains were performed on a Leica Bond RX automated stainer using the Bond Polymer Refine detection kit (Leica Biosystem DS9800). Sections were also stained by the TUNEL method as previously described. All slides were examined by a board-certified veterinary pathologist.

2.2.12 Statistics

Volume-time profiles were compared between the two treatment groups using robust standard errors calculated by a generalized estimating equations approach (Zeger et al., 1988). Tumor growth profiles over time for particle treatment, with and without inhibitor, were compared using a linear model. The longitudinal aspect of the data was taken into account by using generalized estimating equations. We assigned statistical significance at $P < 0.05$.

2.3 RESULTS

2.3.1 αMSH-PEG-C' dot particles localize to the lysosome network

To examine the effects of nanoparticle ingestion on cells, we utilized ~6 nm surface-functionalized poly(ethylene glycol)-coated (PEGylated) near-infrared (NIR) fluorescent silica nanoparticles, referred to as Cornell dots (C' dots), with diameters controllable down to the sub-10 nm range, reported in detail elsewhere (Ma et al.,

2015). This FDA-IND approved hybrid organo-silica particle was previously shown to be a promising cancer molecular imaging agent in metastatic melanoma patients after functionalizing its surface with a_vb_3 integrin-targeting peptides and radiolabels (Bradbury et al., 2013; Phillips et al., 2014). Preferential accumulation was observed within integrin-expressing primary and/or metastatic melanomatous lesions in human subjects and animal melanoma models (Benezra et al., 2011; Bradbury et al., 2013), while, at the same time, demonstrating rapid renal clearance.

Given its potential clinical utility and its early adaptation for drug delivery applications (Yoo et al., 2015), we performed detailed baseline studies using the latest generation of C dots, referred to as C' dots (Ma et al., 2015), that are surface-functionalized with a 14-mer peptide analog, alpha-melanocyte stimulating hormone (αMSH) (Miao et al., 2007), which targets a different surface receptor expressed on malignant melanoma cells (i.e., melanocortin-1 receptor, MC1-R). The resulting αMSH-PEG-C' dots (Fig. 2.1a) were used herein to determine the effects of dose- and/or time-dependent alterations in cellular survival, under particle-exposed, and also nutrient-deprived conditions, in cells and tumors *in vivo*. Live imaging of human melanoma cells (M21) treated with particles for 24 hours revealed colocalization of fluorescent αMSH-PEG-C' dots with lysosomes, visualized by expression of a GFP-tagged lysosomal-associated membrane protein 1 (LAMP1), indicating that ingested particles reside in lysosomal or late endosomal networks (Fig. 2.1b).

2.3.2 αMSH-PEG-C' dot particles induce cell death in amino acid-deprived conditions

M21 cells treated with increasing concentrations of αMSH-PEG-C' dots up to 15 μM showed similar survival and proliferation rates to control cells (Fig. 2.2a),

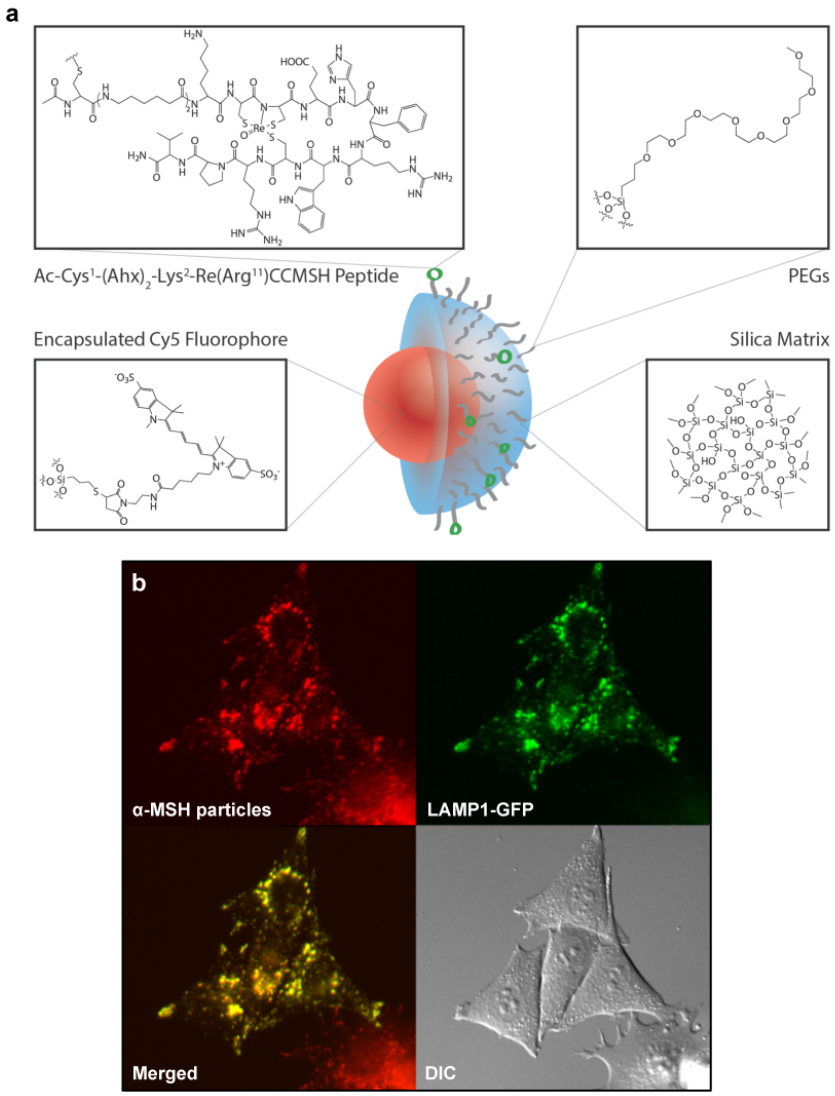

Figure 2.1 αMSH-PEG-C' dot particles and their localization to lysosomal networks. a, αMSH-PEG-C' dots are ultrasmall, 6 nm diameter silica-based particles with a fluorescent (Cy5 encapsulated) core and polyethylene glycol (PEG) and alpha melanocyte-stimulating hormone (αMSH)-modified exterior. **b**, αMSH-PEG-C' dots localize to lysosomal networks in cells. M21 melanoma cells expressing LAMP1-GFP (green) were treated with αMSH-PEG-C' dots (15 μM) for 24 hours. Note colocalization between nanoparticles (Cy5 fluorescence, pseudo-colored red) and LAMP1-GFP in merged image.

demonstrating that incubation with even high concentrations of these nanoparticles is well-tolerated. We also examined the autophagy pathway and lysosome function in nanoparticle-treated cells, by quantifying the basal levels and turnover rates of the autophagy protein microtubule-associated protein 1 light chain 3 (LC3), which is lipidated onto autophagosomal membranes. Accumulation of the autophagosome-associated, lipidated form of LC3 (called LC3-II) can be quantified as a measure of autophagy induction versus the cytosolic, non-lipidated form (called LC3-I), by western blotting (Fig. 2.2b). The turnover of LC3-II that occurs in a lysosome-dependent manner can also be measured as a readout of lysosome function. When lysosomes are functioning properly, treatment with lysosomal inhibitors such as concanamycin A (ConA), which inhibits the lysosomal vacuolar-type H+-ATPase (V-ATPase), leads to accumulation of LC3-II due to a lack of degradation; if lysosomes are dysfunctional, treatment with ConA will not change LC3-II levels (Mizushima et al., 2010). Cells treated with increasing concentrations of αMSH-PEG-C' dots for 24 hours, from 0.15 to 15 μM, had similar relative LC3-II levels compared to control cells, suggesting that autophagy is not induced by nanoparticle treatment. Moreover, ConA treatment induced similar accumulation of LC3-II in particle-treated cells as compared to controls, demonstrating that lysosomes are functioning properly even when cells are loaded with high concentrations of αMSH-PEG-C' dots (Fig. 2.2b).

Although αMSH-PEG-C' dots were well-tolerated by cells cultured under nutrient-replete conditions, and the autophagy pathway and lysosome function appeared to be unperturbed, we further examined if particle treatment might affect cells cultured under nutrient-deprived conditions where autophagy is induced. Cells cultured in amino acid-free media were treated with αMSH-PEG-C' dots and examined by time-lapse imaging. While amino acid deprivation was well-tolerated by

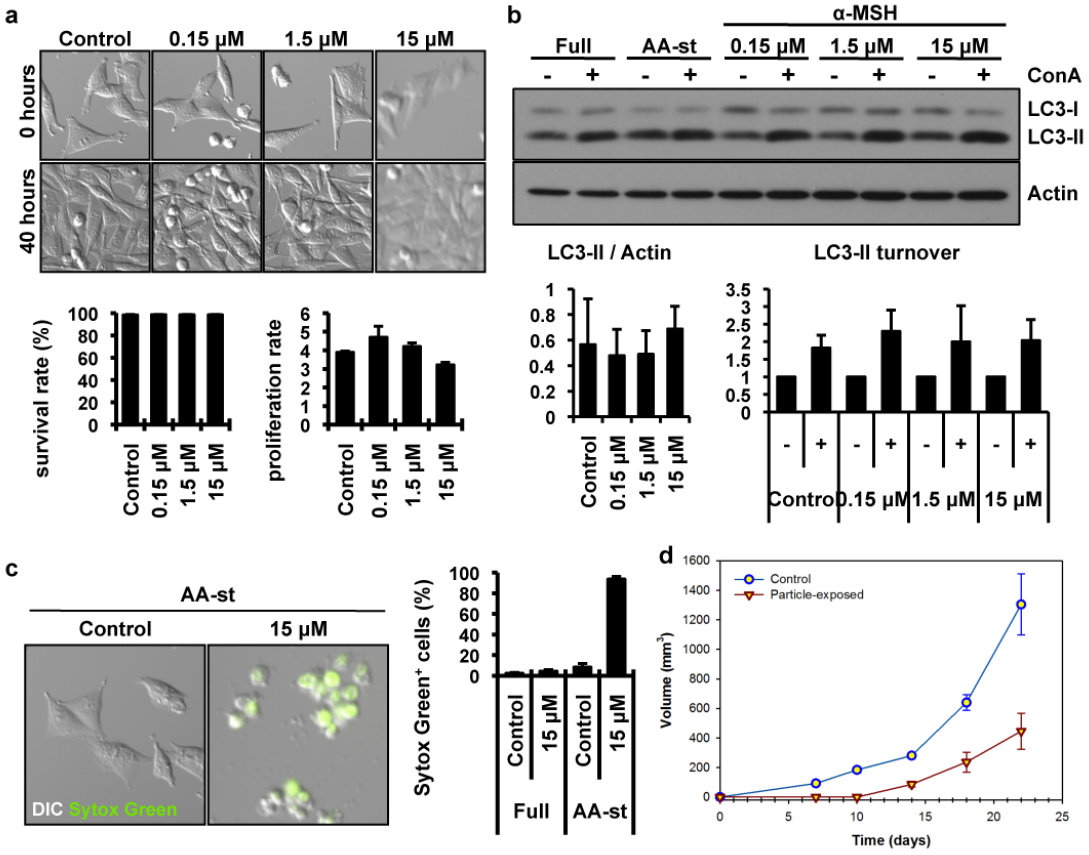

Figure 2.2 αMSH-PEG-C' dot particles induce cell death in amino acid-deprived conditions. a, Nanoparticles are well-tolerated in nutrient-replete media. Images show M21 cells treated with the indicated αMSH-PEG-C' dot concentrations and cultured for 40 hours. Nanoparticles had no significant effect on cell survival (left graph) or cell proliferation (right graph); error bars indicate S.D. **b**, Autophagy and lysosome function in nanoparticle-treated cells are unperturbed. Blot shows LC3-I and –II in cells treated with increasing doses of αMSH-PEG-C' dots for 24 hours compared to untreated and amino acid-starved (AA-st) cells, in the presence (+) and absence (-) of the lysosome inhibitor concanamycin A (ConA, 1 hour at 100 nM). Levels of LC3-II (left graph) are unaltered by nanoparticle treatment, and ConA-inducible LC3-II accumulation (right graph), a measure of autophagy flux, is similar between treated and control cells. Error bars represent SEM. **c**, Nanoparticle treatment induces cell death of M21 cells cultured in amino acid-free media. Images show live control cells and dead (Sytox green-positive) nanoparticle-treated cells in AA-st conditions. Graph shows percent Sytox green-positive cells in full media (Full) or AA-st conditions after 50 hours, as determined by time-lapse microscopy. Error bars represent S.D. **d**, M21 cells treated with 15 μM αMSH-PEG-C' dots in full media for 72 hours prior to create xenografts in immunodeficient (SCID/Beige) mice demonstrate growth inhibition (open inverted triangles) relative to untreated cells (open circles). Data show mean tumor volume over 18 days of growth from three tumors per group, error bars indicate S.D. Particle-treated M21 cells showed statistically significant ($p<0.001$) growth inhibition compared with controls over the study interval.

M21 cells in the absence of particles, the treatment of amino acid-deprived cells with 15 μM αMSH-PEG-C' dots, which had no effect on cells in nutrient-replete media, led to cell death at high rates, detected by the uptake of Sytox Green, a membrane-impermeable nucleic acid dye that labels cells with ruptured plasma membranes (Fig. 2.2c). When injected in mice as flank tumor xenografts, which is known to cause nutrient deprivation (Nelson et al., 2004), M21 melanoma cells loaded with αMSH-PEG-C' dots demonstrated statistically significant growth-inhibition ($p<0.001$) over the study interval relative to non-particle exposed cells (Fig. 2.2d). In fact, no measurable growth occurred in treated tumors up to 10 days following cell injection. These findings suggested that αMSH-PEG-C' dots at high concentrations may induce cell death under conditions of nutrient deprivation in culture and *in vivo.*

2.3.3 αMSH-PEG-C' dot particle-induced cell death is not apoptosis, necroptosis or autosis

We sought to identify the mechanism of how cells treated with αMSH-PEG-C' dots undergo cell death under nutrient-deprived conditions. Careful inspection of the morphology of dying cells suggested a form of necrosis, involving cell swelling and plasma membrane rupture, in the absence of cell blebbing and fragmentation that is typically observed during apoptosis (Fig. 2.3a, Fig. 2.4a). In order to more definitively identify the mechanism of cell death, we utilized two non-tumor cell lines, MCF10A human mammary epithelial cells and mouse embryo fibroblasts (MEF), that were also observed to die at high rates when cultured in amino acid-free media in the presence of αMSH-PEG-C' dots (Fig. 2.3b). Cells rendered resistant to apoptosis, by overexpression of the anti-apoptotic protein Bcl-2 (MCF10A-Bcl2) (Fig. 2.4b) or by genetic deletion of *Bax* and *Bak* (*Bax/Bak*-/- MEFs) (Jacobson et al., 1993;

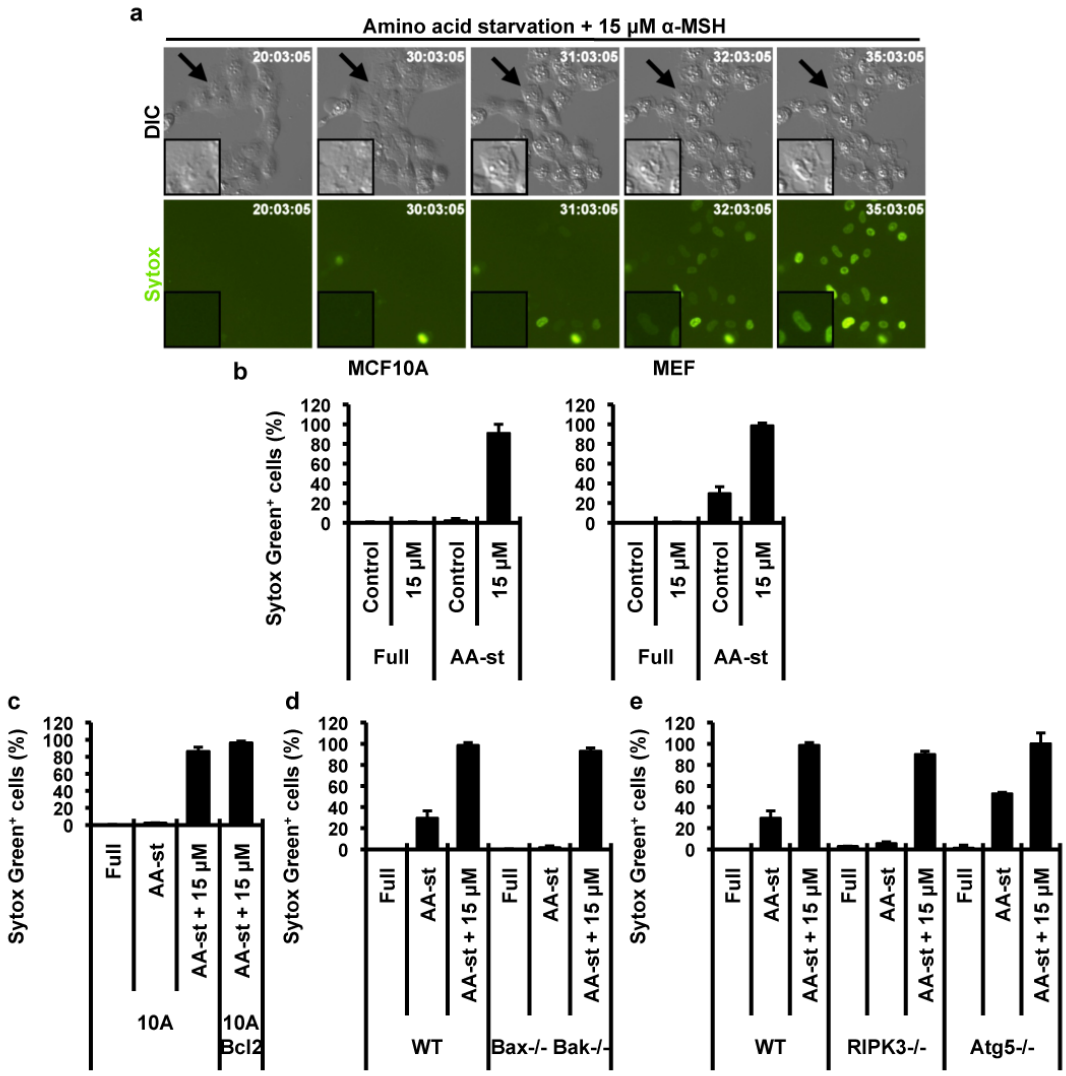

Figure 2.3 αMSH-PEG-C' dot particle-induced cell death is not apoptosis, necroptosis or autosis. a, MCF10A human mammary epithelial cells cultured in the absence of amino acids with 15 μM αMSH-PEG-C' dots undergo cell death after 30 hours with necrotic features. Insets show a dying cell indicated by an arrow. Fluorescence images show Sytox green-labeling of dead cell nuclei. **b**, Quantification of cell death (Sytox green +) in MCF10A and mouse embryo fibroblast (MEF) cultures in full media or amino acid-starved (AA-st) conditions in the presence or absence of 15 μM αMSH-PEG-C' dots, and after 40 hours (MCF10A) or 45 hours (MEF), as determined by time-lapse microscopy. **c-e**, Cell death assays, as in (b), indicate that inhibition of apoptosis by Bcl2 overexpression in MCF10A (c), quantified after a 38 hour time-lapse experiment, or deletion of Bax and Bak in MEF (d), quantified after 45 hours, or inhibition of necroptosis by deletion of Ripk3 in in MEF, (e) quantified after 45 hours, or inhibition of autophagy by knockout of Atg5 in MEF after 45 hours (e) does not inhibit cell death induced by amino acid starvation and treatment with 15 μM αMSH-PEG-C' dots. Error bars represent S.D.

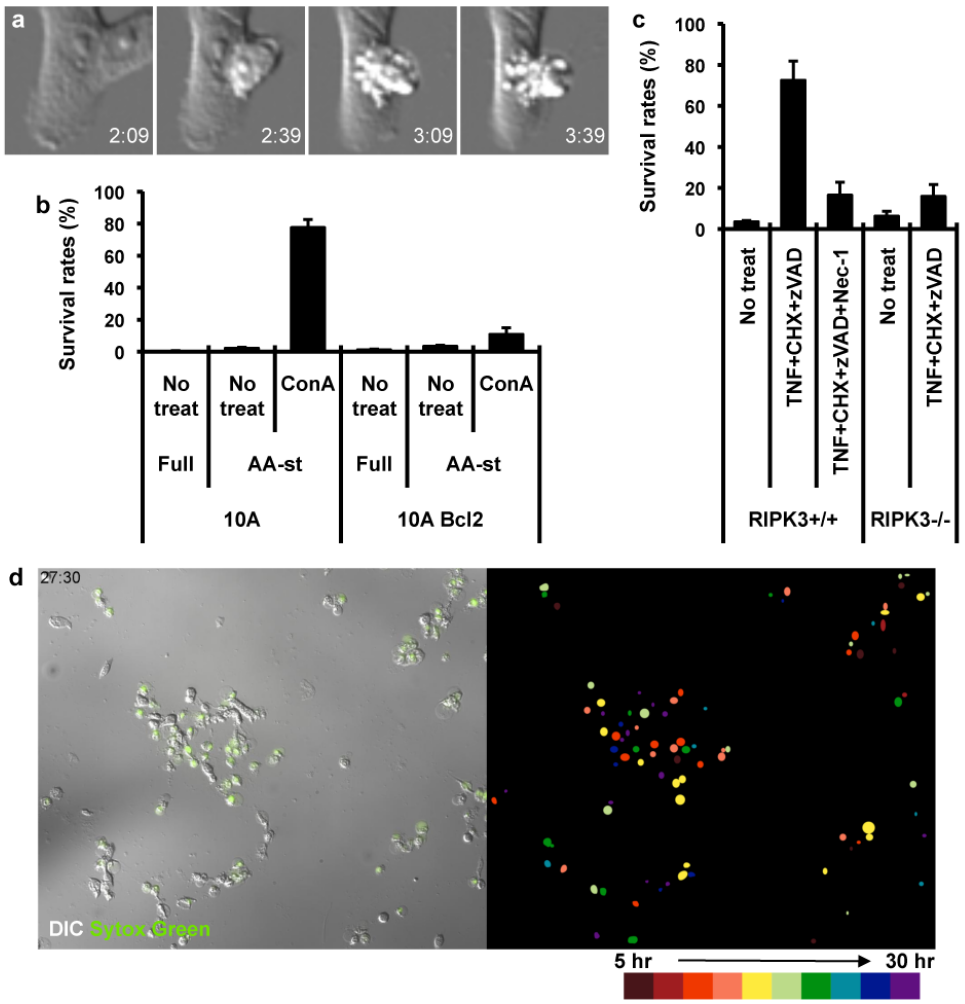

Figure 2.4 Control assays for apoptosis and necroptosis-inhibited cells. a, MCF10A cells cultured in amino acid-free media and treated with 100 nM concanamycin A (ConA) undergo cell death with morphologic features of apoptosis involving cell blebbing and fragmentation. **b,** Quantification of cell death (Sytox green +) in MCF10A cells cultured in full media (Full) or amino acid-starved (AA-st) conditions, in the presence or absence of Bcl2 overexpression and treatment with ConA. Note Bcl2 inhibits apoptosis induced by ConA treatment in AA-st conditions. **c,** Knockout of RIPK3 inhibits necroptosis. Graph shows percent cell death (Sytox green +) of wild-type (wt) and RIPK3-/- MEFs treated with a combination of 100 ng/ml TNFa, 1 μg/ml cycloheximide (CHX) and 20 μM zVAD to induce necroptosis. Note RIPK3 -/- MEFs do not undergo cell death, similar to wt cells treated with 30 μM necrostatin-1 (Nec-1), a necroptosis inhibitor. **d,** MCF10A cells undergoing apoptosis in response to treatment with 50 μg/ml cycloheximide exhibit an asynchronous pattern of cell death. Left image shows image from time-lapse microscopy of cells that have undergone apoptosis (green = Sytox green). Right image shows Sytox green-positive nuclei from left image, pseudocolored to represent the timing of individual cell deaths. The temporal pattern of cell death here is asynchronous compared to Fig 4d.

Kandasamy et al., 2003) underwent cell death at similar rates compared to control cells, suggesting that αMSH-PEG-C' dot-induced cell death does not occur by apoptosis (Fig. 2.3c, d). Next, we examined if cell death was occurring by necroptosis, a programmed form of necrosis that requires the RIPK3 kinase (He et al., 2009). *Ripk3*-/- knockout MEFs, which are resistant to necroptosis (Fig. 2.4c), also underwent cell death at similar rates as controls, suggesting that nanoparticle treatment does not induce necroptosis (Fig. 2.3e). We further determined if a recently-described form of cell death involving the autophagy pathway, called autosis (Liu et al., 2013), could be involved, by treating autophagy-related gene 5 knockout MEFs (*Atg5* -/- MEFs) that are completely deficient for autophagy, with α-MSH-PEG-C' dots in the absence of amino acids. *Atg5* -/- MEFs underwent cell death at similar rates to control cells, demonstrating that αMSH-PEG-C' dot-induced cell death does not involve autophagy, and is not autosis (Fig. 2.3e). Together, these data demonstrate that cell death, induced by a combination of αMSH-PEG-C' dot treatment and amino acid deprivation, occurs independently of apoptosis, necroptosis, and autosis.

2.3.4 Ferroptosis is the underlying mechanism of αMSH particle-induced cell death

We next examined if ferroptosis, a recently described cell death mechanism that occurs via an iron- and reactive oxygen species (ROS)-dependent process and induced by glutathione depletion (Dixon et al., 2012), could be involved in αMSH-PEG-C' dot-induced cell death. We first tested whether ferrostatin-1, a pharmacological inhibitor of ferroptosis, can block cell death in this context. Indeed, ferrostatin-1 treatment rescued cell viability, reducing cell death to the level that occurs under amino acid-deprived conditions in the absence of nanoparticles (Fig. 2.5a). To further examine if nanoparticle-induced death is dependent on iron, we treated cells with

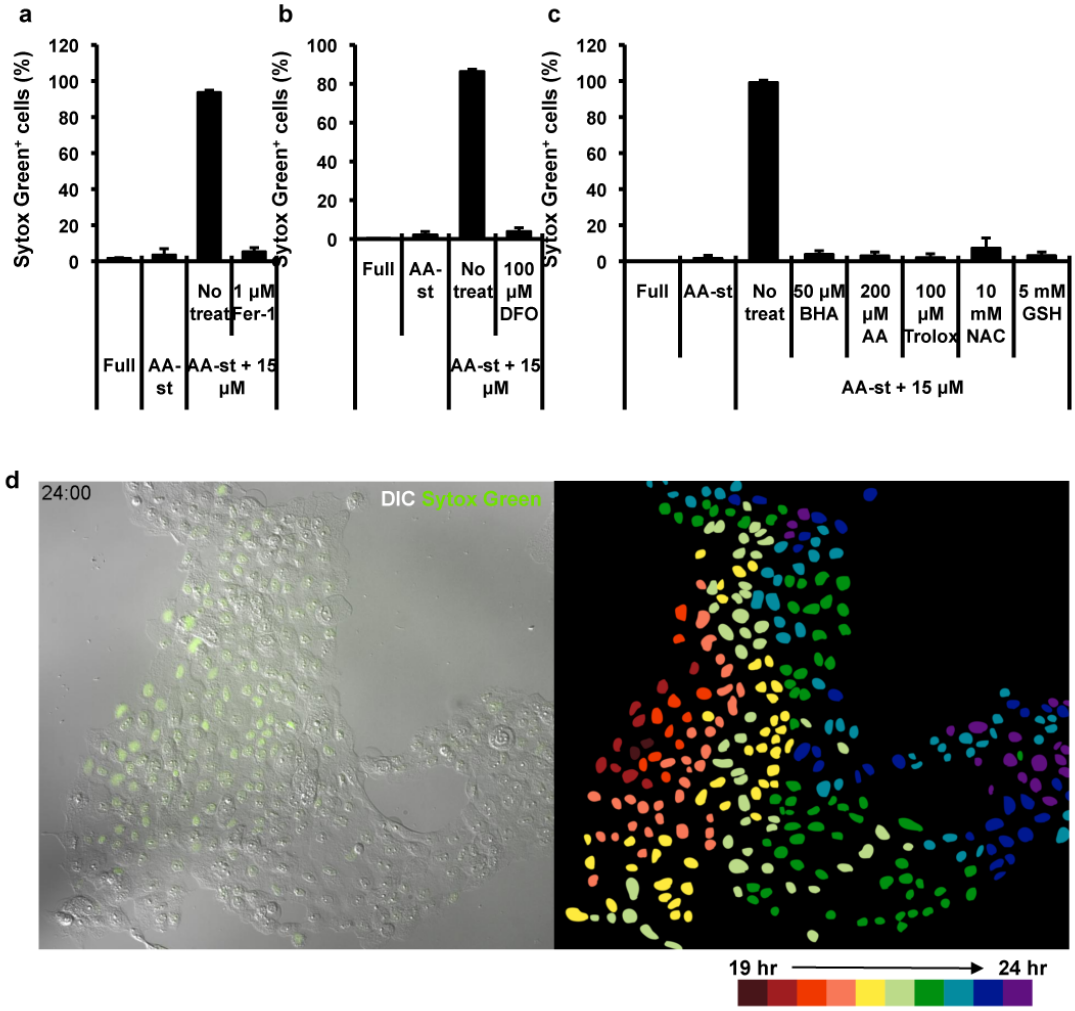

Figure 2.5 Ferroptosis is the underlying mechanism of αMSH particle-induced cell death. a-c, Quantification of cell death (Sytox green +) in MCF10A cells cultured in full media (Full) or amino acid-starved (AA-st) conditions in the presence or absence of 15 μM α-MSH-PEG-C' dot nanoparticles and (a) 1 μM Ferrostatin-1 (Fer-1) after 40 hours, (b) 100 μM deferoxamine (DFO) after 38 hours, and (c) 50 μM butylated hydroxyanisole (BHA), 200 μM ascorbic acid (AA), 100 μM Trolox, 10 mM N-acetylcysteine (NAC), or 5 mM glutathione (GSH), after 40 hours. Error bars represent S.D. **d**, Images from time-lapse analysis of MCF10A undergoing ferroptosis in amino acid-starved conditions with 15 μM αMSH-PEG-C' dots. Note that death (Sytox green positivity) spreads cell-to-cell from the left side of the image to the right.

deferoxamine (DFO), an iron chelator used for treating iron overload and reported to block ferroptosis, and observed that DFO treatment also almost completely inhibited cell death (Fig. 2.5b). In addition, the scavenging of ROS by treatment of cells with different types of antioxidants, including butylated hydroxyanisole (BHA), ascorbic acid (AA), or trolox, or, alternatively, by glutathione repletion through the addition of glutathione or N-acetylcysteine (NAC), a precursor of glutathione, could also block nanoparticle-induced death. Taken together, results indicated that cells cultured in the absence of amino acids and treated with αMSH-PEG-C' dots undergo cell death by ferroptosis (Fig. 2.5c). Interestingly, ferroptosis in this context was also observed to propagate from cell to cell in a wave-like manner (Fig. 2.5d), unlike when cells undergo other types of death such as apoptosis (Fig. 2.4d), suggesting cell-cell communication of a death-inducing signal, and similar to a recent report of ferroptosis occurring in renal tubules in response to the ferroptosis-inducing agent erastin (Linkermann et al., 2014).

2.3.5 αMSH-PEG-C' dots induce partial tumor regression and growth inhibition in HT1080 xenograft models

Having determined that MCF10A cells and MEFs undergo cell death by ferroptosis, we next wanted to examine if cell death could be induced in this manner by amino acid deprivation and nanoparticle treatment in a wider panel of cancer cells. Like MCF10A, MEF, and M21 cells, BxPC3 pancreatic carcinoma cells, H1650 lung carcinoma cells, and HT1080 fibrosarcoma cells underwent high rates of necrosis when treated with αMSH-PEG-C' dots in the absence of amino acids, indicating that

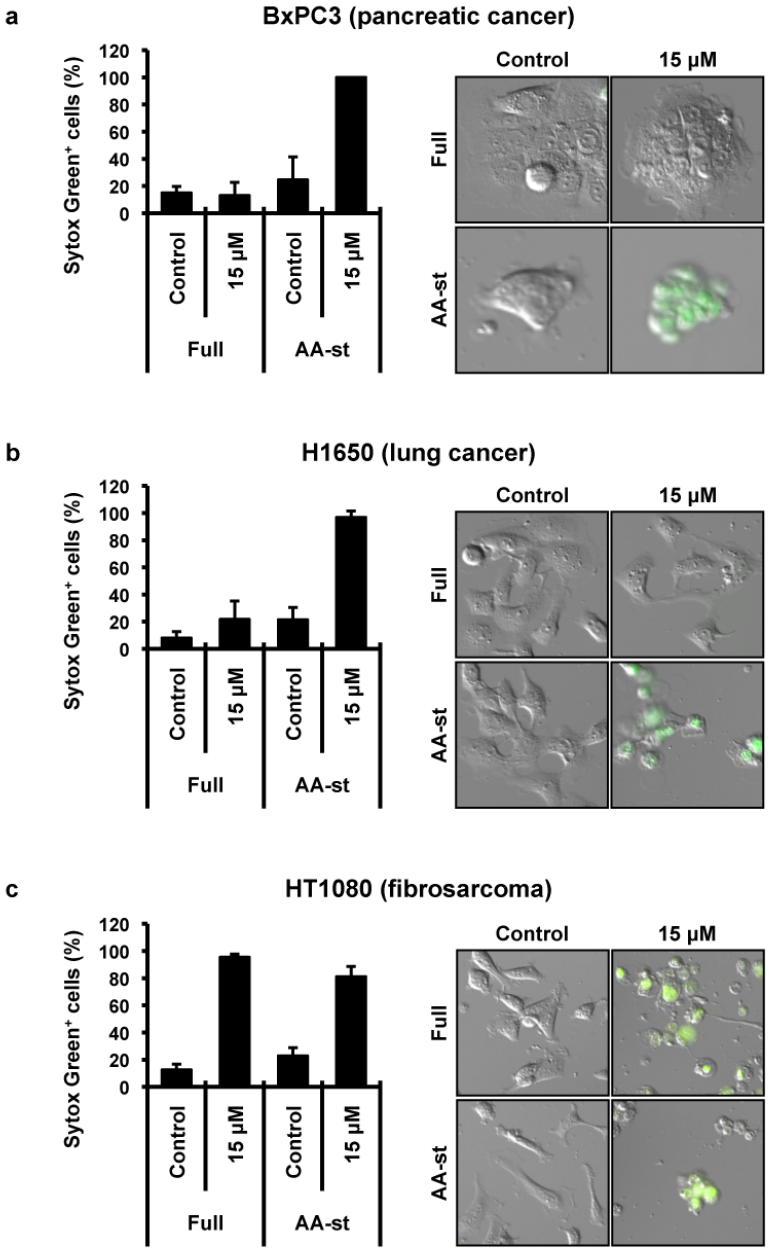

Figure 2.6 αMSH-PEG-C' dots induce cell death in different types of cancer cells. a-c, Quantification of cell death (Sytox green +) in (a) BxPC3 pancreatic carcinoma cells after 40 hours, (b) H1650 lung carcinoma cells after 45 hours, and (c) HT1080 fibrosarcoma cells after 65 hours in full media (Full) or amino acid-free media (AA-st), in the presence or absence of 15 μM αMSH-PEG-C' dot nanoparticles. Error bars represent S.D.

cell death can be induced by this combination in a variety of different cancer cell types (Fig. 2.6a-c).

Based on the foregoing findings, we further investigated whether particle-induced treatment responses could be generated in HT1080 xenograft models. Using a multi-dosing delivery scheme, tumor growth was assessed over a 10-day period after three high-dose intravenous (i.v.) treatments of either the targeted particle probe (n = 5) or 0.9% saline solution (n = 3) in immunosuppressed mice bearing flank HT1080 fibrosarcomas. Relative to the rapidly increasing tumor volumes measured after injection with saline vehicle, statistically significant inhibition of tumor growth was observed with multiple-dose particle treatments over the study interval (Fig. 2.7a). Surprisingly, this was accompanied by partial tumor regression that exceeded 50% for all particle-treated tumors (range: 57% - 78%; mean 64%) within a 4 – 5 day interval after initial injection (Fig. 2.7b). In addition, by the termination of the study, statistically significant reductions in treated tumor volumes (mean ~85%; $p<0.001$) were found relative to control volumes (Fig. 2.7a,b). Representative whole-body optical imaging in mice bearing HT1080 flank xenografts demonstrated intense fluorescence signal at the site of tumor placement after initial αMSH-PEG-C' dot injections, suggesting localization of the intravenously injected particles (Fig. 2.7c).

H&E-stained tissue sections from representative control (n=1) and treated (n=2) tumors (Fig. 2.7d) revealed a poorly demarcated and invasive neoplasm, which was densely cellular, and composed of sheets of fusiform to polygonal cells associated with a fine scant stroma, and exhibiting multifocal necrosis. Control tumors were significantly larger on average than those of treated tumors, but no morphological differences were otherwise observed. Immunohistochemical staining of the control tumor with Mac-2, a murine macrophage marker, demonstrated small numbers of

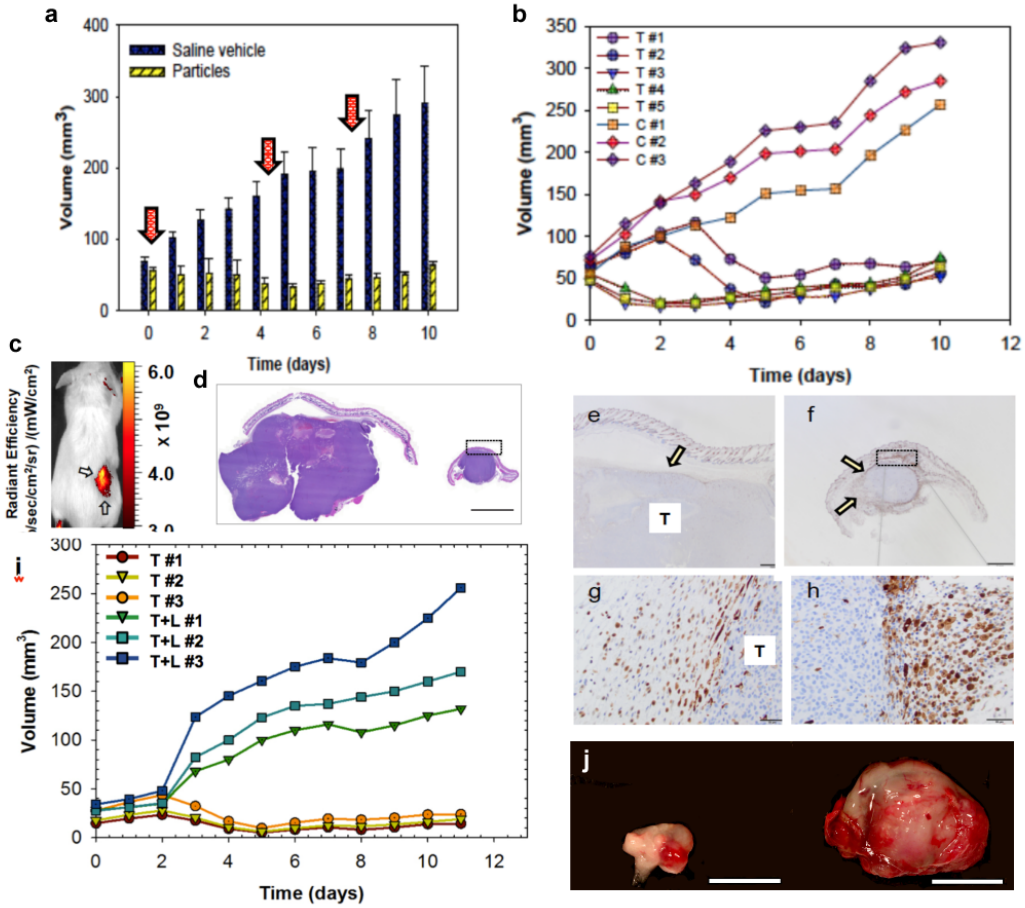

Figure 2.7 αMSH-PEG-C' dots induce partial tumor regression and growth inhibition in HT1080 xenograft models. a,b, Graphical summary of (a) average and (b) individual HT1080 tumor volume measurements in αMSH-PEG-C' dot-treated (T; n=5) and saline-treated (C; n=3) mice; error bars indicate S.D. Three, high-dose αMSH particle (or control vehicle) treatments were i.v.-injected (a; arrows) over a 10-day period. Relative to control tumor volumes, data show marked inhibition of tumor growth and partial tumor regression after particle treatments ($p<0.001$). **c**, Whole body Cy5 fluorescent imaging of a representative H1080 tumor xenograft. **d**, Low-power view of H&E-stained tissue sections from representative control and treated tumors reveal control specimens to be disproportionately larger in size than the corresponding treated ones. **e-h,** Immunohistochemical staining of tumor sections with Mac-2 shows scattered macrophages (arrow) surrounding control tumor sections (T) on (e) low and (g) high power views, while corresponding (f) low and (h) high power views of Mac-2 stained treated sections show large numbers of Mac-2 positive cells circumscribing the tumor at similar locations (boxes, d, f; arrows). Small numbers of intratumoral Mac-2 positive cells are also noted. **i,** Graphical summary of individual HT1080 tumor volume measurements in mice undergoing combined inhibitor and particle treatment (T+L; n=3) versus particle treatment alone (T; n=3). Three high-dose αMSH particle treatments (with and without i.p.-injected inhibitor) over a 10-day period. Relative to particle treatment alone, there is marked progression of tumor growth following combined inhibitor and particle treatment ($p<0.001$). **j,** Representative particle-exposed tumors reveal specimens to be disproportionately larger in size when additionally treated with inhibitor. Scale bars: 1 mm (D, E, and F); 50 μm (G, H); 1 cm (J).

Mac-2 positive macrophages in the soft tissues surrounding the tumor, while treated tumors were circumscribed by much larger numbers of Mac-2 positive cells in the same locations, as shown at both low and high magnification (Fig. 2.7e–h). Intratumoral Mac-2 positive cells were present in similarly small number in all tumors.

We additionally found significantly reduced growth inhibition in HT1080 xenografted mice (n = 3) administered three high-dose particle treatments and daily intraperitoneal (i.p.) doses of liproxstatin-1, a ferroptosis inhibitor recently found to have efficacy *in vivo* (Friedmann Angeli et al., 2014), over a 10-day period, relative to that seen with particle treatment alone (n = 3) (Fig. 2.7i). Average daily growth in particle-exposed tumors treated with liproxstatin-1 was 14.6 (95% CI: 10.1 – 18.9), as compared with -0.87 (95% CI: -1.06 to -0.69) for particle treatment alone, a difference of 15.3 (CI: 13.1 to 17.6; $p < 0.001$). Corresponding particle-exposed tumor specimens are noted, in fact, to be significantly smaller on average than particle-treated tumors receiving daily liproxstatin-1 (Fig. 2.7j).

2.4 DISCUSSION

Here we demonstrate that the combination of treatment of cells with αMSH-PEG-C' dots and starvation for amino acids that can synergize to induce the cell death program ferroptosis. These data suggest that targeted high-dose particle delivery to cancers and their ingestion within cells, under conditions that can lead to dysregulation of cellular redox metabolism, could render cells highly susceptible to cell death without the requirement for additional conjugation of cytotoxic compounds. We note that the combined requirement of nutrient deprivation and nanoparticle treatment for ferroptosis induction in this context could potentially engage tumor cells *in vivo,* while

sparing normal cells, as tumor tissues are known to undergo metabolic stress and are nutrient-limited compared to normal tissues. Ultrasmall targeted silica nanoparticles themselves have also been shown to preferentially accumulate within tumor tissues relative to non-tumor tissues when modified with ligands that promote targeting (Benezra et al., 2011; Phillips et al., 2014).

In this study, the accumulation of nanoparticles within HT1080 xenografts after intravenous delivery was found to significantly inhibit tumor growth and induce partial tumor regression, while the further addition of liproxstatin-1 reversed these effects to levels nearly equivalent to those seen in tumors not exposed to particles. These findings underscore the potential synergy between particle treatment and nutrient deprivation observed in select cancer types, and suggest that, by exploiting such a metabolic strategy, engagement of ferroptosis could hold promising therapeutic potential. The significance of the marked increase in the number of macrophages surrounding particle-treated tumors relative to that about control lesions is not entirely clear, although their role in disease protection and wound repair by engulfing cellular debris is well-established (Ruhrberg and De Palma, 2010). It can be further acknowledged that macrophages are known to demonstrate a high degree of plasticity in response to local cues from the tumor microenvironment (Biswas and Mantovani, 2010; Van Overmeire et al., 2014), and can assume a spectrum of roles upon activation that are required for maintaining tissue homeostasis (Mosser and Edwards, 2008), including shifts in their function associated with tumor shrinkage (Guiducci et al., 2005).

While the concentration of nanoparticles used here to either induce *in vitro* cell death or promote *in vivo* growth inhibition and regression is at least four orders of magnitude higher than what is used currently in human subjects for single-dose imaging-based studies (Phillips et al., 2014), local concentrations could be driven to

much higher levels at tumor sites as part of a multi-dosing strategy, combinatorial treatment regimen, and/or by direct catheter infusion at the target site. Such a dosing schedule would be designed to yield maximum tumor-to-background ratios while reducing off-target toxicities and promoting efficient renal clearance. It is notable that the leakiness of tumor vasculature is thought to allow the accumulation of systemically injected nanoparticles in tumor tissues (Gabizon et al., 2014), while contributing to nutrient deprivation within tumors, again suggesting that the synergism between nanoparticles and nutrient deprivation may be restricted to tumor sites *in vivo*.

We also note that different tumor cell lines apparently differ in their sensitivity to this ferroptosis-inducing mechanism, as we have found, for example, that HT1080 fibrosarcoma cells underwent αMSH-PEG-C' dot-induced ferroptosis even under nutrient-replete conditions (Fig. 2.6c), and in amino acid-deprived conditions with 10-fold lower nanoparticle concentration (1.5 μM) (Fig. 2.8). Targeted particle uptake into HT1080 cells, in this instance, presumably occurred via a non-specific endocytic route, as previous studies identified this route as one of two possible cellular internalization pathways utilized by these probes (Benezra et al., 2014). As ferroptosis is an iron-dependent cell death, it is conceivable that differential susceptibilities may relate in part to the amount of iron that is available in cells. Iron is not only an essential component for cellular homeostasis, but can also generate ROS that can damage organelles. Cells regulate iron availability by uptake, export, or a shift from storage to the labile iron pool (LIP) and some of these processes are altered in cancer (Richardson et al., 2009). The oncogenes c-myc and E1a reduce levels of ferritin, the main cytosolic iron storage protein, which can shift iron from storage to the metabolically active LIP (Tsuji et al., 1993; Wu et al., 1999) and repression of ferritin can stimulate Ras-dependent proliferation most likely by activating DNA synthesis (Kakhlon et al., 2002). Interestingly, ferroptosis-inducing drugs were initially

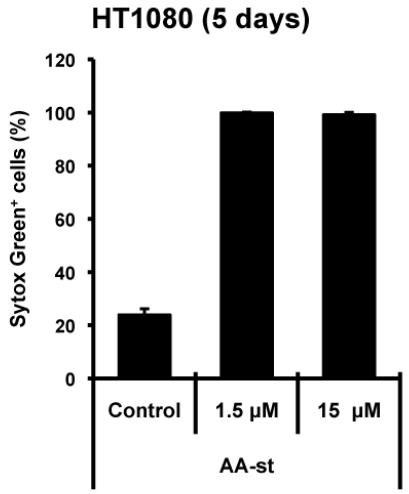

Figure 2.8 Differential sensitivity of HT1080 cancer cells to αMSH-PEG-C' dot-induced ferroptosis. Quantification of cell death (Sytox green +) in HT1080 fibrosarcoma cells after 5 days. Cells were cultured in full media (Full) or amino acid-free media (AA-st) in the presence or absence of the indicated concentrations of αMSH-PEG-C' dot nanoparticles. Error bars represent S.D.

discovered in a screen of small molecules that confer selective killing of Ras-driven tumor cells (Yang and Stockwell, 2008), and among the tested cancer cell lines above, HT1080 is the only cell line harboring a Ras mutation. Therefore, it may be interesting to examine whether cancer cells with mutant Ras are generally more sensitive to nanoparticle treatment.

Some nanomaterials, including uncoated silica particles with diameters on the order of 63 nm (i.e., order of magnitude larger than C' dots) have been shown to induce ROS in cells (Yu et al., 2014). By contrast, we have not detected increased levels of either cytosolic or lipid ROS in cells treated for 24 hours with sub 10-nm diameter α-MSH-PEG-C' dots (Fig. 2.9b), which have an essentially neutral charge. We have found that amino acid starvation and nanoparticle treatment both lower glutathione levels in cells, and also have an additive effect (Fig. 2.9c), suggesting that cell death in this context may be triggered, at least in part, by glutathione depletion (Fig. 2.9d), similar to the ferroptosis-inducing agent erastin that inhibits glutathione production by limiting cystine uptake. The nanoparticles used here are surface-modified with αMSH peptides for targeting cancers *in vivo*, and this modification also enhances cellular uptake (data not shown). In this context, particle modification does not appear to be involved in ferroptosis, as we have observed ferroptosis induction even with PEG-coated C' dots that are unmodified with αMSH targeting ligands, although death in this context occurs with slower kinetics, likely due to slower uptake of the base particles than of αMSH-modified platforms in MC1-R-expressing melanoma cells (Fig. 2.9a). On the other hand, particle size was found to play a critical role in the induction of ferroptotic effects under amino acid deprived conditions. Relative to the high percentage of Sytox Green labeled HT1080 cells (i.e., 80%) found 48 hours after exposure to smaller diameter (~6 nm) PEGylated C' dots, the

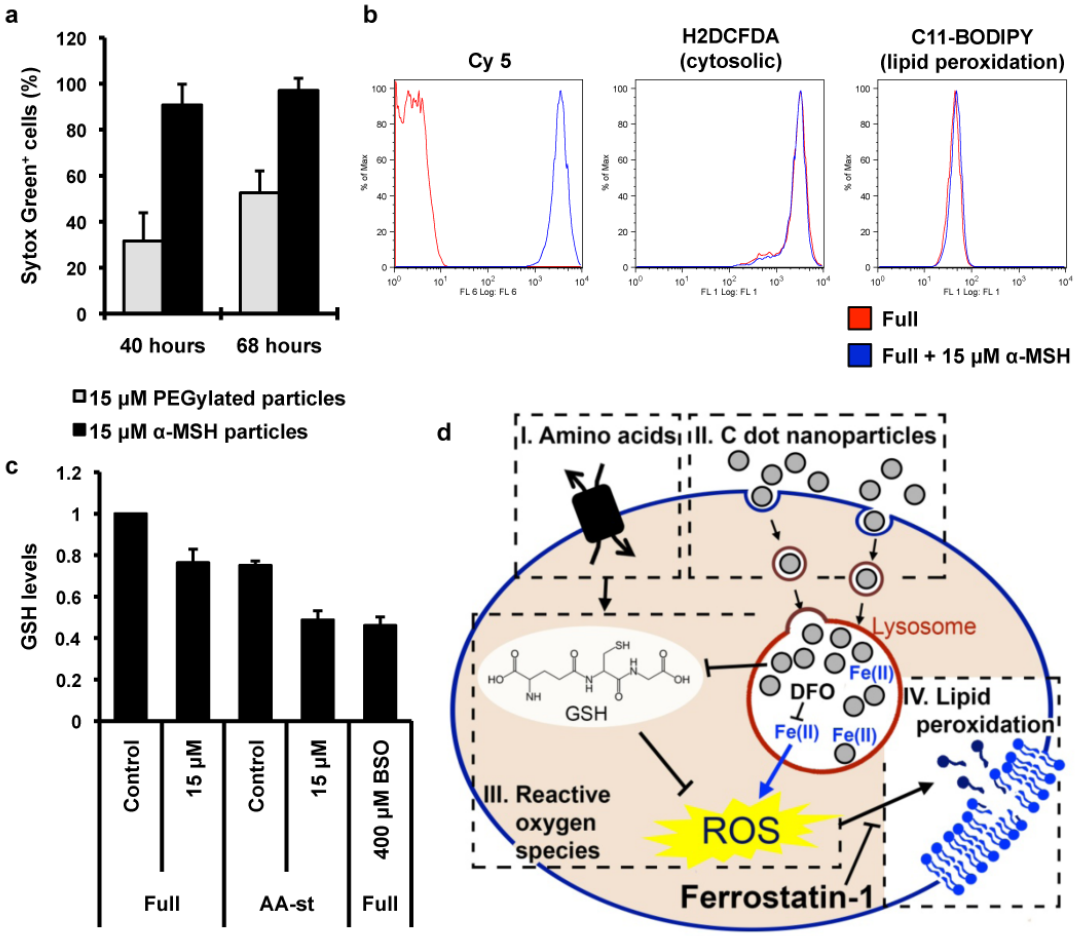

Figure 2.9 ROS, glutathione, and cell death measurements in MCF10A cells treated with and without αMSH-PEG-C' dots or PEG-C' dots. a, Quantification of cell death (Sytox green +) of MCF10A cells cultured in AA-st conditions in the presence of 15mM αMSH-PEG-C' dots (black bars) or PEG-C' dots lacking the aMSH peptide (gray bars). Error bars represent S.D. **b**, MCF10A cells treated with 15 μM αMSH-PEG-C' dots in full media for 24 hours were examined by flow cytometry for levels of cytosolic ROS using 25 μM H_2DCFDA (middle panel) and lipid peroxidation using 2 μM C11-BODIPY(581/591) (right panel). Left panel shows Cy5 fluorescence of particle-treated cells (blue population). **c**, Quantification of glutathione levels in MCF10A cells cultured in full media (Full) or amino acid-free media (AA-st) for 24 hours, in the presence or absence of 15 μM αMSH-PEG-C' dots or 400 μM buthionine sulphoximine (BSO), an inhibitor of γ-glutamylcysteine synthetase, the rate-limiting enzyme for glutathione. Note that nanoparticle treatment and amino acid deprivation reduce glutathione levels alone and in combination, similar to treatment with BSO. Error bars represent S.D. **d**, Model for amino acid starvation and αMSH-PEG-C' dot-induced cell death by ferroptosis. Amino acid deprivation (I) and nanoparticle ingestion by lysosomes (II) lead to depletion of glutathione (see Supp. Figure 2c) and, when combined, induction of ferroptosis that is dependent upon lysosomal iron, a known inducer of reactive oxygen species (ROS), and lipid peroxidation, the latter blocked by Ferrostatin-1.

percentage of labeled cells found after incubation with larger diameter (~10 nm) particles was much lower, on the order of 25%, only slightly increased over non-treated cells (Fig. 2.10).

It will be important in future studies to identify mechanisms whereby C' dots contribute to ferroptosis, and whether other controlled variations in particle structure, composition, or surface chemical properties may alter, or even abrogate, induction of ferroptotic effects. The discovery of nanoparticle-induced ferroptosis as a redox modulator of cell fate, as well as a mediator of tumor regression and growth inhibition, suggests that it may be possible to exploit this process therapeutically to synchronously and selectively kill cancers sensitive to an iron-dependent, non-apoptotic cell death program.

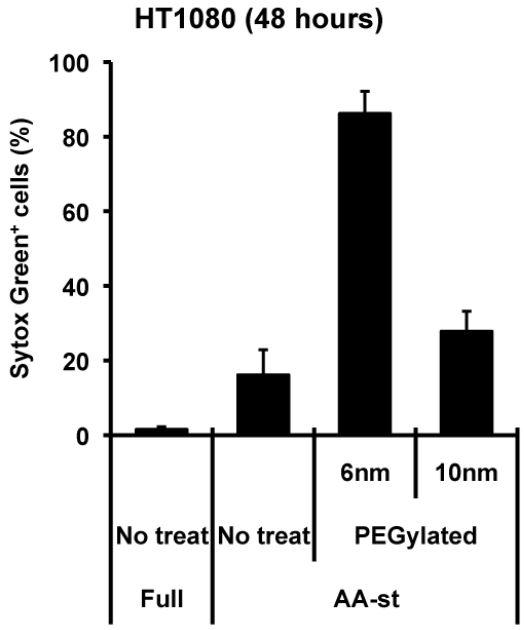

Figure 2.10 Cell death measurements in HT1080 cells treated with different sized PEG-C' dots. Quantification of cell death (Sytox green +) of HT1080 cells cultured in full media or AA-st conditions in the presence of 15 μM PEG-C' dots, 6 nm or 10 nm, lacking the aMSH peptide for 48 hours. Error bars represent S.D.

2.5 REFERENCES

Benezra, M., O. Penate-Medina, P.B. Zanzonico, D. Schaer, H. Ow, A. Burns, E. DeStanchina, V. Longo, E. Herz, S. Iyer, J. Wolchok, S.M. Larson, U. Wiesner, and M.S. Bradbury. 2011. Multimodal silica nanoparticles are effective cancer-targeted probes in a model of human melanoma. *J Clin Invest*. 121:2768-2780.

Benezra, M., E. Phillips, M. Overholtzer, P.B. Zanzonico, E. Tuominen, U. Wiesner, and M.S. Bradbury. 2014. Ultrasmall Integrin-Targeted Silica Nanoparticles Modulate Signaling Events and Cellular Processes in a Concentration-Dependent Manner. *Small*.

Biswas, S.K., and A. Mantovani. 2010. Macrophage plasticity and interaction with lymphocyte subsets: cancer as a paradigm. *Nat Immunol*. 11:889-896.

Bradbury, M.S., E. Phillips, P.H. Montero, S.M. Cheal, H. Stambuk, J.C. Durack, C.T. Sofocleous, R.J. Meester, U. Wiesner, and S. Patel. 2013. Clinically-translated silica nanoparticles as dual-modality cancer-targeted probes for image-guided surgery and interventions. *Integr Biol (Camb)*. 5:74-86.

Chen, N., H. Wang, Q. Huang, J. Li, J. Yan, D. He, C. Fan, and H. Song. 2014. Long-term effects of nanoparticles on nutrition and metabolism. *Small*. 10:3603-3611.

Davis, M.E., Z.G. Chen, and D.M. Shin. 2008. Nanoparticle therapeutics: an emerging treatment modality for cancer. *Nat Rev Drug Discov*. 7:771-782.

Dixon, S.J., K.M. Lemberg, M.R. Lamprecht, R. Skouta, E.M. Zaitsev, C.E. Gleason, D.N. Patel, A.J. Bauer, A.M. Cantley, W.S. Yang, B. Morrison, 3rd, and B.R. Stockwell. 2012. Ferroptosis: an iron-dependent form of nonapoptotic cell death. *Cell*. 149:1060-1072.

Duncan, R., and R. Gaspar. 2011. Nanomedicine(s) under the microscope. *Mol Pharm*. 8:2101-2141.

Duncan, R., and S.C. Richardson. 2012. Endocytosis and intracellular trafficking as gateways for nanomedicine delivery: opportunities and challenges. *Mol Pharm*. 9:2380-2402.

Friedmann Angeli, J.P., M. Schneider, B. Proneth, Y.Y. Tyurina, V.A. Tyurin, V.J. Hammond, N. Herbach, M. Aichler, A. Walch, E. Eggenhofer, D. Basavarajappa, O. Radmark, S. Kobayashi, T. Seibt, H. Beck, F. Neff, I. Esposito, R. Wanke, H. Forster, O. Yefremova, M. Heinrichmeyer, G.W. Bornkamm, E.K. Geissler, S.B. Thomas, B.R. Stockwell, V.B. O'Donnell, V.E. Kagan, J.A. Schick, and M. Conrad. 2014. Inactivation of the ferroptosis regulator Gpx4 triggers acute renal failure in mice. *Nature cell biology*. 16:1180-1191.

Gabizon, A., M. Bradbury, U. Prabhakar, W. Zamboni, S. Libutti, and P. Grodzinski. 2014. Cancer nanomedicines: closing the translational gap. *Lancet*. 384:2175-2176.

Gao, M., P. Monian, N. Quadri, R. Ramasamy, and X. Jiang. 2015. Glutaminolysis and Transferrin Regulate Ferroptosis. *Molecular Cell*. 59:298-308.

Guiducci, C., A.P. Vicari, S. Sangaletti, G. Trinchieri, and M.P. Colombo. 2005. Redirecting in vivo elicited tumor infiltrating macrophages and dendritic cells towards tumor rejection. *Cancer Res*. 65:3437-3446.

Hayano, M., W.S. Yang, C.K. Corn, N.C. Pagano, and B.R. Stockwell. 2015. Loss of cysteinyl-tRNA synthetase (CARS) induces the transsulfuration pathway and inhibits ferroptosis induced by cystine deprivation. *Cell Death Differ*.

He, S., L. Wang, L. Miao, T. Wang, F. Du, L. Zhao, and X. Wang. 2009. Receptor interacting protein kinase-3 determines cellular necrotic response to TNF-alpha. *Cell*. 137:1100-1111.

Jacobson, M.D., J.F. Burne, M.P. King, T. Miyashita, J.C. Reed, and M.C. Raff. 1993. Bcl-2 blocks apoptosis in cells lacking mitochondrial DNA. *Nature*. 361:365-369.

Jiang, L., N. Kon, T. Li, S.-J. Wang, T. Su, H. Hibshoosh, R. Baer, and W. Gu. 2015. Ferroptosis as a p53-mediated activity during tumour suppression. *Nature*. 520:57-62.

Kakhlon, O., Y. Gruenbaum, and Z.I. Cabantchik. 2002. Ferritin expression modulates cell cycle dynamics and cell responsiveness to H-ras-induced growth via expansion of the labile iron pool. *Biochem J*. 363:431-436.

Kandasamy, K., S.M. Srinivasula, E.S. Alnemri, C.B. Thompson, S.J. Korsmeyer, J.L. Bryant, and R.K. Srivastava. 2003. Involvement of proapoptotic molecules Bax and Bak in tumor necrosis factor-related apoptosis-inducing ligand (TRAIL)-induced mitochondrial disruption and apoptosis: differential regulation of cytochrome c and Smac/DIABLO release. *Cancer Res*. 63:1712-1721.

Li, C., H. Liu, Y. Sun, H. Wang, F. Guo, S. Rao, J. Deng, Y. Zhang, Y. Miao, C. Guo, J. Meng, X. Chen, L. Li, D. Li, H. Xu, B. Li, and C. Jiang. 2009. PAMAM nanoparticles promote acute lung injury by inducing autophagic cell death through the Akt-TSC2-mTOR signaling pathway. *J Mol Cell Biol*. 1:37-45.

Li, J.J., D. Hartono, C.N. Ong, B.H. Bay, and L.Y. Yung. 2010. Autophagy and oxidative stress associated with gold nanoparticles. *Biomaterials*. 31:5996-6003.

Linkermann, A., R. Skouta, N. Himmerkus, S.R. Mulay, C. Dewitz, F. De Zen, A. Prokai, G. Zuchtriegel, F. Krombach, P.S. Welz, R. Weinlich, T. Vanden Berghe, P. Vandenabeele, M. Pasparakis, M. Bleich, J.M. Weinberg, C.A. Reichel, J.H. Brasen, U. Kunzendorf, H.J. Anders, B.R. Stockwell, D.R. Green, and S. Krautwald. 2014.

Synchronized renal tubular cell death involves ferroptosis. *Proceedings of the National Academy of Sciences of the United States of America*. 111:16836-16841.

Liu, Y., S. Shoji-Kawata, R.M. Sumpter, Jr., Y. Wei, V. Ginet, L. Zhang, B. Posner, K.A. Tran, D.R. Green, R.J. Xavier, S.Y. Shaw, P.G. Clarke, J. Puyal, and B. Levine. 2013. Autosis is a Na+,K+-ATPase-regulated form of cell death triggered by autophagy-inducing peptides, starvation, and hypoxia-ischemia. *Proceedings of the National Academy of Sciences of the United States of America*. 110:20364-20371.

Ma, K., C. Mendoza, M. Hanson, U. Werner-Zwanziger, J. Zwanziger, and U. Wiesner. 2015. Control of ultrasmall sub-10 nm ligand-functionalized fluorescent core–shell silica nanoparticle growth in water. *Chem Mat*.

Ma, X., Y. Wu, S. Jin, Y. Tian, X. Zhang, Y. Zhao, L. Yu, and X.J. Liang. 2011. Gold nanoparticles induce autophagosome accumulation through size-dependent nanoparticle uptake and lysosome impairment. *ACS Nano*. 5:8629-8639.

Miao, Y., K. Benwell, and T.P. Quinn. 2007. 99mTc- and 111In-labeled alpha-melanocyte-stimulating hormone peptides as imaging probes for primary and pulmonary metastatic melanoma detection. *J Nucl Med*. 48:73-80.

Mizushima, N., T. Yoshimori, and B. Levine. 2010. Methods in mammalian autophagy research. *Cell*. 140:313-326.

Mosser, D.M., and J.P. Edwards. 2008. Exploring the full spectrum of macrophage activation. *Nat Rev Immunol*. 8:958-969.

Nelson, D.A., T.T. Tan, A.B. Rabson, D. Anderson, K. Degenhardt, and E. White. 2004. Hypoxia and defective apoptosis drive genomic instability and tumorigenesis. *Genes Dev*. 18:2095-2107.

Phillips, E., O. Penate-Medina, P.B. Zanzonico, R.D. Carvajal, P. Mohan, Y. Ye, J. Humm, M. Gonen, H. Kalaigian, H. Schoder, H.W. Strauss, S.M. Larson, U. Wiesner, and M.S. Bradbury. 2014. Clinical translation of an ultrasmall inorganic optical-PET imaging nanoparticle probe. *Science translational medicine*. 6:260ra149.

Richardson, D.R., D.S. Kalinowski, S. Lau, P.J. Jansson, and D.B. Lovejoy. 2009. Cancer cell iron metabolism and the development of potent iron chelators as anti-tumour agents. *Biochim Biophys Acta*. 1790:702-717.

Ruhrberg, C., and M. De Palma. 2010. A double agent in cancer: deciphering macrophage roles in human tumors. *Nat Med*. 16:861-862.

Sadasivan, S., A. Dubey, Y. Li, and D. Rasmussen. 1998. Alcoholic solvent effect on silica synthesis—NMR and DLS investigation. *J Sol-Gel Sci Technol*. 12:5-14.

Stern, S.T., P.P. Adiseshaiah, and R.M. Crist. 2012. Autophagy and lysosomal dysfunction as emerging mechanisms of nanomaterial toxicity. *Part Fibre Toxicol*. 9:20.

Tsuji, Y., E. Kwak, T. Saika, S.V. Torti, and F.M. Torti. 1993. Preferential repression of the H subunit of ferritin by adenovirus E1A in NIH-3T3 mouse fibroblasts. *J Biol Chem*. 268:7270-7275.

Van Overmeire, E., D. Laoui, J. Keirsse, J.A. Van Ginderachter, and A. Sarukhan. 2014. Mechanisms driving macrophage diversity and specialization in distinct tumor microenvironments and parallelisms with other tissues. *Front Immunol*. 5:127.

Wu, K.J., A. Polack, and R. Dalla-Favera. 1999. Coordinated regulation of iron-controlling genes, H-ferritin and IRP2, by c-MYC. *Science*. 283:676-679.

Xie, Y., W. Hou, X. Song, Y. Yu, J. Huang, X. Sun, R. Kang, and D. Tang. 2016. Ferroptosis: process and function. *Cell Death Differ*. 23:369-379.

Yang, W.S., and B.R. Stockwell. 2008. Synthetic lethal screening identifies compounds activating iron-dependent, nonapoptotic cell death in oncogenic-RAS-harboring cancer cells. *Chem Biol*. 15:234-245.

Yoo, B., K. Ma, Z. Li, A.A. Burns, S. Sequeira, C. Brennan, I. Mellinghoff, U. Wiesner, and M. Bradbury. 2015. Ultrasmall dual-modality nanoparticle drug conjugates for nanomedicine. *Submitted*.

Yu, Y., J. Duan, Y. Yu, Y. Li, X. Liu, X. Zhou, K.F. Ho, L. Tian, and Z. Sun. 2014. Silica nanoparticles induce autophagy and autophagic cell death in HepG2 cells triggered by reactive oxygen species. *Journal of hazardous materials*. 270:176-186.

Zeger, S.L., K.Y. Liang, and P.S. Albert. 1988. Models for longitudinal data: a generalized estimating equation approach. *Biometrics*. 44:1049-1060.

CHAPTER 3: Amino acids and mTOR regulate the fate of live engulfed cells

3.1. INTRODUCTION

As discussed in chapter one, in addition to apoptosis, or type I cell death, which is well known to control cell turnover during metazoan development and in adult tissues, other alternative, non-apoptotic forms of programmed cell death have been identified recently, and these also contribute to physiologic cell turnover in some contexts (Galluzzi et al., 2012; Tait et al., 2014; Yuan and Kroemer, 2010). For example, forms of programmed necrosis, or type III cell death, eliminate cells during viral infection or ischemia-reperfusion (Linkermann and Green, 2014), and autophagic, or type II, cell death participates in development (Das et al., 2012) and may eliminate stressed cells in adult tissues (Liu et al., 2013). In addition to these programs, it is also evident that cells can be targeted for death by being engulfed by professional phagocytes or by neighboring cells (Brown and Neher, 2012; Overholtzer and Brugge, 2008). Examples of cell death-inducing engulfment mechanisms include entosis (Overholtzer et al., 2007), emperitosis (Wang et al., 2013), suicidal emperipolesis (Benseler et al., 2011), phagoptosis (Brown and Neher, 2012), and homotypic cell cannibalism (HoCC) (Cano et al., 2012). While cell engulfment appears to be the cause of cell death for these programs, little is known about the molecular mechanisms that regulate the death of ingested cells in these contexts. In fact, engulfment appears to be insufficient to cause cell death in some circumstances, as entotic cells and those engulfed by HoCC have been shown to escape, post-engulfment, and thereby avoid execution (Cano et al., 2012; Overholtzer et al., 2007).

We have previously found that engulfed entotic cells do not have access to growth factors, have low levels of mTOR activity compared to neighboring cells, and

upregulate autophagy, suggesting that they are shielded from the extracellular medium and are nutrient-deprived. However, many of these live engulfed cells can survive for prolonged periods, from hours to days, within entotic vacuoles of host cells and can even undergo division in some cases (Overholtzer et al., 2007). Their prolonged survival appears to depend at least in part on the induction of autophagy, as autophagy inhibition by siRNA-mediated knockdowns within engulfed cells leads to a high rate of apoptosis (Florey et al., 2011). Intriguingly, autophagy proteins also function to execute the non-apoptotic death of ingested cells, by acting within engulfing cells to lipidate the autophagy protein microtubule-associated protein light chain 3 (LC3) onto entotic vacuoles (Florey et al., 2011). LC3 lipidation is followed by the fusion of lysosomes, whose enzymes appear to kill and digest engulfed cells. A similar activity of autophagy pathway proteins occurs during phagocytosis and macropinocytosis and is thought to control vacuole maturation, perhaps by facilitating lysosome fusion (Florey and Overholtzer, 2012).

But while phagosome maturation involving LC3 lipidation occurs rapidly after engulfment, entotic vacuoles exhibit a maturation delay of hours or even days, suggesting that engulfment *per se* is insufficient to trigger LC3 lipidation and the death of internalized cells, and that there may be additional signals (Florey et al., 2011). Why entotic vacuoles exhibit delayed maturation, and the nature of the signal that ultimately triggers maturation, are unknown. Like cells ingested by entosis, the predominant fate of cells ingested by suicidal emperipolesis or phagoptosis is considered to be cell death (Benseler et al., 2011), but detailed imaging-based quantification of the fates of engulfed cells, including the kinetics of death and whether targeted cells can be rescued post-engulfment, have not been performed.

To investigate the regulation live cell engulfment-induced cell death, we sought to identify pathways that might control cell death initiation, or contribute to the

prolonged survival of engulfed cells, potentially by inhibiting cell death. Surprisingly, even though engulfed cells appear to be shielded from the outside environment, we found that the withdrawal of amino acids from culture medium induced live engulfed cells to undergo apoptosis. Similarly, inhibition of the mTOR kinase, which is regulated by amino acids, induced apoptosis of engulfed cells, dependent on the expression within engulfed cells of 4E-BP1, a known negative regulator of mRNA translation and an mTORC1 effector protein. Similar to entosis, we find that the fate of cells ingested by HoCC, but not phagoptosis, is also controlled by mTOR signaling and amino acids from media, suggesting that live engulfed cells may acquire nutrients from the external environment that prolong cell survival. Interestingly, mTOR inhibition also affected the rate of non-apoptotic cell death by acting within engulfing cells, in a manner not requiring 4E-BP1. Together these data identify amino acid signaling and mTOR activity as key determinants controlling the fate of live engulfed cells, and further suggest that engulfed cells may feed through an unknown mechanism that prolongs their survival.

3.2 MATERIALS AND METHODS

3.2.1 Cell culture and constructs

MCF10A cells (ATCC) were cultured in DMEM/F12 (Gibco, Grand Island, NY) supplemented with 5% horse serum (Atlanta Biologicals, Flowery Branch, GA), 20 ng/ml EGF (Peprotech, Rocky Hill, NJ), 10 μg/ml insulin (Sigma, St. Louis, MO), 0.5 μg/ml hydrocortisone (Sigma), and 100 ng/ml cholera toxin (Sigma) with penicillin/streptomycin. BxPC3 cells (ATCC) were cultured in RPMI-1640 (Gibco) supplemented with 10% FBS with penicillin/streptomycin. RAW 264.7 and Jurkat cells (ATCC) were cultured in DMEM (Gibco) supplemented with 10% FBS with

penicillin/streptomycin. Cells were routinely verified as mycoplasma-free by DAPI imaging. Amino acid-free medium was prepared by dialyzing heat-inactivated FBS (for BxPC3, RAW 264.7, and Jurkat cells) or horse serum (for MCF10A cells) for 4 h, followed by overnight incubation at 4°C in phosphate-buffered saline (PBS) in MWCO 3500 dialysis tubing (21-152-9; Fisherbrand, Pittsburgh, PA) and addition to base media prepared without amino acids. GFP-LC3, H2B-mCherry, and H2B-GFP were introduced into MCF10A, BxPC3, or RAW 264.7 cells by retroviral transduction, and stable cell lines were selected with blasticidin, puromycin, and geneticin, respectively.

3.2.2 Reagents

The following reagents were used at the indicated concentrations: Torin1 (Tocris, Ellisville, MO) 0.5 μM, 5-Bromo-2-Deoxyuridine (BrdU) (Sigma) 10 μM; Concanamycin A (ConA) (Sigma) 100 nM; anti-CD47 antibody (ab3283; Abcam, Cambridge, MA) 10 μg/ml.

3.2.3 Immunofluorescence

The following antibodies were used for immunofluorescence (IF): Anti-phospho-mTOR (5536; Cell Signaling, Danvers, MA), Anti-LAMP1 (555798; BD Biosciences, San Jose, CA), Anti-BrdU (5292; Cell Signaling). IF was performed on cells cultured on glass-bottom dishes (Mattek), essentially as described (Overholtzer et al., 2007). Confocal microscopy was performed with the Ultraview Vox spinning-disc confocal system (Perkin Elmer) equipped with a Yokogawa CSU-X1 spinning-disc head and an EMCCD camera (Hamamatsu C9100-13), and coupled to a Nikon Ti-E microscope.

3.2.4 Western blotting

Cells were scraped into ice-cold RIPA buffer (50 mM Tris at pH 7.4, 150 mM NaCl, 2 mM EDTA, 1% NP40, 0.1% SDS with protease inhibitor cocktail) and lysed for 10 min on ice. Lysates were then centrifuged at 15,870g for 20 min at 4 °C and protein was quantified by BCA assay (Pierce, Waltham, MA). Samples were separated on 15% polyacrylamide SDS–PAGE gels and transferred to a polyvinyldifluoride membrane which was blocked with TBST plus 5% BSA and incubated overnight at 4 °C with the following primary antibodies: Anti-mTOR (2983; Cell Signaling), Anti-4E-BP1 (Cell Signaling), Anti-LC3A/B (4108; Cell Signaling) and anti-Actin (A1978; Sigma), diluted in blocking buffer. Blots were incubated with horseradish peroxidase conjugated to secondary antibodies and protein was detected using enhanced chemiluminescence detection (Invitrogen, Carlsbad, CA). Densitometry analysis was carried out using ImageJ software (NIH).

3.2.5 siRNA and shRNA mediated protein knockdown

siGenome SMART pool siRNA against human *mTOR, FIP200* as well as Control 2 non-targeting siRNAs, were obtained from Dharmacon. MCF10A cells were seeded in a 6-well plate at 5 x 10^4 per well and transfected with 100 nM siRNA using Oligofectamine (Invitrogen). Cells were assayed 48 hours post-transfection. shRNA constructs targeting human *Atg13* in the pLKO.1 vector, as well as empty vector, were acquired from the MSKCC core facility. Cells were selected with puromycin and assayed 72 hours after selection.

3.2.6.CRISPR/Cas9 gene knockout system

Vectors encoding guide RNA (sequence) targeting exon of 4E-BP1 were cloned as previously described (Mali et al., 2013). MCF10A cells were co-transfected with

gRNA vector and the Cas9 vector. After 3 days, cells were seeded as single colonies in 96-well plates and left to grow for 2-3 weeks. Clones were selected based on western blotting.

3.2.7 Time-lapse microscopy

Cells were plated onto glass-bottom 6-well plates (MatTek, Ashland, MA) overnight and fluorescence and differential interference contrast (DIC) images were acquired every 10 min for indicated times using a Nikon TI-E inverted microscope, a CoolSNAP HQ^2 CCD (charge-coupled device) camera (Photometrics, Tucson, AZ), a live-cell incubation chamber to maintain cells at 37 °C and 5% CO_2, and NIS Elements software (Nikon, Melville, NY). Cell fates, including cell survival, death, and proliferation, were manually quantified and processed using NIS Elements software and Image J.

3.2.8 BrdU incorporation assay

MCF10A cells were plated in glass-bottom 6-well plates and treated with DMSO or Torin1 with the addition of BrdU. After 24 hours, cells were fixed and immunostained with an anti-BrdU antibody.

3.2.9. Phagoptosis assay

RAW 264.7 cells were plated in glass-bottom 6-well plates in full media with 200 U/ml IFN-γ. After 48 hours, RAW 264.7 cells were overlayed with $2.5x10^5$ trypsinized MCF10A cells expressing H2B-mCherry and imaged for 15 hours. Cell fates, including engulfment and death, were manually quantified and processed using NIS Elements software and Image J.

3.3 RESULTS

3.3.1 Amino acid starvation or mTOR inhibition induces apoptosis of live engulfed entotic cells.

Entosis leads to the formation of cell-in-cell structures that harbor viable epithelial cells that have been engulfed by their neighbors. These engulfed cells do not appear to have access to culture media, as they have been shown to lack access to a fluorescent-tagged epidermal growth factor (EGF), and they also upregulate autophagy, a known starvation response that is required for entotic cell survival (Florey et al., 2011). Consistent with a lack of access to nutrients, we found that internalized entotic cells also display low levels of mTOR activity compared to host and neighboring cells, as determined by immunostaining for mTOR phosphorylated on serine 2448, that indicates activated mTOR kinase (Fig. 3.1a). As shown previously, when cell-in-cell structures cultured in nutrient-replete conditions were observed by time-lapse microscopy for 20 hours, the majority of cell deaths that were observed were non-apoptotic in nature, as determined by nuclear morphology, while only about 5-10% of engulfed cells underwent apoptotic cell death, indicated by nuclear condensation and fragmentation, as well as membrane blebbing (Fig. 3.1b). We also found that the autophagy protein LC3, which is lipidated onto entotic vacuoles prior to non-apoptotic cell death, was not lipidated prior to apoptotic cell death, as reported (Fig. 3.1b). Surprisingly, although internalized cells are shielded from the extracellular environment, have low levels of mTOR activity, and upregulate autophagy, we found that the removal of amino acids from culture medium induced cell death by apoptosis (Fig. 3.1c). Furthermore, although internalized cells exhibit low levels of immunostaining for active mTOR, the inhibition of mTOR kinase activity, by treatment with the inhibitor Torin1, similarly resulted in apoptosis (Fig. 3.1d). These

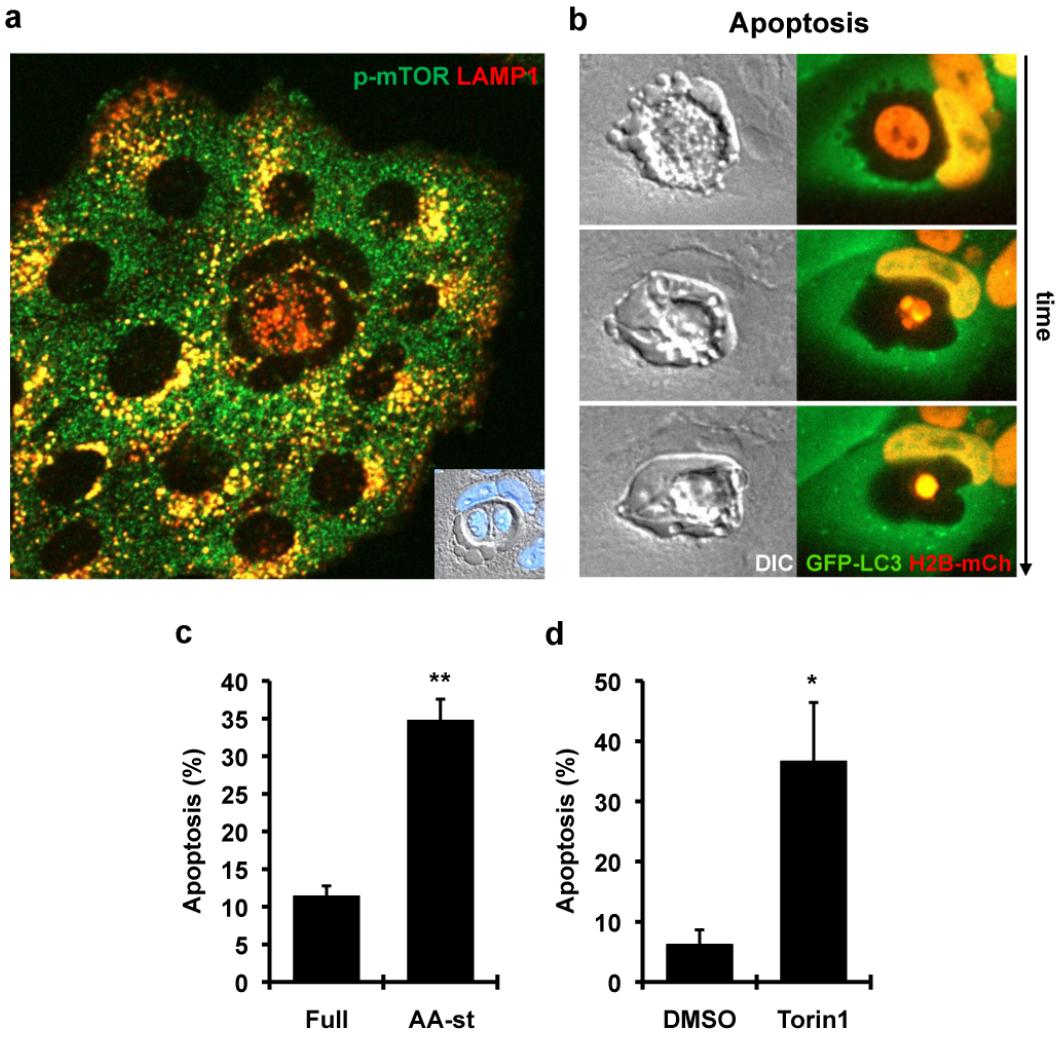

Figure 3.1. Amino acid starvation or mTOR inhibition induces apoptosis of live engulfed cells in entosis. a, Engulfed cells have low mTOR activity, indicated by low levels of phosphorylated mTOR, compared to neighboring cells in full media. b, Representative image of apoptotic death through time. Note distinct membrane blebbing and nuclear condensation of engulfed cell. c-d, Quantification of apoptosis of internalized cell fate over 20 hours in amino acid starvation (c) or Torin1 treatment (d). * $p<0.05$, ** $p<0.01$.

data demonstrate that the fate of live engulfed cells during entosis is regulated, surprisingly, by the availability of extracellular amino acids and activity of the amino acid-responsive mTOR kinase.

3.3.2 Amino acid starvation or mTOR inhibition induces apoptosis of live engulfed cells during HoCC.

To examine if the fates of live engulfed cells formed by other engulfment process are also regulated by amino acid signaling, we examined cell-in-cell structures formed by pancreatic carcinoma BxPC3 cells, which have been shown to be formed by a process called homotypic cell cannibalism (HoCC), argued to be distinct from entosis (Cano et al., 2012). Similar to entotic cell structures, some engulfed cells resulting from HoCC underwent cell death with an apoptotic morphology, with membrane blebbing and nuclear condensation, and an absence of LC3 lipidation (Fig. 3.2a). When cells were starved for amino acids or treated with Torin1, the rates of apoptosis increased significantly, similarly to the fates of entotic cells (Fig. 3.2b). This demonstrates that the fates of engulfed cells within HoCC-mediated cell-in-cell structures are also regulated by amino acids and mTOR activity in a similar manner to entotic cells.

3.3.3 mTOR activity is required within engulfed cells for survival.

To further examine how mTOR controls the survival of engulfed cells, we sought to determine which cells, the host or internalized cells, might require amino acid signaling and mTOR activity. We examined the requirement of mTOR for cell survival in different cell populations by mixing control cells expressing a green fluorescent marker of the nucleus (H2B-GFP) with those expressing a red fluorescent marker of the nucleus (H2B-mCherry), and then treated red cells with mTOR-targeted

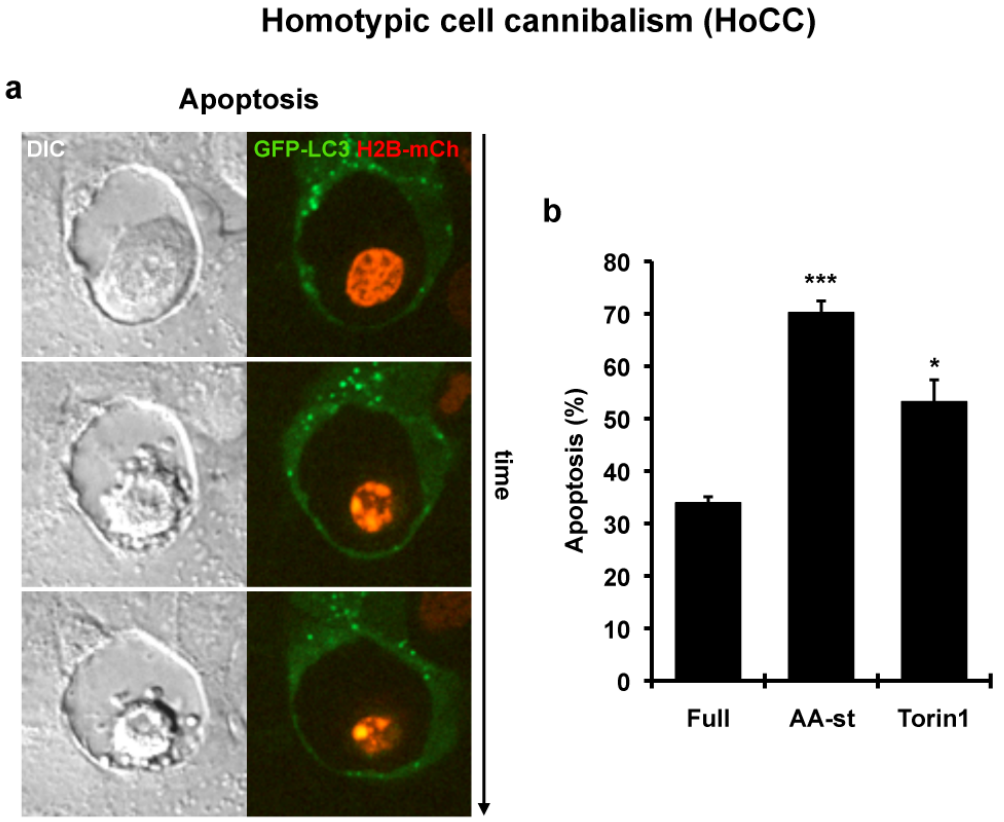

Figure 3.2. The live engulfed cells of HoCC cell-in-cell structures can also undergo apoptosis and are regulated by amino acid starvation and mTOR. a, Engulfed cells of HoCC cell-in-cell structures can also undergo apoptosis with characteristics of membrane blebbing and nuclear condensation. b, Amino acid starvation or Torin1 treatment induces apoptosis of engulfed cells in HoCC similar to entosis. * $p<0.05$, *** $p<0.001$.

siRNA (Fig. 3.3a). Cell-in-cell structures in mixed cultures were examined by time-lapse microscopy and the frequencies of apoptotic cell death were quantified over time. Among the possible combinations of host and engulfed cell relationships, we found that when mTOR was depleted from engulfed cells, not host cells (Fig. 3.3b), the frequency of apoptosis was significantly increased (Fig. 3.3c), consistent with a requirement for amino acid signaling and mTOR activity to maintain the viability of engulfed cells in an autonomous manner.

3.3.4 4E-BP1 is required for apoptosis occurring in response to mTOR inhibition.

As the amino acid-responsive mTORC1 kinase complex is known to phosphorylate translational machinery to regulate protein synthesis, we examined the potential involvement of the known mTOR effector 4E-binding protein 1 (4E-BP1) (Dowling et al., 2010). 4E-BP1 interferes with the interaction between eukaryotic translation initiation factor 4E (eIF4E) and eIF4G, leading to a block of translation initiation, but when phosphorylated by mTOR, 4E-BP1 dissociates from eIF4E and allows protein synthesis to begin (Ma and Blenis, 2009). Therefore, in cells depleted for 4E-BP1, translation initiation, as well as cell proliferation, are rescued in the context of mTOR inhibition (Dowling et al., 2010). We generated cells depleted of 4E-BP1 (Fig. 3.4a), using the CRISPR/Cas9 system, and observed that the proliferation arrest that is normally caused by mTOR inhibition was partially relieved, consistent with a previous report (Fig. 3.4b). We next examined the frequencies of apoptosis of these cells in mTOR-inhibited conditions, and observed that 4E-BP1-depleted cells were rescued from apoptotic death caused by the inhibition of mTOR (Fig. 3.4c). Furthermore, consistent with the requirement of mTOR signaling within in engulfed cells to promote cell survival, we found that the knockout of 4E-BP1 within engulfed cells

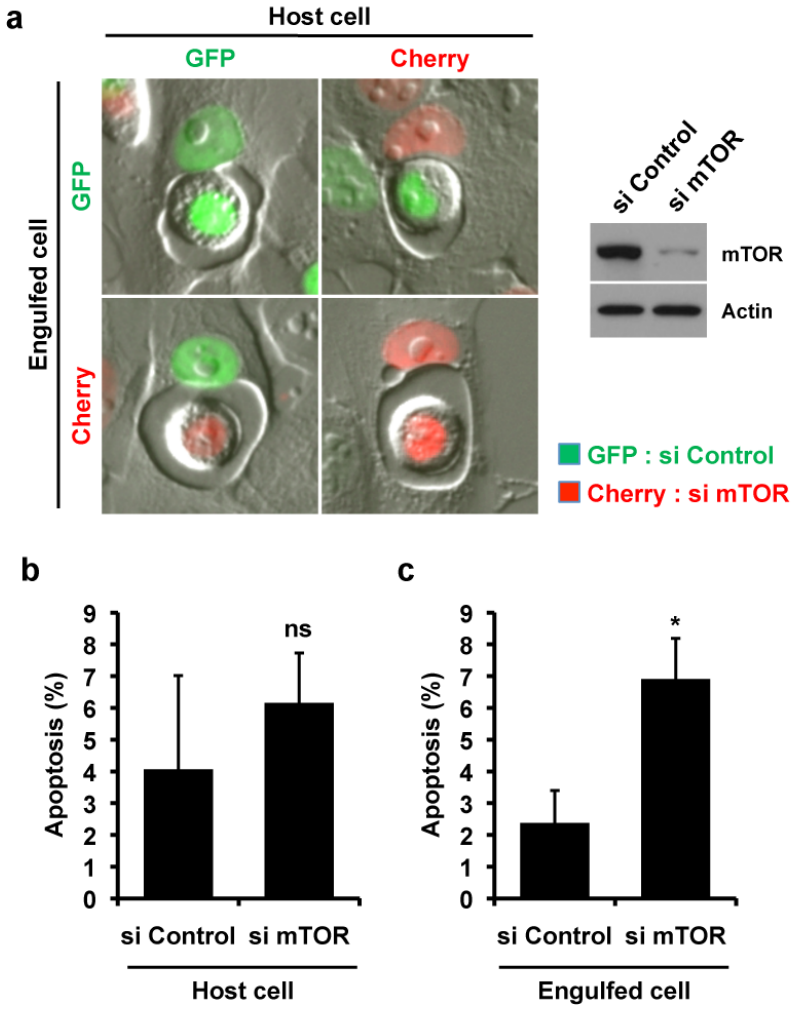

Figure 3.3. The activity of mTOR in required in the engulfed cell for survival. a, Representative images of cell-in-cell structures formed between control (H2B-GFP) and mTOR-depleted (H2B-mCherry) mixed cultures. Western blot shows knockdown of mTOR. b, Quantification of apoptosis grouped by the identity, control of mTOR-depleted, of host cells. c, Quantification of apoptosis grouped by the identity, control of mTOR-depleted, of engulfed cells. * $p<0.05$.

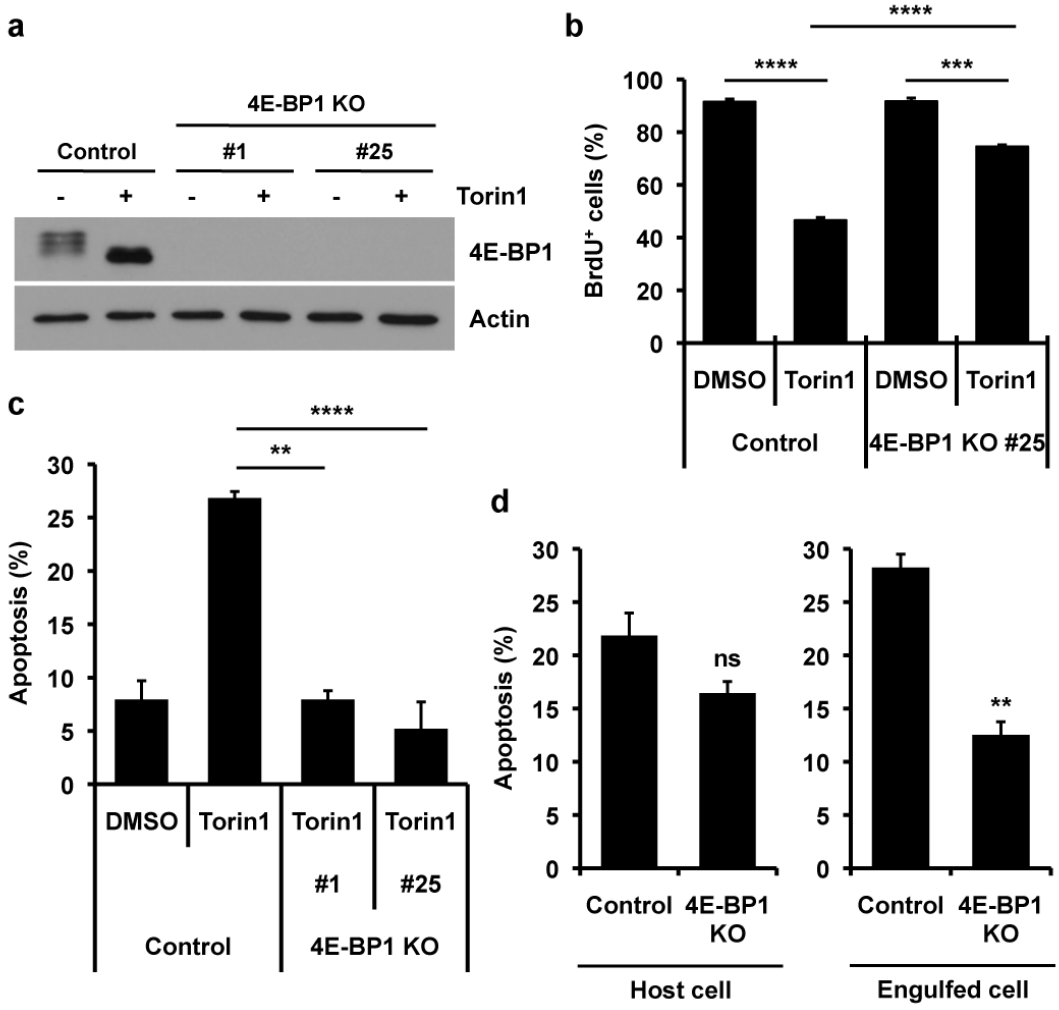

Figure 3.4. Knockout of 4E-BP1 specifically in engulfed cells rescues cells from apoptosis. a, Western blot showing 4E-BP1 knockout (note the dephosphorylated form of 4E-BP1 with Torin1 treatment). b, 4E-BP1 depletion leads to a rescue of proliferation rates, indicated by BrdU uptake, in Torin1 treatment compared to control cells. c, Apoptosis frequencies are rescued in 4E-BP1-depleted cells treated with Torin1. d, The activity of 4E-BP1 to rescue cells from apoptosis comes from the engulfed cell. ** $p<0.01$, *** $p<0.001$, **** $p<0.0001$.

could rescue, in a cell-autonomous manner, apoptosis induced by mTOR inhibition (Fig. 3.4d).

3.3.5 Non-apoptotic death of engulfed cells in entosis is also regulated by amino acids and mTOR.

Live engulfed cells in entosis can undergo another type of cell death that is morphologically and genetically distinct from apoptosis, but rather requires autophagy proteins from the host cell and is dependent on the lysosomal fusion to vacuoles that harbour engulfed cells (Fig. 3.5a) (Florey et al., 2011). We observed the frequencies of this cell death and noticed that amino acid starvation and mTOR inhibition led to a decrease in rates of non-apoptotic death (Fig. 3.5b). It has been shown previously that the autophagy proteins, which are required for lysosomal fusion and subsequent death of engulfed cells, are specifically required within the host cells (Florey et al., 2011). To examine which cell requires mTOR activity for regulation of non-apoptotic cell death, we performed mixing experiments with red and green cells and examined the non-apoptotic cell death rates of engulfed cells within mixed cell-in-cell structures. Unlike apoptotic cell death, the siRNA-mediated knockdown of mTOR within host cells, but not internalized cells, reduced the rate of non-apoptotic cell death (Fig. 3.5c). However, when we depleted the mTOR effector protein 4E-BP1 from host cells, the rates of non-apoptotic cell death were unchanged, suggesting that mTOR does not regulate non-apoptotic death through 4E-BP1 (Fig. 3.5d).

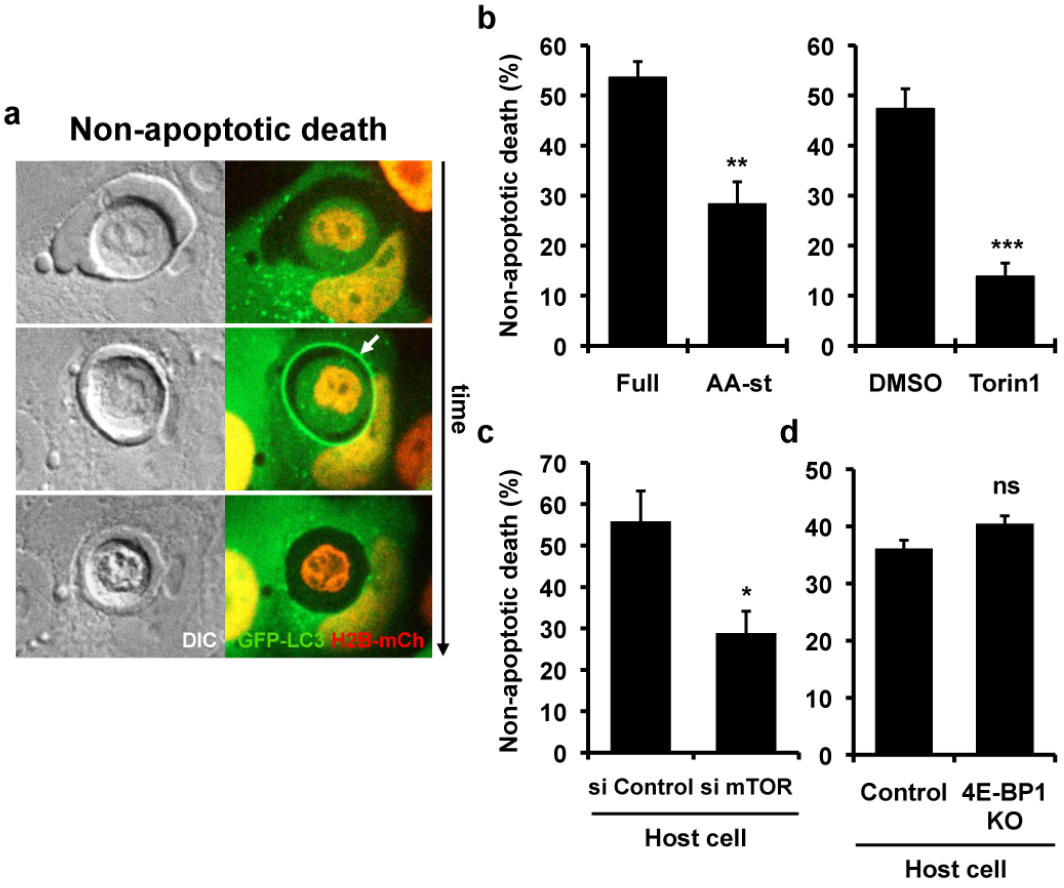

Figure 3.5. Amino acid starvation or mTOR inhibition inhibits non-apoptotic death in entosis and HoCC. a, Non-apoptotic death of live engulfed cells in entotic cell-in-cell structures undergo a process of LC3 lipidation (arrow) and subsequent death caused by lysosomal fusion without noticeable membrane blebbing or nuclear condensation. b, Amino acid starvation and mTOR inhibition by Torin1 leads to decreased rates of non-apoptotic death of engulfed cells. c, Specific knockdown of mTOR in host cells reduced non-apoptotic death in entosis, suggesting a role of mTOR in the host cells regulating non-apoptotic death of engulfed cells. d, Depletion of 4E-BP1 in host cells was not able to reverse the effects of mTOR inhibition, suggesting that mTOR does not act through 4E-BP1 to regulated non-apoptotic death. * $p<0.05$, ** $p<0.01$, *** $p<0.001$.

3.3.6 mTOR does not act through autophagy to regulate non-apoptotic death during entosis.

As amino acid starvation and mTOR inhibition are known to upregulate autophagy, and autophagy proteins contribute to regulating entotic cell death (Florey et al., 2011), we sought to determine whether it was the upregulation of autophagy by these treatments that was inhibiting non-apoptotic death frequencies, perhaps by inducing competition between these processes for shared autophagy proteins such as LC3. To examine this, we took advantage of the fact that non-apoptotic cell death is regulated independently of the ULK1/2/FIP200/ATG13 complex that is required for autophagy (Florey et al., 2011). As shown in Figure 3.6a-b, the siRNA-mediated knockdown of FIP200, or shRNA-mediated knockdown of ATG13, reduced the amount of lipidated LC3 (LC3-II) induced by treatment with Torin1, consistent with the inhibition of autophagy. However, these autophagy-inhibited cells still exhibited reduced non-apoptotic cell death frequencies upon treatment with Torin1 (Figure 3.6c-d), suggesting that mTOR inhibition does not regulate non-apoptotic cell death frequencies by inducing autophagy and sequestering autophagy proteins.

3.3.7 The fates of live engulfed cells within HoCC cell-in-cell structures, but not CD47-blockade-induced phagocytosis, are regulated by amino acids and mTOR.

To ask whether other live engulfment programs undergo similar non-apoptotic cell deaths that are also regulated by amino acids and mTOR, we decided to look at HoCC and phagoptosis, a process of live engulfment induced by the blockage of CD47, a "don't-eat-me" signal in cells (Brown and Neher, 2012). First, we found that live engulfed cells within HoCC cell-in-cell structures can also undergo non-apoptotic cell death associated with LC3 lipidation onto vacuoles (Fig. 3.7a), and we found that the

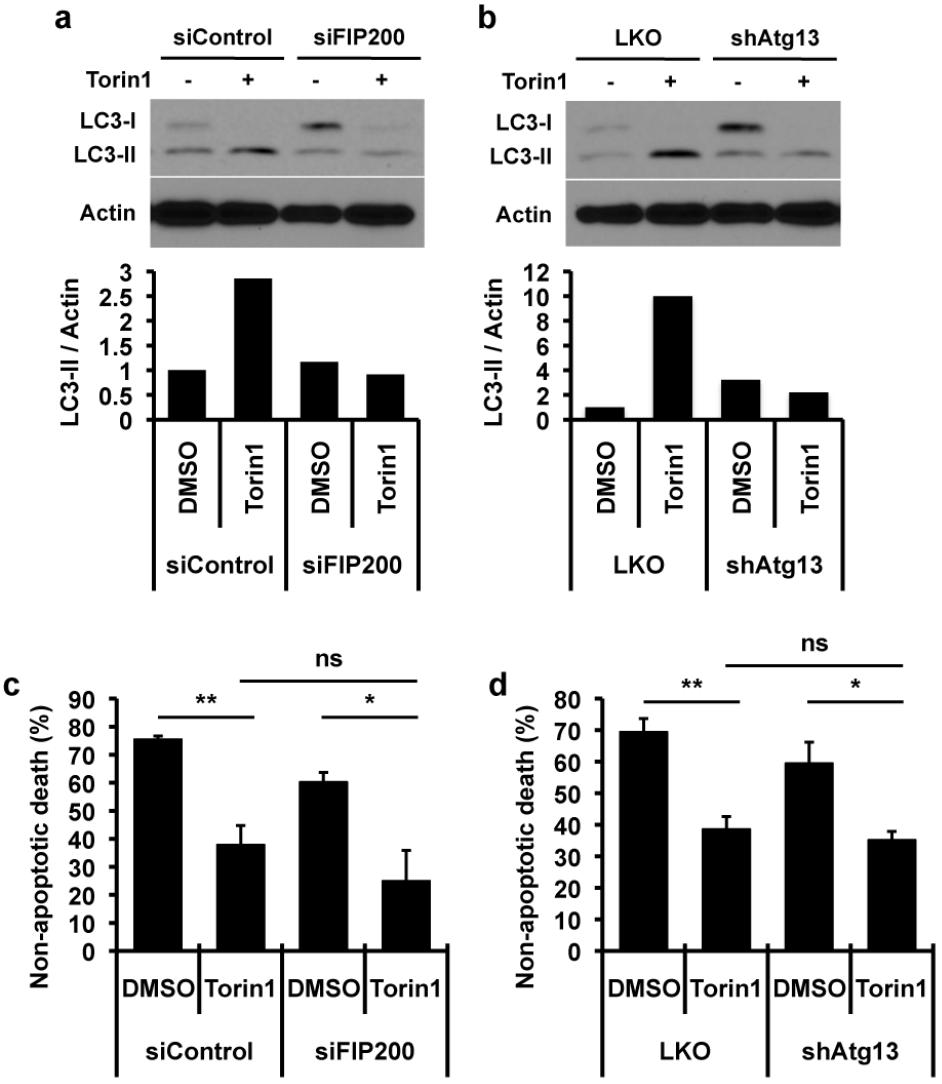

Figure 3.6. Autophagy-inhibited cells still have decreased rates of non-apoptotic death with mTOR inhibition. a-b, Knocdown of FIP200 (a) or Atg13 (b) blocks the induction of LC3-II form, indicative of autophagosome formation, with Torin1 treatments compared to control conditions. c-d, Even in these autophagy-inhibited cells, Torin1 treatment had similar effects of decreasing the frequencies of non-apoptotic death compared to control conditions. * $p<0.05$, ** $p<0.01$.

frequencies of these deaths were also decreased with amino acid starvation or mTOR inhibition, similar to entosis (Fig. 3.7b). Anti-CD47 antibody-mediated phagocytosis, also termed phagoptosis, is a type of live cell engulfment that is induced by the blockade of CD47, a molecule which functions as a "don't-eat-me" signal, on viable cells (Chao et al., 2012). Normally, live lymphocytes are not engulfed by macrophages when incubated together even for a prolonged time (Fig. 3.8aA-A'''). However, when they are incubated in the presence of an anti-CD47 antibody that targets CD47 on the lymphocytes, this induces phagocytosis of the lymphocytes by the macrophages (Fig. 3.8aB-B'''), as previously reported (Chao et al., 2012). We found that phagosomes containing live lymphocytes follow a similar maturation process to entotic vacuoles, consisting of LC3 lipidation and lysosome fusion, occurring prior to internalized cell death (Fig. 3.8b). The death of the lymphocytes was dependent on lysosome function, as pre-treatment with the lysosome inhibitor concanamycin A, which blocks the vacuolar type ATP-dependent H+ pump (V-ATPase), inhibited cell death, and engulfed cells under this condition appeared to survive and move continuously within phagosomes for prolonged periods, up to more than 5 hours (Fig. 3.8aC-C'''). To ask whether mTOR can regulate this non-apoptotic cell death caused by phagoptosis, we treated macrophages with Torin1 and added cells targeted with CD47 antibodies. Unlike entotic or HoCC-related non-apoptotic cell deaths, treatment with Torin1 did not alter the frequencies of cell death by phagoptosis (Fig. 3.8c), suggesting that the observed regulation of cell death by amino acids or mTOR during entosis and HoCC does not occur during phagoptosis. This may be related to the observation that engulfment and death of the engulfed cell is tightly correlated during phagoptosis, as phagosomes mature rapidly after engulfment, and engulfed cells die quickly, becoming acidified and ceasing movement within approximately 30 minutes to one

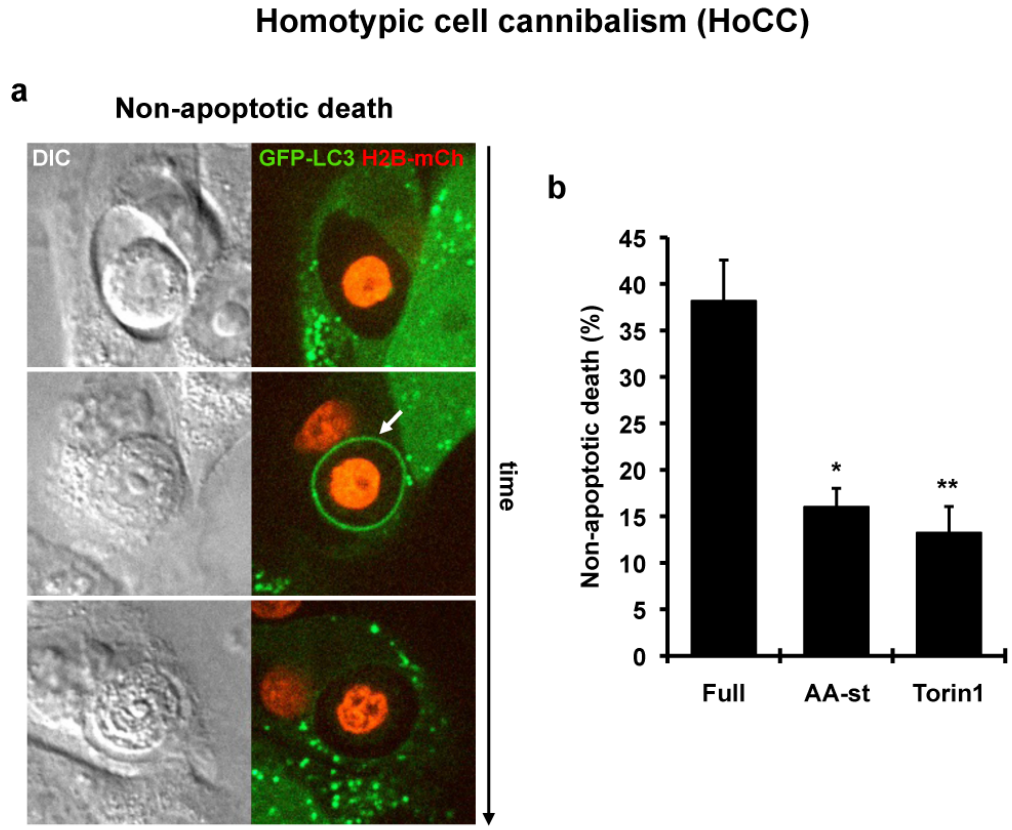

Figure 3.7. The live engulfed cells of HoCC cell-in-cell structures can undergo non-apoptotic death and are regulated by amino acid starvation and mTOR. a, Engulfed cells of HoCC cell-in-cell structures can also undergo non-apoptotic death associated with LC3 lipidation (white arrow) and lysosome fusion that leads to subsequent death of engulfed cells. b, The frequencies of non-apoptotic death of HoCC cell-in-cell structures are decreased by amino acid starvation and mTOR inhibition, similar to entosis. * $p<0.05$, ** $p<0.01$.

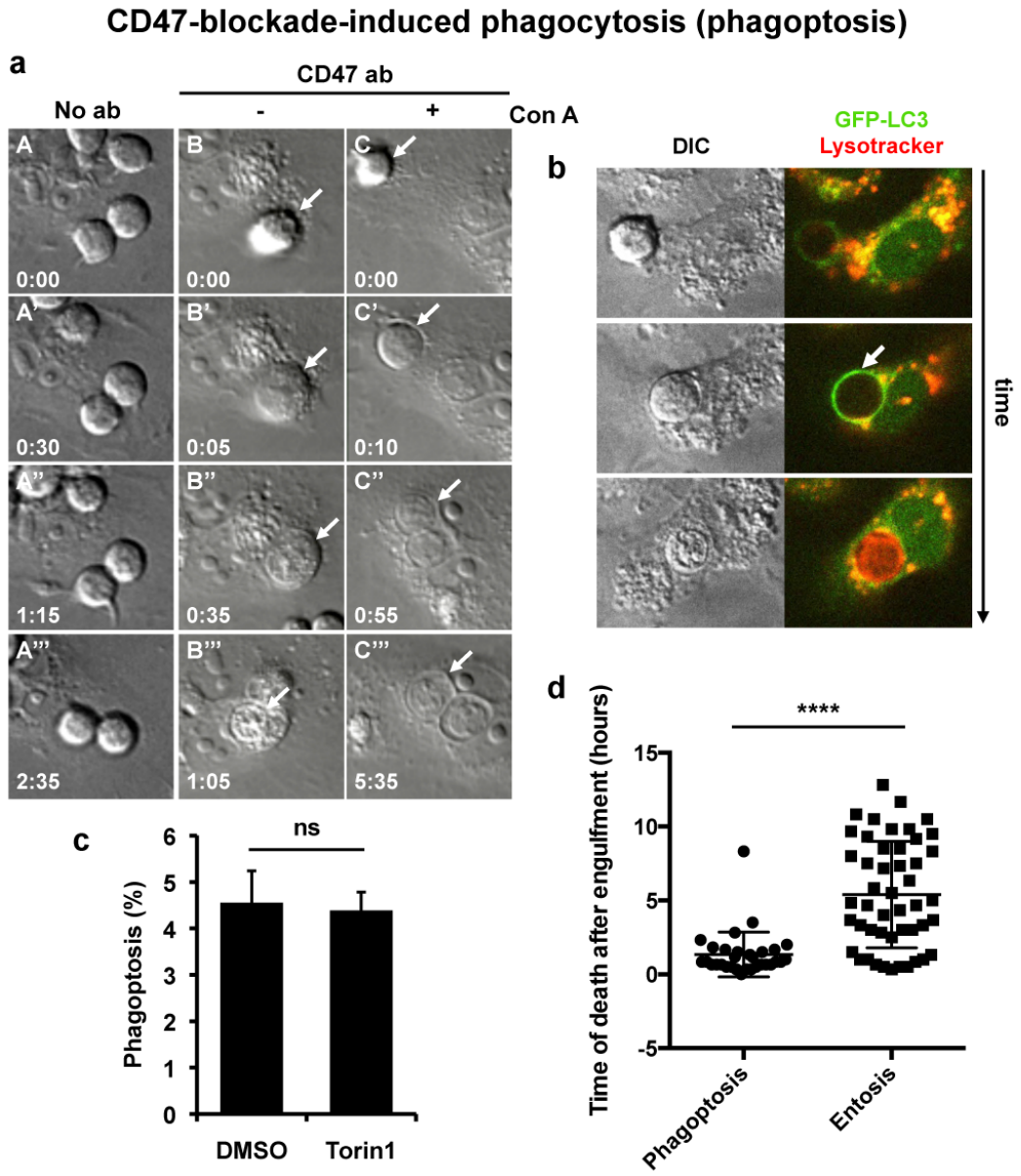

Figure 3.8 Live engulfed cells of phagoptosis undergo non-apoptotic death but are not affected by amino acid starvation and mTOR. a, CD47-blockade-induced phagocytosis, also known as phagoptosis, is a lysosomal fusion-induced cell death process, similar to entosis and HoCC. (A-A''') Macrophages do not engulf live lymphocytes in the absence of CD47 antibodies. (B-B''') In the presence of anti-CD47 antibodies that target the lymphocytes, these cells are engulfed by the macrophages and undergo a rapid killing process in approximately an hour (White arrow indicates newly engulfed cell that undergoes death. (C-C''') With a pretreatment of concanamycin A, which inhibits lysosome acidification, engulfed lymphocytes are viable and exhibit cell movement even up to 5 hours after engulfement (White arrows indicate engulfed cells that show movement up to 5 hours). b, Similar to entosis and HoCC, phagoptosis follows a sequence of LC3 lipidation after live cell engulfment that is followed by lysosome fusion and subsequent non-apoptotic death of engulfed cell. c, However, unlike entosis and HoCC, rates of engulfed cell death caused by phagoptosis was not affected by mTOR inhibition. d, A clear distinction between phagoptosis and entosis is the time of death after engulfment which is rapid in phagoptosis compared to entosis. **** $p<0.0001$.

hour after ingestion (Fig. 3.8a). Even when cells were targeted for either phagoptosis or entosis in the same culture conditions, engulfed cells formed by phagoptosis died rapidly after engulfment, unlike those formed by entosis or HoCC, in which death of engulfed cell was widely distributed between 0-15 hours after engulfment occurred (Fig. 3.8d).

3.4 DISCUSSION

Here we identify the amino acid-mTOR-4E-BP1 pathway as a regulator of apoptosis of live engulfed cells formed by entosis or HoCC. Amino acid withdrawal or mTOR inhibition increases the frequencies of apoptosis compared to when cells are cultured in nutrient-replete conditions. This increase of apoptosis by mTOR inhibition is completely rescued by depletion of the 4E-BP1 protein, suggesting that amino acid-mTOR signaling exerts control over this process by regulating mRNA translation. The activity of the mTOR-4E-BP1 pathway is specifically required within engulfed cells to prevent their death through apoptosis. This is a somewhat surprising result as we have previously shown that live engulfed cells formed by entosis already have decreased mTOR activity, even in nutrient-replete conditions. This suggests that some engulfed cells may retain a certain threshold of mTOR activity, although lowered compared to control cells, perhaps through amino acid signaling from the medium. When the culture medium is devoid of amino acids or when mTOR activity is blocked by inhibitor treatment, engulfed cells then succumb to apoptosis. It is possible therefore that engulfed cells acquire small amounts of amino acids that function to sustain a low, yet sufficient level of mTOR activity that promotes cell survival. While the methods of mTOR inhibition shown here (Torin 1 treatment or siRNA-mediated knockdown) both block mTORC1 and mTORC2 activity, the finding that the known mTORC1

effector 4E-BP1 plays a role in cell death, specifically implicate the mTORC1 complex as a regulator of entotic cell death in this context.

How engulfed cells can acquire nutrients from medium is unknown and an important question to be addressed by further studies. It is possible that engulfed cells could acquire amino acids from the cytosol of host cells, as these can be shared directly through gap junctions. We have evidence that the entotic vacuole membrane, within which live engulfed cells are contained, retains characteristics of the plasma membrane for prolonged periods, including localization of E-cadherin and transferrin receptor (data not shown). It may be possible that gap junction complexes could also be present and could mediate the transfer of amino acids to internalized cells. Alternatively, it may possible that endocytic vesicles, such as macropinosomes, could be ingested by host cells and recycled to the membrane surrounding engulfed cells, which could also deliver nutrients.

Live engulfed cells ingested by entosis or HoCC can also undergo another, more frequent type of death that requires the autophagy proteins within host cells, and we also find that mTOR is a regulator of this process. The mTOR effector(s) that may participate as regulators of non-apoptotic cell death in this context are unknown. We have previously shown that autophagy pathway proteins participate in entotic cell death by facilitating vacuole maturation, and that depletion of the autophagy machinery that controls LC3 lipidation also reduces non-apoptotic cell death frequencies in entosis (Florey et al., 2011). But here we find that the regulation of non-apoptotic cell death by mTOR appears unrelated to its control over autophagy, consistent with previous findings that autophagy induction is unrelated to phagosome maturation (Sanjuan et al., 2007).

Here we also found that the death of tumor cells ingested by HoCC is, like entotic cell death, regulated by the availability of extracellular amino acids and mTOR

activity, while the death of live cells ingested by phagoptosis is not; although both types of engulfments engage in LC3 lipidation and lysosome fusion. As entosis and HoCC are associated with an apparent vacuole maturation delay compared to phagoptosis (Fig. 3.8d), we speculate that the initiation of vacuole maturation in the context of epithelial cell-cell engulfment requires a secondary, post-engulfment signal, regulated by mTOR, that is not directly related to the engulfment itself, and perhaps macrophage-driven phagoptosis bypasses this requirement. Indeed, we show here that ingestion of the same target epithelial cell (MCF10A) is associated with a maturation delay only when neighboring epithelial cells, and not macrophages, mediate the engulfment. The engagement of Fcγ-receptors on macrophages by the anti-CD47 antibody used to trigger phagoptosis could conceivably play a role to facilitate rapid phagosome maturation in this context. The identity of the protein or proteins required for vacuole maturation during entosis or HoCC that are synthesized in an mTOR-dependent manner is an important topic for future studies.

Our findings highlight an important concept for the study of live cell engulfment programs; that internalized cells can undergo cell death, which occurs post-engulfment, by distinct mechanisms. Our findings here demonstrate that, to our surprise, the withdrawal of amino acids from culture medium induces apoptosis of internalized cells, while inhibiting entotic cell death. This makes an important prediction that cells engulfed by entosis or HoCC within tumors may also undergo cell death, post-engulfment, by apoptosis, especially when amino acids are limiting in the environment. Therefore, the identification of apoptotic engulfed cells within tumor sections does not necessarily indicate the mechanism by which those cells were engulfed, as entosis, which typically leads to non-apoptotic cell death in nutrient-replete conditions, is associated with apoptosis during starvation. Finally, while nutrient restriction is shown here to change the mechanism of cell death for engulfed

cells, it does not alter the frequency of death, unless cells overexpress a strong inhibitor of apoptosis like Bcl2. Therefore, we find that cells can still cause the death of their neighbors, by entosis or HoCC-mediated ingestion, in the absence of exogenous amino acids, suggesting that the inhibition of transformed growth by entosis (Florey et al., 2011; Overholtzer et al., 2007), as well as nutrient recovery from ingested entotic cells (Krajcovic et al., 2013), may occur similarly under conditions of nutrient restriction.

3.5 REFERENCES

Benseler, V., A. Warren, M. Vo, L.E. Holz, S.S. Tay, D.G. Le Couteur, E. Breen, A.C. Allison, N. van Rooijen, C. McGuffog, H.J. Schlitt, D.G. Bowen, G.W. McCaughan, and P. Bertolino. 2011. Hepatocyte entry leads to degradation of autoreactive CD8 T cells. *Proceedings of the National Academy of Sciences of the United States of America*. 108:16735-16740.

Brown, G.C., and J.J. Neher. 2012. Eaten alive! Cell death by primary phagocytosis: 'phagoptosis'. *Trends in Biochemical Sciences*. 37:325-332.

Cano, C.E., M.J. Sandi, T. Hamidi, E.L. Calvo, O. Turrini, L. Bartholin, C. Loncle, V. Secq, S. Garcia, G. Lomberk, G. Kroemer, R. Urrutia, and J.L. Iovanna. 2012. Homotypic cell cannibalism, a cell-death process regulated by the nuclear protein 1, opposes to metastasis in pancreatic cancer. *EMBO molecular medicine*. 4:964-979.

Chao, M.P., I.L. Weissman, and R. Majeti. 2012. The CD47-SIRPalpha pathway in cancer immune evasion and potential therapeutic implications. *Curr Opin Immunol*. 24:225-232.

Das, G., B.V. Shravage, and E.H. Baehrecke. 2012. Regulation and function of autophagy during cell survival and cell death. *Cold Spring Harb Perspect Biol*. 4.

Dowling, R.J., I. Topisirovic, T. Alain, M. Bidinosti, B.D. Fonseca, E. Petroulakis, X. Wang, O. Larsson, A. Selvaraj, Y. Liu, S.C. Kozma, G. Thomas, and N. Sonenberg. 2010. mTORC1-mediated cell proliferation, but not cell growth, controlled by the 4E-BPs. *Science*. 328:1172-1176.

Florey, O., S.E. Kim, C.P. Sandoval, C.M. Haynes, and M. Overholtzer. 2011. Autophagy machinery mediates macroendocytic processing and entotic cell death by targeting single membranes. *Nature Cell Biology*. 13:1335-1343.

Florey, O., and M. Overholtzer. 2012. Autophagy proteins in macroendocytic engulfment. *Trends Cell Biol*. 22:374-380.

Galluzzi, L., I. Vitale, J.M. Abrams, E.S. Alnemri, E.H. Baehrecke, M.V. Blagosklonny, T.M. Dawson, V.L. Dawson, W.S. El-Deiry, S. Fulda, E. Gottlieb, D.R. Green, M.O. Hengartner, O. Kepp, R.A. Knight, S. Kumar, S.A. Lipton, X. Lu, F. Madeo, W. Malorni, P. Mehlen, G. Nunez, M.E. Peter, M. Piacentini, D.C. Rubinsztein, Y. Shi, H.U. Simon, P. Vandenabeele, E. White, J. Yuan, B. Zhivotovsky, G. Melino, and G. Kroemer. 2012. Molecular definitions of cell death subroutines: recommendations of the Nomenclature Committee on Cell Death 2012. *Cell Death Differ*. 19:107-120.

Krajcovic, M., S. Krishna, L. Akkari, J.A. Joyce, and M. Overholtzer. 2013. mTOR regulates phagosome and entotic vacuole fission. *Molecular biology of the cell*. 24:3736-3745.

Linkermann, A., and D.R. Green. 2014. Necroptosis. *The New England journal of medicine*. 370:455-465.

Liu, Y., S. Shoji-Kawata, R.M. Sumpter, Jr., Y. Wei, V. Ginet, L. Zhang, B. Posner, K.A. Tran, D.R. Green, R.J. Xavier, S.Y. Shaw, P.G. Clarke, J. Puyal, and B. Levine. 2013. Autosis is a Na+,K+-ATPase-regulated form of cell death triggered by autophagy-inducing peptides, starvation, and hypoxia-ischemia. *Proceedings of the National Academy of Sciences of the United States of America*. 110:20364-20371.

Ma, X.M., and J. Blenis. 2009. Molecular mechanisms of mTOR-mediated translational control. *Nat Rev Mol Cell Biol*. 10:307-318.

Mali, P., L. Yang, K.M. Esvelt, J. Aach, M. Guell, J.E. DiCarlo, J.E. Norville, and G.M. Church. 2013. RNA-Guided Human Genome Engineering via Cas9. *Science*. 339:823-826.

Overholtzer, M., and J.S. Brugge. 2008. The cell biology of cell-in-cell structures. *Nat Rev Mol Cell Biol*. 9:796-809.

Overholtzer, M., A.A. Mailleux, G. Mouneimne, G. Normand, S.J. Schnitt, R.W. King, E.S. Cibas, and J.S. Brugge. 2007. A nonapoptotic cell death process, entosis, that occurs by cell-in-cell invasion. *Cell*. 131:966-979.

Sanjuan, M.A., C.P. Dillon, S.W. Tait, S. Moshiach, F. Dorsey, S. Connell, M. Komatsu, K. Tanaka, J.L. Cleveland, S. Withoff, and D.R. Green. 2007. Toll-like receptor signalling in macrophages links the autophagy pathway to phagocytosis. *Nature*. 450:1253-1257.

Tait, S.W., G. Ichim, and D.R. Green. 2014. Die another way--non-apoptotic mechanisms of cell death. *Journal of cell science*. 127:2135-2144.

Wang, S., M.F. He, Y.H. Chen, M.Y. Wang, X.M. Yu, J. Bai, H.Y. Zhu, Y.Y. Wang, H. Zhao, Q. Mei, J. Nie, J. Ma, J.F. Wang, Q. Wen, L. Ma, Y. Wang, and X.N. Wang. 2013. Rapid reuptake of granzyme B leads to emperitosis: an apoptotic cell-in-cell death of immune killer cells inside tumor cells. *Cell death & disease*. 4:e856.

Yuan, J., and G. Kroemer. 2010. Alternative cell death mechanisms in development and beyond. *Genes & development*. 24:2592-2602.

CHAPTER 4: Conclusions and perspectives

4.1. SUMMARY

The mechanisms of recently discovered non-apoptotic cell death forms and the metabolic regulation of these cell death processes are poorly understood. In my thesis research, we have found that amino acid starvation can lead to ferroptosis of cells that have been treated with ultrasmall particles through depletion of cellular glutathione levels. This suggests that these ultrasmall silica nanoparticles, under nutrient-deprived conditions, can be utilized as inducers of ferroptosis. Starvation of amino acids, in this scenario, leads to a decrease in intracellular glutathione levels, most likely caused by a deprivation of cystine, and causes cells to become more susceptible to oxidative stress. We have found that *in vivo* xenograft growth, which is accompanied by nutrient deprivation, was also inhibited with intravenous injections of these nanoparticles. As these ultrasmall silica particles have been approved by FDA-IND to be used as a cancer molecular imaging agent, this opens the possibility of the utilization of these particles as therapeutic agents to induce ferroptosis. An interesting observation we have made of nanoparticle-induced ferroptosis is that the death of cells in a clonal population can be propagated to neighboring cells in a wave-like manner. This is a novel mechanism of cell death that is not observed in other forms of death such as apoptosis and necroptosis. This spread of death may be dependent on cell-to-cell contact in which a death-inducing molecule, or molecules, propagates to neighboring cells.

We have also found that the death of live engulfed cells can be regulated by amino acids and mTOR activity. We find that amino acid withdrawal or mTOR inhibition induces apoptosis of engulfed cells and also disrupts entotic cell death that

is associated with the lipidation of LC3 to entotic vacuoles. The knockdown of mTOR in engulfed cells induces apoptosis of these cells, suggesting that mTOR is needed for survival of these cells. Conversely, the knockdown of mTOR specifically within host cells inhibits entotic cell death, suggesting that mTOR plays a role in vacuole maturation in this context. We find that cells ingested by two other live cell engulfment programs, homotypic cell cannibalism (HoCC) and anti-CD47 antibody-mediated phagocytosis, also known as phagoptosis, also undergo a similar vacuole maturation sequence involving LC3 lipidation and lysosome fusion, but only HoCC involves mTOR-dependent regulation of vacuole maturation and cell death, similar to entosis. We further find that the regulation of apoptosis by mTOR involves the 4E-BP1 protein that is a known regulator of mRNA translation. The knockout of 4E-BP1 in engulfed cells rescues these cells from undergoing apoptosis caused by mTOR inhibition. These data identify amino acid signaling and the mTOR-4EBP-1 pathway as a survival pathway for live engulfed cells formed by entosis and HoCC.

4.2. FUTURE DIRECTIONS

4.2.1 Molecular mechanism of ferroptosis

We have identified a novel mechanism of inducing ferroptosis of cells by the combination of amino acid starvation and nanoparticle treatment. Ferroptosis itself is a newly described form of cell death and not many molecular players have been identified for the signaling pathways related to the death process, at least by comparison to another mechanism of programmed necrosis, necroptosis. For necroptosis, it is becoming clear that necrosis is a highly regulated process involving kinase-mediated control over a protein complex that may function as a pore to promote cell rupture. These layers of molecular control are not yet apparent for

ferroptosis, but if more machinery exists for this mechanism it will be important to identify. The potent ability of ferroptosis to eliminate entire cell populations should facilitate screening efforts to identify, by loss-of-function approaches, genes whose products are required for cell death in this context, as resistant cells may be able to grow out over a clean background in cellular assays. In the case of necroptosis, the discovery of the RIP1 kinase and its inhibitor, necrostatin-1, accelerated the field not only by elucidating molecular mechanism, but also by identifying a kinase inhibitor that could be used as a test to examine if particular death processes occur by this program. If kinases also control ferroptosis, their identification could similarly accelerate the field. Using CRISPR-Cas9 technology, it should be possible to conduct a pooled kinase knockout screen to enrich for resistant cells in ferroptosis-inducing conditions, in order to discover potential kinases that may be essential to this death process.

We have found that ultrasmall nanoparticle treatment can inhibit the growth of melanoma and fibrosarcoma xenograft tumors *in vivo* by inducing ferroptosis, It will be important in future work to expand these studies to investigate if other types of tumors are also susceptible to this treatment. Renal cancer cells have been shown to be more sensitive to ferroptosis than other cell types (Yang et al., 2014), and by analyzing the susceptibility for ferroptosis in a panel of patient-derived renal cancer cell lines (Hakimi et al., 2016), it may be possible to identify certain pathways or mutations that confer ferroptotic sensitivity to cells. For example, a recent study has shown that glutaminolysis is required for ferroptosis (Gao et al., 2015) and there may be other pathways whose activity confers sensitivity to this form of cell death. The identification of mutations or expression patterns that confer sensitivity will be invaluable for future studies to identify cancers that could potentially be treated by

strategies aimed at inducing ferroptosis, or to identify potential efficacious combination treatments, and also for gaining insight into the ferroptosis mechanism.

4.2.2 Synchronous cell-to-cell spreading of ferroptosis

The phenomenon of the synchronous wave-like death spreading in cell colonies undergoing ferroptosis is a very unusual process that is not observed in other types of cell death such as apoptosis or necroptosis. This feature of ferroptosis has also been observed in *ex vivo* cultures of renal tubules (Linkermann et al., 2014). The spreading of cell death may be dependent on cell contact between neighboring cells and may involve the transmission of molecules through gap junctions. Gap junctions are intercellular connections of the cytoplasm between cells that allow small molecules, ions and calcium to move between cells. Gap junction channels are composed of connexin protein subunits and can allow transfer of molecules smaller than 1,000 daltons (Loewenstein, 1966). Apart from some terminally differentiated cell types, such as some nerve cells, skeletal muscle, and circulating lymphocytes, most cells in normal tissues form gap junctions. Interestingly, gap junctions have previously been implicated in a "bystander effect" occurring mostly during apoptosis, where neighboring cells adjacent to those that become damaged can be killed (Feine et al., 2012; Guo et al., 2014). The bystander effect has been described mostly in the context of radiation exposure and treatment with chemotherapy agents, but has also been implicated in development processes (Cusato et al., 2003; Prise and O'Sullivan, 2009). To examine if gap junctions play a role to spread cell death signals during ferroptosis, cells that have been depleted of connexin 43, a commonly expressed and required component of gap junctions, can be treated and the synchronous nature of ferroptotic cell death can be quantified. Such studies could also be extended to *in vivo* contexts where it will be interesting to examine if ferroptosis can kill cells in trans in mixed

tumors, potentially in a gap junction-dependent manner. The inducible knockdown of the lipid peroxidase enzyme GPX4, for example, which has been shown to lead to ferroptosis induction, may be able to kill control cells within mixed tumors, but not when gap junction proteins such as connexin 43 are depleted.

4.2.3 Nutrient uptake of live engulfed cells

In addition to ferroptosis, I have also investigated the cell death mechanism entosis and uncovered regulation controlling apoptosis of live engulfed cells involving the amino acid-responsive mTOR kinase pathway within engulfed cells. The mTOR kinase exists in two distinct complexes, called mTORC1 and mTORC2, where mTORC1 is involved in amino acid sensing and the regulation of mRNA translation and autophagy. We have previously shown that entotic cells sometimes undergo death by apoptosis (Overholtzer et al., 2007), particularly when autophagy, which likely allows for nutrient recycling within engulfed cells, is inhibited. Our findings here demonstrate that, to our surprise, the withdrawal of amino acids from culture media also induces apoptosis of internalized cells. In conditions of mTOR inhibition or knockdown, engulfed cells undergo apoptosis at an increased rate, but if translation is kept active, by a knockout of 4E-BP1, engulfed cells are rescued and do not undergo apoptosis. This suggests that translation of a certain protein, or proteins, can enable live engulfed cells to survive instead of undergoing apoptosis. As mentioned previously, anti-apoptotic proteins such as MCL-1 or cFLIP, may be such candidate proteins. These data are quite surprising as in a previous study, we have shown that most engulfed cells do not have access to growth factors and have decreased mTOR activity even in amino acid replete media, consistent with their induction of autophagy (Florey et al., 2011). If engulfed cells already have lowered mTOR activity and poor access to nutrients, why do these cells undergo apoptosis more often when cultured in

amino acid deprived conditions? It may be possible that although engulfed cells have decreased mTOR activity compared to control cells, they still retain a threshold that is high enough to block apoptosis. Therefore, when mTOR activity is further reduced (by mTOR knockdowns or treatment with an mTOR inhibitor), engulfed cells may undergo apoptosis more often. This model also suggests that engulfed cells may have some degree of access to amino acids, perhaps transiently, that could be responsible for sustaining a lowered level of mTOR activity. It is possible that engulfed cells could acquire amino acids from the cytosol of host cells directly through gap junctions that mediate the transfer of amino acids to internalized cells. Alternatively, it may possible that amino acids could reach engulfed cells through vesicle transport from host cells. Macropinosomes, for example, have been shown to recycle back to the plasma membrane (Hewlett et al., 1994) and we have found evidence that entotic membranes retain characteristics of the plasma membrane for extended periods (for hours, or even up to more than a day), including localization of E-cadherin and transferrin receptor. It is therefore conceivable that endocytc vesicles could "recycle" from host cells to engulfed cells by fusing to the entotic membrane that separates them, and in this manner engulfed cells could acquire some amount of nutrients, such as amino acids, from media. It will be interesting to investigate this hypothesis, potentially by imaging-based approaches, to determine if fluorescent media tracers (e.g. labeled dextrans) that are internalized into cells by endocytosis or macrpinocytosis can gain access to the luminal side of entotic membranes and to engulfed cells.

4.2.4 mTOR-dependent upstream trigger of entotic death

Another interesting observation arising from my entosis studies is the regulation of the non-apoptotic death of engulfed cells involving the amino acid-responsive mTOR kinase pathway. We have shown that mTOR activity is required within host cells of

cell-in-cell structures for the maturation of entotic vacuoles and subsequent death of engulfed cells. The sequence of events that is known to control entotic vacuole maturation involves formation of phosphatidylinositol 3-phosphate (PI3P), through Vps34 activity, which leads to the recruitment of the Atg12-Atg5-Atg16 autophagy protein complex that promotes LC3 lipidation. We have previously shown that autophagy pathway proteins participate in entotic cell death by facilitating vacuole maturation, and that depletion of the autophagy machinery that controls LC3 lipidation also reduces entotic cell death frequencies (Florey et al., 2011). But here we find that the regulation of entotic cell death by mTOR is unrelated to its control over autophagy, The identity of this secondary, post-engulfment signal that initiates vacuole maturation during entosis or HoCC, will be an important topic for future studies.

4.3 CONCLUSION

The findings discussed here arising from my studies have illuminated two examples of crosstalk between nutrient availability and cell survival. Importantly, nutrient limitation through amino acid withdrawal influences cell death occurring by multiple cell death mechanisms. As the field of cell death continues to expand and a deeper understanding of regulated forms of cell death begins to emerge, it will be important to consider how these multiple mechanisms may participate together in the context of complicated pathologies such as cancer, where nutrients are often limiting and rapid cellular evolution also occurs. Cell death occurring over time in complex cancer cell populations is likely to proceed through different mechanisms of execution, where some regions of solid tumors may undergo forms of regulated necrosis, entosis, or apoptosis, perhaps at different times, in manner that is influenced by different nutrient

stresses and genetic variation. Entotic cell death for example, which is known to act as a mechanism of cell competition, is disrupted to some extent by amino acid starvation and may occur through its normal regulation only in regions of tumors where mTORC1 is still at least partially active. Ferroptosis, on the other hand, which has clear non-cell autonomous activity to spread through cell populations, is promoted by amino acid withdrawal. My studies have therefore shown that nutrient availability has distinct, and often complex, effects on different modes of cell death, and, further, that one particular form, ferroptosis, may be a therapeutic strategy that can be leveraged for the treatment of cancer.

4.4 REFERENCES

Cusato, K., A. Bosco, R. Rozental, C.A. Guimar√£es, B.E. Reese, R. Linden, and D.C. Spray. 2003. Gap junctions mediate bystander cell death in developing retina. *The Journal of neuroscience*. 23:6413-6422.

Feine, I., I. Pinkas, Y. Salomon, and A. Scherz. 2012. Local Oxidative Stress Expansion through Endothelial Cells ‚Äì A Key Role for Gap Junction Intercellular Communication. *PLoS ONE*. 7:e41633.

Florey, O., S.E. Kim, C.P. Sandoval, C.M. Haynes, and M. Overholtzer. 2011. Autophagy machinery mediates macroendocytic processing and entotic cell death by targeting single membranes. *Nature Cell Biology*. 13:1335-1343.

Gao, M., P. Monian, N. Quadri, R. Ramasamy, and X. Jiang. 2015. Glutaminolysis and Transferrin Regulate Ferroptosis. *Molecular Cell*. 59:298-308.

Guo, S., J. Zhou, X. Chen, Y. Yu, M. Ren, G. Hu, Y. Liu, and F. Zou. 2014. Bystander effects of PC12 cells treated with Pb2+ depend on ROS-mitochondria-dependent apoptotic signaling via gap-junctional intercellular communication. *Toxicology Letters*. 229:150-157.

Hakimi, A.A., E. Reznik, C.-H. Lee, C.J. Creighton, A.R. Brannon, A. Luna, B.A. Aksoy, E.M. Liu, R. Shen, W. Lee, Y. Chen, S.M. Stirdivant, P. Russo, Y.-B. Chen, S.K. Tickoo, V.E. Reuter, E.H. Cheng, C. Sander, and J.J. Hsieh. 2016. An Integrated Metabolic Atlas of Clear Cell Renal Cell Carcinoma. *Cancer Cell*. 29:104-116.

Hewlett, L.J., A.R. Prescott, and C. Watts. 1994. The coated pit and macropinocytic pathways serve distinct endosome populations. *The Journal of Cell Biology*. 124:689-703.

Linkermann, A., R. Skouta, N. Himmerkus, S.R. Mulay, C. Dewitz, F. De Zen, A. Prokai, G. Zuchtriegel, F. Krombach, P.-S. Welz, R. Weinlich, T. Vanden Berghe, P. Vandenabeele, M. Pasparakis, M. Bleich, J.M. Weinberg, C.A. Reichel, J.H. Br√ § sen, U. Kunzendorf, H.-J. Anders, B.R. Stockwell, D.R. Green, and S. Krautwald. 2014. Synchronized renal tubular cell death involves ferroptosis. *Proceedings of the National Academy of Sciences*. 111:16836-16841.

Loewenstein, W.R. 1966. PERMEABILITY OF MEMBRANE JUNCTIONS*. *Annals of the New York Academy of Sciences*. 137:441-472.

Overholtzer, M., A.A. Mailleux, G. Mouneimne, G. Normand, S.J. Schnitt, R.W. King, E.S. Cibas, and J.S. Brugge. 2007. A nonapoptotic cell death process, entosis, that occurs by cell-in-cell invasion. *Cell*. 131:966-979.

Prise, K.M., and J.M. O'Sullivan. 2009. Radiation-induced bystander signalling in cancer therapy. *Nature Reviews Cancer*. 9:351-360.

Yang, W.S., R. SriRamaratnam, M.E. Welsch, K. Shimada, R. Skouta, V.S. Viswanathan, J.H. Cheah, P.A. Clemons, A.F. Shamji, C.B. Clish, L.M. Brown, A.W. Girotti, V.W. Cornish, S.L. Schreiber, and B.R. Stockwell. 2014. Regulation of Ferroptotic Cancer Cell Death by GPX4. *Cell*. 156:317-331.